DEPARTMENT OF ELECTRICAL AND COMPUTER ENGINEERING

ENHANCING THE PRIMARY FREQUENCY RESERVES WITH ADVANCED UNDERFREQUENCY LOAD SHEDDING SCHEMES

YIANNIS TOFIS

A dissertation submitted to the University of Cyprus in partial fulfillment of the requirements for the degree of Doctor of Philosophy

May 2018

VALIDATION PAGE

Doctoral Candidate: Yiannis Tofis

Doctoral Thesis Title: Enhancing the Primary Frequency Reserves with Advanced Underfrequency Load Shedding Schemes

The present Doctoral Dissertation was submitted in partial fulfilment of the requirements for the degree of Doctor of Philosophy at the Department of Electrical and Computer Engineering and was approved on the 17th of May 2018 by the members of the Examination Committee.

Examination Committee:

Research Supervisor: _____

(Dr. Elias Kyriakides, Associate Professor)

Committee Member: _____

(Dr. Marios Polycarpou, Professor)

Committee Member: _____

(Dr. Christos Panayiotou, Associate Professor)

Committee Member: _____

(Dr. Vladimir Terzija, Professor)

Committee Member: _____

(Dr. Gustavo Valverde, Associate Professor)

DECLARATION OF DOCTORAL CANDIDATE

The present doctoral dissertation was submitted in partial fulfillment of the requirements for the degree of Doctor of Philosophy of the University of Cyprus. It is a product of original work of my own, unless otherwise mentioned through references, notes, or any other statements.

…….... **[**Full name of Doctoral candidate]

…….... **[**Signature]

ΠΕΡΙΛΗΨΗ

Στα σύγχρονα συστήματα ηλεκτρικής ενέργειας χρησιμοποιούνται ως επί το πλείστον συμβατικά σχήματα αποκοπής φορτίου σε περιπτώσεις όπου υπάρχει έλλειμα παραγωγής. Αυτά τα συμβατικά σχήματα χρησιμοποιούν μια αρχιτεκτονική που βασίζεται στη βηματική αποκοπή φορτίου προκειμένου να επιτευχθεί η διατήρηση της συχνότητας του ηλεκτρικού δικτύου σε επιθυμητά επίπεδα σε περιπτώσεις σοβαρής έκτακτης ανάγκης (π.χ., μαζική απώλεια παραγωγής). Υπάρχουν προκαθορισμένα υποψήφια προς αποκοπή κυκλώματα που βασίζονται στη σημαντικότητά τους, τα ιστορικά δεδομένα, τη ζήτηση ηλεκτρικής ισχύος σε κάθε υποσταθμό και την εμπειρία του διαχειριστή του συστήματος. Οι συνθήκες κάτω από τις οποίες συμβαίνει κάποιο σφάλμα ή μια βλάβη διαφέρουν και έχουν ως αποτέλεσμα την αποκοπή μικρότερης ή μεγαλύτερης ποσότητας ηλεκτρικού φορτίου από την απαιτούμενη και συνεπώς στη μη-βέλτιστη λειτουργία του σχήματος αποκοπής φορτίου. Επιπρόσθετα, τα πρόσφατα προτεινόμενα ημί-προσαρμοστικά σχήματα αποκοπής φορτίου είναι λειτουργικά μόνο στη θεωρία μια και για να λειτουργήσουν ικανοποιητικά στην πράξη χρειάζονται μεγάλο αριθμού δεδομένων συλλεχθέντων σε πραγματικό χρόνο. Αυτά τα δεδομένα δεν μπορούν εύκολα να συλλεγούν σε μεγάλη κλίματα και με τρόπο αποδοτικό από οικονομικής άποψης. Επιπλέον, τα προηγούμενα προταθέντα σχήματα αποκοπής φορτίου αποτυγχάνουν να ανταποκριθούν με επάρκεια σε πρωτόγνωρα ή συνδιαστικά συμβάντα, είναι συντηρητικά ως προς την ποσότητα του φορτίου που πρέπει να αποκοπεί και δεν καταπιάνονται με την επιλεκτική διάσταση του φαινομένου της αποκοπής φορτίου. Σ' αυτή την διδακτορική διατριβή, προτείνεται αριθμός από καινοφανή σχήματα αποκοπής φορτίου (βασιζόμενα σε μοντέλο, πλήρως προσαρμοστικά και αναλυτικά), τα οποία ελαχιστοποιούν το συνολικό φορτίο που πρέπει να αποκοπεί και είναι εύρωστα σε διαδοχικές διαταραχές. Προσθετικά, οι επιπτώσεις του συνολικού χρόνου ανταπόκρισης των προτεινόμενων συστημάτων αποκοπής φορτίου σε σχέση με την ποσότητα του φορτίου προς αποκοπή έχουν μελετηθεί και ποσοτικοποιηθεί. Περαιτέρω, η παρούσα διδακτορική διατριβή μοντελοποιεί το ίχνος των σχημάτων αποκοπής φορτίου στην διάρκεια ζωής των περιστρεφόμενων μαζών του συστήματος ηλεκτρικής ενέργειας και παρέχει τη βέλτιστη ποσότητα φορτίου προς αποκοπή που εξασφαλίζει τη μέγιστη βιωσιμότητα από οικονομικής άποψης, λαμβάνοντας υπόψη το κόστος της μη εξυπηρετούμενης ενέργειας καθώς και το κόστος της μηχανικής καταπόνησης στην οποία υπόκεινται οι μονάδες ηλεκτροπαραγωγής.

ABSTRACT

In contemporary power systems conventional Under Frequency Load Shedding (UFLS) schemes are typically used. These UFLS schemes employ a step-level structure to calculate the amount of load to be shed in the case of a severe contingency (e.g., massive loss of generation). There are pre-defined candidate circuit breakers to be opened, based on the importance of loads, historical data for the load demand at each substation, and the operator's experience. However, real conditions at the time of fault differ, resulting to the shedding of a larger or smaller amount of load and to a non-optimal operation of the load shedding scheme. Furthermore, the recently proposed semi-adaptive load shedding schemes are usually only theoretically functional due to the large amount of real time monitoring data required to perform satisfactorily. These data cannot be obtained at a large scale and on a cost effective manner. Also, previously proposed UFLS schemes fail to respond adequately against newly emerging or combinational events, are conservative in terms of the amount of load to be shed and do not address the selectivity dimension as far as the combination of loads to be shed is concerned. In this Ph.D. thesis, a number of novel UFLS schemes are proposed (model based, fully adaptive and analytical) that minimize the total amount of UFLS and are robust to consecutive disturbances. Also, the impact of the total response time of the proposed UFLS schemes with regards to the load shedding amount was investigated and quantified. Additionally, this Ph.D. thesis models the footprint of the UFLS to the lifetime of the rotating equipment of the power system and provides the optimal amount of load shedding that ensures maximum sustainability from the economical point of view, taking into account the cost of unserved energy as well as the cost of the incurred fatigue of the generating units.

ACKNOWLEDGMENTS

The completion of a Ph.D. thesis constitutes a long journey interlarded with a variety of feelings; excitements and disappointments, successes and failures, opportunities and reversals. It is a mainly lonely journey of self-discovery and sitting up late, pushing you beyond the limits you have just discovered. A journey that made me "wealthy with all I have gained on the way". All these features render the journey unique. Unique and marvelous.

This marvelous journey would have not been possible without the advice, coordination, supervision, assistance and support of others. Fellow travelers or not. I take this opportunity to thank all those who contributed to the successful fulfillment of this venture.

First and foremost, I would like to thank my thesis supervisor, teacher in both science and life, Elias Kyriakides who has embraced me and unselfishly integrated me in this research group, providing me all the opportunities, guarantees, academic security, freedom and focus at the same time, for the successful completion of this venture. I am very grateful for his help, patience, tolerance, understanding and constant support. I am also very grateful for his always open door policy, his accurate directions as well as the timely and complete responses to my endless enquiries. I cannot overlook the lessons of ethos, dignity and integrity that Elias Kyriakides provided in abundance.

I would also like to equally thank Stelios Timotheou for his genuine and unadulterated interest in successfully completing this journey. Stelios has dedicated a lot of time to familiarize himself with the topic of my Ph.D. in order to be able to substantially contribute with his unique broad knowledge and background. He both inspired and excited me numerous times with his compelling inputs and bright ideas. I cannot fail to mention the very enjoyable meetings and brainstorming sessions that we have had as well as his outstanding mental courtesy and moral stature.

I feel privileged that I had the chance to meet and interact with the Power research group of the KIOS Research and Innovation Center of Excellence. Especially I would like to thank Yiasoumis Yiasemi for providing tirelessly his expertise in DigSilent simulations, his endless inner power and the unwavering friendship, Markos Asprou for the presentation of a paper of mine at IEEE PES GM 2017, his support and the unforgettable times that we have had during conferences, Lenos Hadjidemetriou for his support and the collaboration to a number of initiatives and Lazaros Zacharia for his everyday smiling welcome.

Working and interacting at a pleasant, comfortable and inspiring work environment was crucial for the successful completion of this endeavor. The KIOS Research and Innovation Center of Excellence generally provided this environment, excluding the fact that my desktop lacked of natural light.

Apart from my research group, I would like to thank all the KIOS faculty, researchers, and administrative staff. My fellow researchers at the KIOS Research and Innovation Center of Excellence are too many to list all of them one by one by their name, but I would like to thank each and every one of them for contributing to the ambiance of the KIOS Center. I am particularly grateful to Alexandros Kyriakides, Agathoklis Papadopoulos, Constantinos Heracleous, Christodoulos Keliris, Charalambos Menelaou, Alexis Kyriacou, Costas Constantinou, Christos Kyrkou and Giorgos Milis who each in their own way contributed to enhancing my experience at the KIOS Research and Innovation Center of Excellence.

My friends Christiana Kenta, Themistoklis Mavrogordatos, Stavros Volos, Constantinos Chailis and Zenonas Antoniou were extremely supportive during this journey while my Violin and Karate teachers Iraklis Mitellas and Andreas Kapardis respectively, provided me new perspectives and spiritual horizons.

Most importantly, I would like to thank my family, my parents and my sister. My parents, in addition to giving me life, have also given me the good life by actively supporting me and providing me the opportunities to equally cultivate both hemispheres of my mind.

TABLE OF CONTENTS

LIST OF TABLES

LIST OF FIGURES

CHAPTER 1
INTRODUCTION

Frequency stability in power systems is of utmost importance since it ensures the maintenance of the delicate balance between generation and demand as well as the operational state of the power system.

During the normal operation of the power system, small variations between generation and demand occur; these are accommodated by the governor action of each committed generator. However, in the case of an unexpected outage of a large portion of the generation or a sudden load increment, the sole action of governors fails to overturn the power deficit between generation and demand due to the limited ramp up rate. The ramp up limit is a safety parameter arising from a mechanical constraint associated with thermal limits. Another constraint is the limited spinning reserve which indicates that even if the generating units were ramping up adequately fast, they would have reached the maximum power output point without managing to cover the whole power deficit in case of a large loss of generation. After the frequency reaches a certain threshold in the under-frequency operation, the power system operator should act accordingly in order to maintain the frequency stability of the power system. Failing to do so, the frequency will exceed the allowed frequency threshold and thus the protection relays of the generating units open. This will cause a cascading blackout [1].

This unfortunate scenario occurred numerous times in the past in various continents affecting millions of people and incurring a very accountable financial and social impact. Only the major Northeast blackout in 2003 contributed to at least eleven deaths and cost an estimated six billion USD [1]. Also the social impact was quite accountable; Internet, telephony and communication systems experienced outages, the Stock Market busted, road/rail traffic restrictions caused accidents, medical facilities came across major challenges and restrictions, business manufacturing processes were interrupted, while payment transactions were compromised and the level of trust to the financial institutions deteriorated significantly [1], [2]. A repetition of such a scenario has increasing chances nowadays given the ever increasing massive penetration of renewables in the contemporary power systems, which shrink the frequency reserve margins due to their short timescale intermittency and their inertia-free nature (solar and wind).

In order to tackle this problem and restore the balance between generation and demand in a timely manner and before a cascading event is triggered, drastic measures should be taken such as underfrequency load shedding (UFLS). UFLS constitutes the last resort for power system operator in order to save the system from the total collapse/whole blackout, a highly unwanted situation that requires a long restoration process that bootstraps the power grid into operation (black start). UFLS is a procedure that disconnects different amounts/chunks of load from the demand side based on the frequency levels in an ongoing effort to counterbalance the unexpected loss of generation. UFLS schemes are strictly conservatively designed in order to ensure that the lower allowed frequency level will never be reached, maintaining in that way the power system in an operational state. However, this practice incurs a substantial amount of cost due to the unserved load and the inconvenience caused to the end customers [3].

A large number of blackouts occurred due to improper amount of load shedding, either because of overshedding or insufficient load shedding [1]. This fact introduced questions regarding the effectiveness and reliability of conventional load shedding schemes and emphasizes the need for the introduction of new schemes that address the large size and complex nature of the smart grid.

The main objectives of this Ph.D. thesis are:

- Optimize the UFLS schemes, quantifying and shedding some light to practices that are common and constitute rules of thumb without their scientific background being adequately quantified.
- To get a deep insight of the already existing load shedding schemes, their advantages and disadvantages. This enables the proposal of new load shedding schemes that take into consideration all the aspects and parameters involved for designing an UFLS scheme. The objective is these parameters to be quantified mathematically.
- Studying thoroughly the already proposed models in the literature and evaluate their adequacy to capture the frequency characteristics of the power system and their ability to respond fast to the time sensitive nature of the UFLS.
- Propose new innovative UFLS schemes that minimize the amount of load shedding and ensure the frequency stability of the power system.
- Propose a benchmark UFLS scheme for comparison purposes and evaluation of the performance of the proposed scheme.

- Quantify the effect of the delays and total response time of the UFLS schemes as well as the "penalty" to be paid in terms of extra amount of load shedding as a function of the total response time of the UFLS scheme.
- Estimate and quantify the fingerprint of UFLS to the generating units' lifetime.

The main contributions of this Ph.D. work are:

- Overshedding and time delays of the conventional UFLS have been studied quantified
- An "ideal" conventional UFLS scheme has been proposed and used as a benchmark to compare with the proposed and future schemes
- The minimum amount of load shedding has been analytically determined according to the grid code; this amount fully exploits the allowed underfrequency operating band in order to minimize the amount of required load shedding. The analytical nature of the solution renders the proposed scheme lightweight since it does not incur any substantial computational burden. This is a great advantage of the proposed scheme due to the time sensitivity of the UFLS problem.
- A widely known second order frequency response model for the power system has been identified online for the first time in the literature. The proposed scheme provides a paradigm shift, from static exploitation of the model for step-wise load shedding schemes, to an adaptive scheme able to accommodate consecutive disturbances
- An approximation based intelligent UFLS scheme has been proposed that approximates the nonlinear and complex form of the swing equation (including damping power) online, bounding the disturbance and model uncertainties bounds.
- The effect of the time delays to the amount of UFLS have been quantified. More specifically, given a certain time delay, the required amount of load shedding is estimated. This is a very useful result not only for evaluating the proposed scheme but in a more general sense since it provides an insight about the employed delays and their effect in every UFLS scheme.
- The impact of underfrequency operation to the ancillary equipment and more specifically to the rotating equipment life time has not been studied in the literature so far. This is a major contribution of this Ph.D. work since for every UFLS scheme the mechanical fatigue that the generating units experience during underfrequency

operation is quantified and the amount of load shedding is adjusted accordingly in a way that the unserved energy and the mechanical exhaustion are compensated.

In this Ph.D. work different UFLS schemes are proposed which fill the gaps of previously proposed schemes in the literature in terms of plug and play operation and optimality, as far as the amount of optimal load shedding from both technical and economic point of view is concerned. More specifically, in Chapter 2 an overview of the state of the art is presented, outlining the most important load shedding technologies that have been proposed so far. In Chapter 3 a load shedding scheme is presented based on a simplistic second order frequency response model, while in Chapter 4 the swing equation is used as a frequency response model to be approximated online. Load disturbance levels are also approximated online by employing adaptive bounding techniques. Furthermore, an important contribution of this Ph.D. work is also the development of an analytical UFLS scheme which is very efficient in regards to its required computational resources since due to its analytical nature it is very lightweight with negligible computational footprint. This is presented in Chapter 5. In Chapter 6 the footprint of total response time of an UFLS scheme arising from the time that a control center load shedding command is issued and the time that the command is executed, has been investigated. The study and evaluation of the total response time provides answers to questions about the preset time delays of the UFLS relays and their impact of the total required amount of load shedding as well as the effects of the processing delays incurred from UFLS schemes on the required amount of load to be shed. Chapter 7 quantifies the mechanical fatigue of the generating units committed during the underfrequency operation and a tradeoff between the minimal amount of load shedding and an economical sound UFLS scheme is demonstrated. Finally, in Chapter 8 the future work along with the conclusions of this ongoing work are presented.

CHAPTER 2
STATE OF THE ART OVERVIEW

2.1 Introduction

Different Underfrequency Load Shedding (UFLS) schemes have been proposed historically which are classified in the literature in three main categories: (a) Conventional or Static UFLS schemes, (b) Semi Adaptive/Dynamic UFLS schemes and (c) Fully Adaptive/Dynamic UFLS schemes. In this chapter the most important UFLS schemes that have been proposed in the literature and/or the industry among the aforementioned categories are presented.

2.2 Conventional UFLS schemes

Conventional UFLS or Automatic Under Frequency Load Shedding (AULS) is the most usually employed UFLS scheme in the electric utility industry [4]. It is a relatively simple, direct and automatic procedure which employs underfrequency relays throughout the whole load area that shed preset increments of loads as a function of the underfrequency levels. In order to determine and preset these levels, it is vital to obtain a previous knowledge of the behavior of the system's frequency as a function of load increment/decrement. However, this is not an easy task due to the size and complexity of the contemporary power systems and the large number of parameters involved. So, a basic and rough knowledge of the system based on historical data has been exploited in order to determine the steps of the conventional UFLS scheme.

According to [5], a load shedding program requires a fast detection of the power deficit between generation and demand and concurrent load shedding performance at this extent that will ensure the frequency stability of the system. The last statement forces load shedding program designers to "generously" design the load shedding schemes with regards to the amount of load shedding to be performed. And this is due to the fact that the oscillatory nature of frequency measurements along different portions of the load area, the different size of UFLS candidate blocks, as well as the preset stepwise relay structure of the conventional UFLS schemes, limit the control on the exact amount of load shedding. The arising

stochasticity of the operation of UFLS schemes usually renders them prone to overshedding [6].

Historical data collected during disturbances [3], [7], [8] introduced in the past, provide valuable information regarding the oscillatory nature of the frequency characteristic of the load buses. However, the robustness of the UFLS schemes under fault or disturbance agnostic situations, where the fault has not emerged in the past, is still questionable.

A UFLS scheme should be able to answer the following questions adequately [5], [6]:

- What is the maximum disturbance magnitude that the UFLS can accommodate?

  It is not an easy task to predict what could be the maximum disturbance magnitude for a certain load area. Especially for large interconnected systems, it is almost impossible to foresee where and how the system will be separated after the introduction of the disturbance and thus to determine the power deficit of the separated area. It is however much easier to come up with a reasonable disturbance margin within migrogrids and industrial systems which are fed over a tie line or a small number of tie lines.

- What is the maximum load shedding amount that can be performed?

  The amount of load that should be shed should be close to (but always smaller than) the disturbance magnitude. It is especially important to ensure that the amount of load to be shed is adequate to reverse the negative frequency decay rate and overcome the minimum of the frequency characteristic. This is of fundamental importance, since after this point the system will be able to recover and restore its frequency back to its nominal levels due to the governing action, which will keep increasing the power output of the generating units, overturning the power deficit. This assumes that the remaining generation in the system maintains a pick up capability. If this is not the case, the network operator should ensure, through the suitable amount of load shedding, a frequency operating level above 49 (59) Hz. Operating above this level does not incur significant mechanical fatigue to the generating units and the auxiliary equipment and provides to the network operator plenty of time to either increase the generation by the commitment of extra units or to shed extra load amount in a more fine-grained and controllable manner.

UFLS usually incurs extended operation of the power system equipment in the underfrequency band. This happens because of, apart from the UFLS schemes inadequacies, the oscillatory nature of the frequency decay, the variation of the demand and generation sides, the distribution of loads, the intermittent nature of renewables and the -difficult to forecast- load-generation composition. The fact that the system equipment is exposed to such an underfrequency operation for a priori undefined time frame poses serious problems for the sustainability of the system equipment and especially the steam turbine generators which constitute the most vulnerable element subjected to cumulatively overwork and permanent damage in a relatively short time for small departures of rotational speed. Mechanical resonances cause extensive vibration to steam turbines and may lead to subsynchronous resonance which is a phenomenon in which the resonant frequency of the turbine generator shaft coincides with a natural resonant frequency of the electrical system such that there is a sustained, cyclic exchange of energy between the mechanical shaft and the electrical system. This exchange of energy results in torsional stress on the turbine generator shaft that can lead to severe damage. In extreme cases, the shaft can actually fracture [9].

The phenomena that take place during underfrequency operation are shown in Figure 2-1 [6], [10] where the vibration stress amplitude of the turbine is presented in terms of electrical frequency. The damage is accumulated when the running frequency of the power system gets outside of the “safe band”, i.e., in the case of underfrequency or overfrequency operating conditions. Three indicative stress levels A, B and C are depicted in Figure 2-1, where the area below stress point A indicates indefinite operation without damage.

The stress amplitude as a function of the number of vibration cycles for failure is depicted in Figure 2-2 [6]. It is depicted in Figure 2-2 that a stress level B causes a failure at 10000 cycles of vibration, while stress level C at 1000 cycles. In the case that the operation takes place at different stress levels, then the number of cycles to failure are calculated by employing a life fraction rule where the life reduction is accumulated across the range of frequencies [6].

The recommended underfrequency and overfrequency time limits for a steam turbine are given in Figure 2-3. Figure 2-3 actually provides the estimated minimum time to cracking for some elements of the bucket structure of the turbines. The elements of the bucket structure that are more prone to crack are the tie wires and the bucket covers.

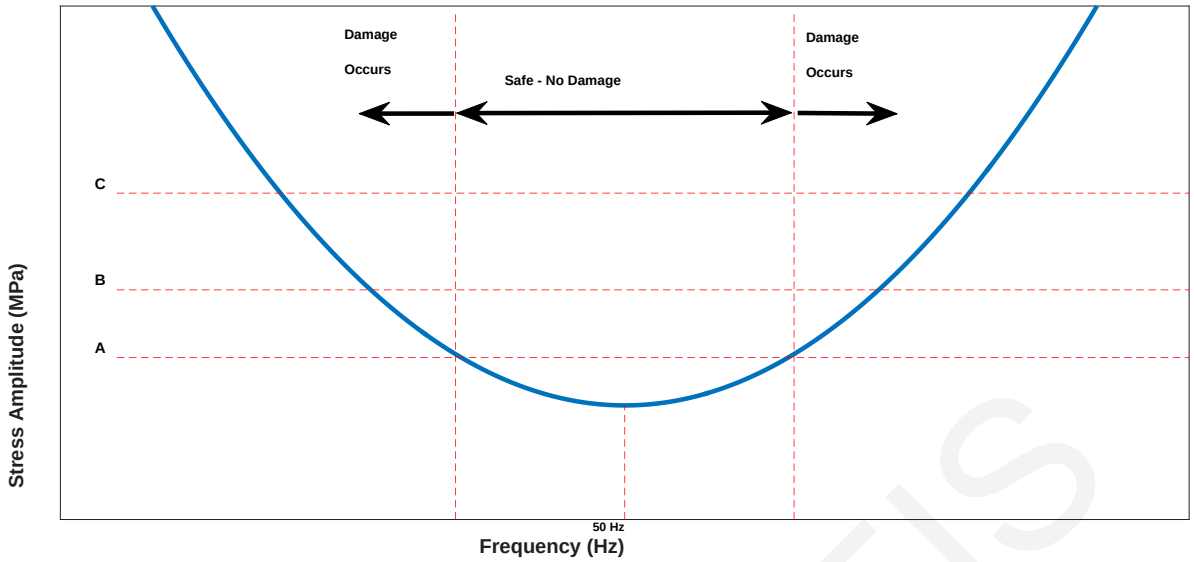

Figure 2-1: Vibration stress amplitude as a function of the electrical frequency of the power system [6]

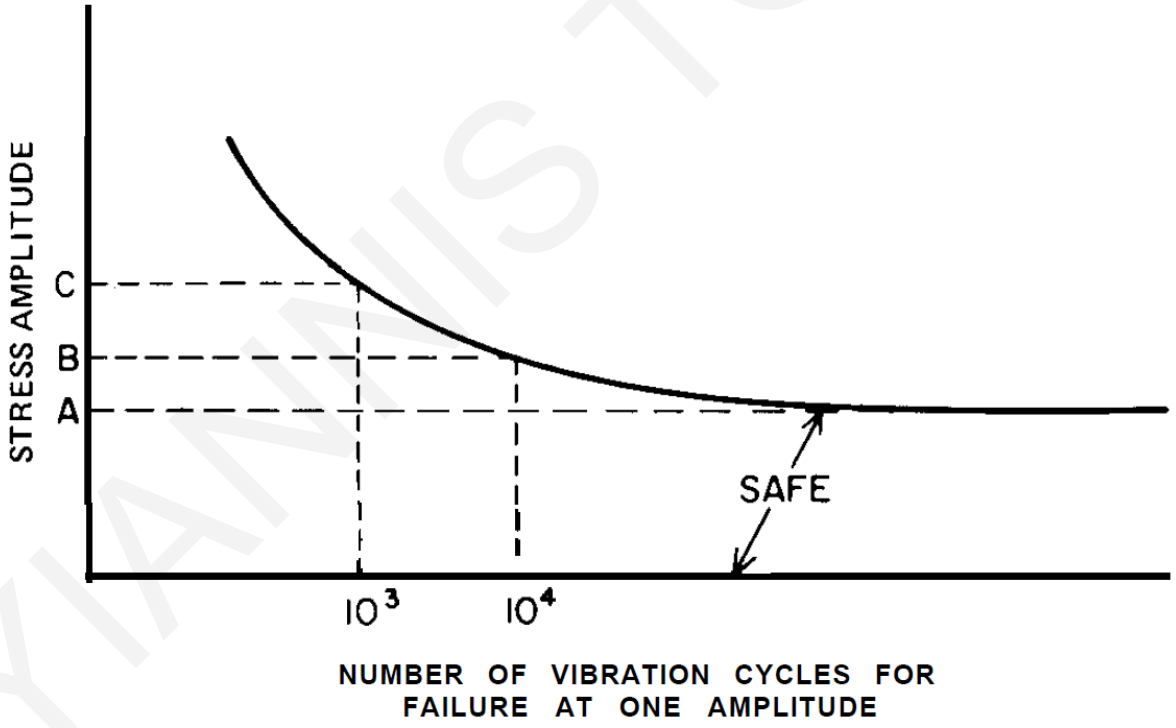

Figure 2-2: Vibration Stress Amplitude as a function of the Number of Cycles to Failure [6]

Although the crack of these elements does not constitute a catastrophic failure by itself, it causes a behavioral change as far as the bucket structure is concerned. This increases the possibility of shifting the natural frequencies of the bucket structure closer to the power system running frequency that causes turbine fatigue failure to the turbine [2]. Figure 2-3 indicates that the time to damage becomes critical after a 5% departure from the nominal

frequency and it is highly recommended to avoid the operation below 47 (56.4) Hz. It is interesting to underline that the lower frequency limit allows only one second of cumulative operation while at a zone close to the nominal frequency the curves are flattened, indicating continuous operation without any effect on the turbine sustainability or life span.

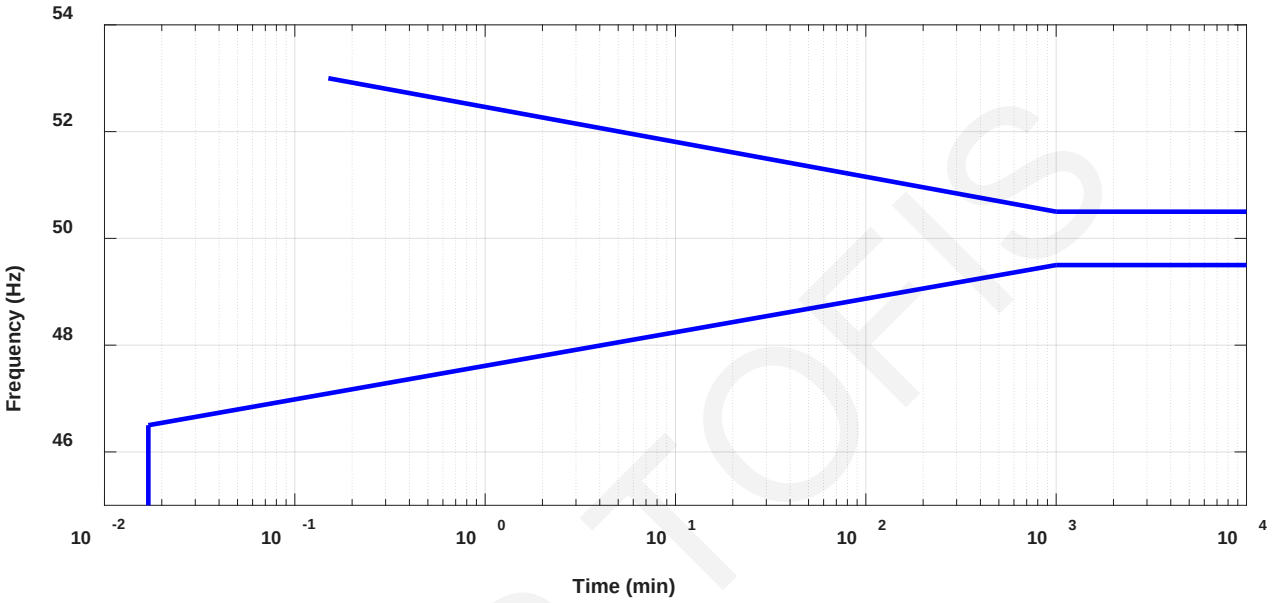

Figure 2-3: Turbine Over/Under-Frequency Limits [6]

Table 2-1 presents estimates of steam-turbine limitations as far as the under-frequency time of operation is concerned. The times shown are cumulative for the life span of a certain unit, i.e., two minutes of operation at 48.5 (58.2) Hz would leave eight minutes of operation at this frequency level, before the turbine is damaged.

Table 2-1: Cumulative time-frequency limitation for steam-turbines [6]

Frequency at Full Load - Hz	**Cumulative Time to Damage**
49.5 (59.4)	continuous
49 (58.8)	90 minutes
48.5 (58.2)	10 minutes
48 (57.6)	1 minute

- What is the allowed underfrequency operating band and how the frequency settings are determined?

Conventional UFLS schemes shed load in steps in order to ensure that the overshedding amount is minimal in the case that the scheme was misled due to the oscillatory nature of the frequency characteristic in less severe underfrequency operating conditions. The first step is decided depending on the size of the system, the possible interconnections or islanded structure of the employed power system. In the case of an interconnected system the first load disconnection step of the UFLS scheme is set at higher frequency levels (at 49.75 (59.7) – 49.83 (59.8) Hz) since these levels indicate the substantial power deficiency. In islanded systems these levels are less conservative and the first step is set at 49.17 (59) Hz [3], [7].

The Union for the Coordination of Transmission of Electricity (UCTE) in its operational handbook [11] advises its members to set the initial frequency setting for the UFLS program not lower than 59 (49) Hz, tripping a 10-20% of the load.

Another important aspect of choosing the first UFLS scheme setting point is the potential swing due to the loss of synchronism of local generation in respect to the system. It is important to make sure that this swing which in this case is not an indication of power deficit and has a duration of a few ms, will not trigger a massive load shedding. In order to do so, we combine a lower frequency setting with an associated time delay.

The design of conventional UFLS schemes employs a trial and error procedure. The ultimate task is the selection of the number and size of the frequency settings that will shed the maximum amount of load shedding that the system is designed for, within the allowed underfrequency band.

The number of load shedding steps lies between three and six since, from experience, this is optimal to the extent of relay coordination and minimal amount of load shedding. The number of the steps is increasing with the total amount of load to be shed, while the amount of load associated with each step is not that critical and is usually equally divided among the steps except from the initial step which is directly associated with the size of the base unit (which is the generating unit with the largest capacity) for islanded systems. In the case of interconnected systems, the initial frequency setting is related with the pick-up capacity of the interconnected tie-lines [6].

Reference [12] proposes two load shedding approaches: a Four and a Six Step Plan. In this work we compare the proposed load shedding scheme to the Six Step Plan. An indicative six step UFLS scheme is presented in Table 2-2 for illustration purposes:

Table 2-2: Frequency settings for a Six Step Load Shedding Plan

Relay	Frequency	Load Trip	Delay
f1	59.5 Hz	0.048 per unit	0.1 s
f2	59.3 Hz	0.048 per unit	0.1 s
f3	59.1 Hz	0.042 per unit	0.1 s
f4	58.8 Hz	0.040 per unit	0.1 s
f5	58.5 Hz	0.036 per unit	0.1 s
f6	58.2 Hz	0.036 per unit	0.1 s
	Total	**0.25 per unit**	

Generally, for *K* load shedding steps the load shedding can be expressed as:

$$u_{UFLS}(t) = \sum_{i=0}^{K} \Delta P_i u(t - t_i)$$

where ΔP_i denotes the incremental amount of load shed while t_i denotes the time instant of the i^{th} load shedding step [13] and $u(t)$ the step function.

The European Network of Transmission System Operators for Electricity (ENTSOE) recommends that the overall delay as shown in Table 2 should be 350 ms including breaker's operating time, while it goes one step further, providing recommendations for emergency operation of the power plants such as the connection of the quick start generators to the system and minimum operating frequency levels with regards to the type of the turbine [14], [15].

2.3 Semi-Adaptive UFLS Schemes

The fact that the conventional load shedding is static and does not take into consideration the magnitude of the disturbance [16] led both academia and the utility industry along with the network operators to a paradigm shift, from the conventional to the dynamic UFLS schemes. These schemes obtain the overload of the system according to [17], based on the equivalent swing equation of the power system without damping power.

$$2Hf(t)\frac{df(t)}{dt} = p_{mp.u.}(t) - p_{ep.u.}(t) \quad (2.1)$$

where

- H is the total normalized inertia constant for the entire system in per unit-seconds (assumed to be known)
- $f(t)$ is the per unit instantaneous electrical frequency of the center of inertia
- $p_{mp.u.}(t)$ is the total per unit mechanical power of the turbines
- $p_{ep.u.}(t)$ is the total per unit electrical power output of the generators

As soon as a load disturbance is introduced to the system, this is reflected to the right part of (2.1), appearing as an accelerating power and thus starts to decay as well as the Rate of Change of Frequency (ROCOF). If H, f and its first time derivative are known, the overvoltage level can be estimated and thus the corresponding amount of load shedding can be deduced. A characteristic example of adaptive UFLS is the ROCOF relay [2]. In the following figure, a general algorithm for the dynamic load shedding practices is presented in Figure 4.

It is generally believed that dynamic UFLS techniques improve the performance of the conventional UFLS since they monitor, besides the frequency per se, its first time derivative. This provides a better indication of the amount of the UFLS to be performed. Nevertheless, the oscillatory nature of the frequency as well as the dependence of the frequency first time derivative on the total inertial of the system does not provide a certain ROCOF for a certain overloading condition, i.e., there is not a one-to-one mapping (injective mapping) between the load disturbance and the ROCOF levels. Also the ROCOF is depended on the operating points of the committed generating units and their loading. Thus, semi-adaptive load shedding schemes fail to estimate the optimal amount of load shedding usually and provide a sub-optimal solution of the load frequency problem [22].

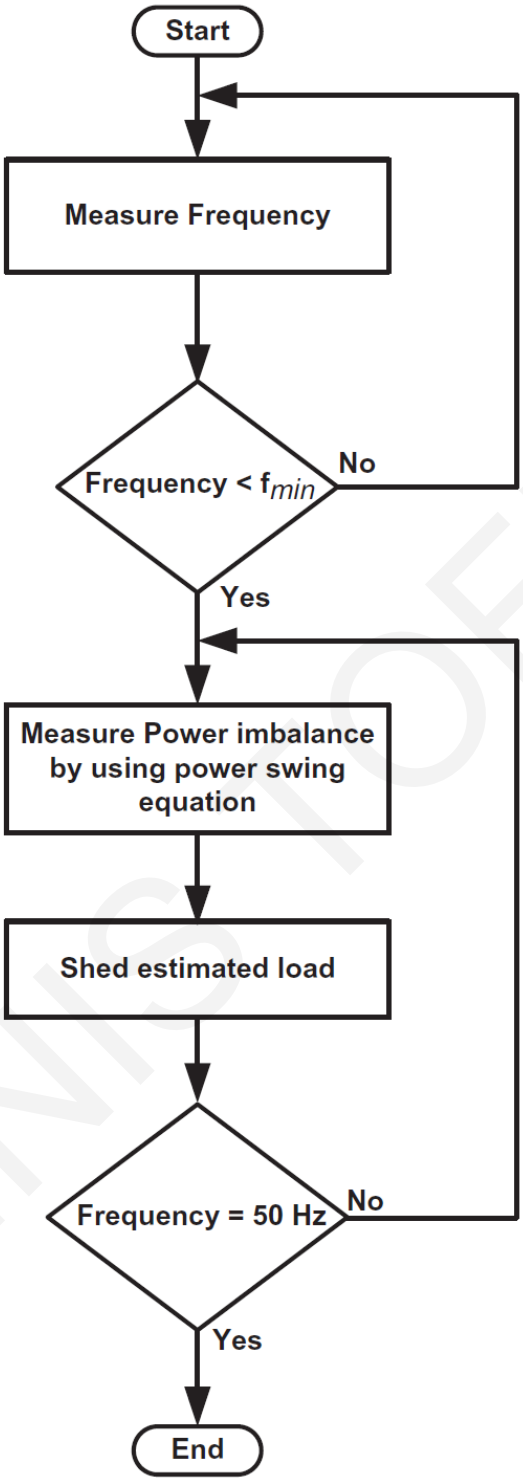

Figure 2-4: Flow chart of dynamic UFLS schemes

2.4 Fully Adaptive Load Shedding Schemes

The highly nonlinear nature of nowadays power systems renders the conventional and semi adaptive schemes insufficient to function optimally in the case of a disturbance or more importantly in the case of consecutive disturbances. Performing more load shedding than required (overshedding), causes extra financial cost and incurs financial losses while

degrading the reliability metrics/indices of the utility/operator due to the increased unserved energy. Moreover, it renders the power system prone to system-wide shut-down due to overfrequency operation. On the other hand, performing less load shedding than required may also cause a cascading blackout due to sequential opening of the protective relays of the generating units due to off nominal/abnormal frequency operation [18]–[20].

The advantage of adaptive UFLS schemes is the ability to deal with the complex non-linear nature of the power grid and approximate it accordingly [21]. Hsu et al. [18] applied Artificial Neural Networks (ANNs) in an effort to find the minimum amount of UFLS in the context of a cogeneration system. The inputs were the frequency decay rate, the total generation and the total demand while the output was the amount of load to be shed. Hsu et al. claim that their proposed UFLS scheme has a faster response time compared to the conventional scheme proposed. References [16], [22] also provide optimal and timely sound UFLS schemes based on ANNs. The performance of these schemes has been evaluated on the IEEE 39-bus test system, verifying enhanced stability margins of the power system due to the optimally performed load shedding amount.

Moreover, another IEEE test system (IEEE 30-bus test system) has been employed to evaluate the performance of UFLS scheme that mitigates the overloading condition experienced from the overloaded lines prior to the system separation process (islanding) [23].

Kottick et al. in [24] have employed an ANN for determining the minimum frequency levels during the transient phenomenon caused from an unexpected outage of a generating unit and a second one for determining the number of UFLS stages required for the certain disturbance caused. Djukanovic et al. in [25] have proposed an ANN which constitutes a decision making process addressed to network operators that ensures the stability of a multi machine system in a timely manner. It proposes the shedding of generators in order to isolate the faulty areas of the system. The ANN is trained in order to approximate the sensitivity of electrical frequency with respect to the tripped generation amount. The output of the ANN is used in order to trip the right generation amount that will prevent the loss of synchronization of committed generating units.

After the major blackout in Taiwan that affected the vast majority of the population [26]–[28], Hsu et al. in [29] proposed an ANN UFLS scheme that improves the stability limits of the country's tie-power system. Purnomo et al. proposed an ANN specially designed to accommodate large disturbances [30] while in [31] Mitchell et al. have proposed an ANN based scheme that is capable to efficiently and effectively predict the dynamic response of

the power system. In [32] Thalassinakis et al. proposed an ANN that has as an output the optimal number of steps of the conventional UFLS scheme. In [33] Javadian et al. have trained an ANN for several fault cases and UFLS was performed in order to maintain the frequency stability in each islanded load area, after the separation of the distribution network into zones.

ANNs present the clear advantages in comparison with conventional UFLS as far as the estimation of the frequency minimum based on certain UFLS amount. However they present certain disadvantages as well. Two papers in the literature focus on these limitations [34], [35]. ANNs have a very good response for the cases that have been trained for. However, they usually fail to generalize well and respond adequately to unseen cases, while the online training constitutes another challenge for the ANNs due to the substantial computational burden required. References [34], [35] evaluate the performance of ANNs in different scenarios. The evaluation is based on the amount of load to be shed for the testing dataset, i.e., for unseen cases that the ANN was not trained for. The poor performance is due to the fact that "the training dataset had relatively few patterns closely associated with unknown cases", while ANNs serve as good interpolator but not equally good extrapolator, according to [6], [34], [35].

Apart from ANNs, Fuzzy Logic Control (FLC) has been applied for UFLS purposes. Reference [36] applies a fuzzy controller for intelligent load shedding as a form of vulnerability control strategy. It employs a neuro-fuzzy UFLS scheme that determines the amount of load that should be shed in order to guarantee the operational state of the power system. The results obtained by using the IEEE 300-bus test system, verify that a FLC UFLS scheme constitutes a fast and sharp vulnerability control action. In [37] a new fuzzy logic based UFLS scheme is presented, especially designed for an islanded system where the electrical frequency is highly affected by the imbalance between generation and demand.

Along the same lines, Genetic Algorithms (GA) have been employed for the solution of the UFLS problem. Genetic Algorithms are suitable for such a problem due to the fact that the global optimum is found in nonlinear, multi objective problems. Sanaye-Pasand et al. [9] proposed a GA for UFLS based on real time power flow data of the IEEE 30-bus system. The GA is used in order to solve the steady state UFLS problem with the constraints of the optimization problem arising from the power flow study. In [38] a GA is employed in order to determine the load shedding amount of each bus of the IEEE 30-bus system. Both the transmission lines as well as the generating units have been characterized based on a contingency ranking and the load shedding candidate buses have been selected accordingly.

Along the same lines, a GA-based scheme for optimal load shedding in distribution networks has been proposed in [39] while an optimal restoration supply strategy is presented. In [21] Lopes et al. propose an effective variant of a GA for optimal UFLS to tackle contingencies. UFLS is performed as a sequence of preset feeder disconnections which take into account the dynamic characteristics of the load while minimizing the amount of load to be shed. The planning of UFLS with the aid of a GA is examined in [40] for minimal load shedding. The system is simulated as a single load-generator and the number of the UFLS relays have been estimated, as well as the amount of load shedding and the shedding ratio per step. The simulation was performed over a dataset including the demand for one year and the results have been directly compared to the conventional UFLS scheme, proving the outperformance of the proposed scheme. Finally, in [41], [42] GA-based approaches have been proposed in order to find out the optimal relay settings of the UFLS program in an isolated grid with varied types of generating units.

CHAPTER 3
ADAPTIVE UNDERFREQUENCY LOAD SHEDDING BASED ON A FREQUENCY RESPONSE MODEL

3.1 Introduction

In this chapter an adaptive approach of load shedding will be presented which controls and manages only the second priority loads (i.e., devices that their operation is not urgent and can be shifted in time, such as boilers, refrigerators, central heating and air-conditioning) in the entire distribution network in an adaptive and optimal way. Further, as soon as the disturbance is overcome, the loads can be smoothly/seamlessly re-committed, skipping long restoration procedures.

In the approach used in this Chapter, the power system is represented as a low order System Frequency Response (SFR) model [12]. This model considers the average frequency of the system. It filters out the synchronizing oscillations between generators and although simplified, it represents the frequency behavior of the system adequately [17]. The parameters of this model are identified online through the Error Filtering Online Learning (EFOL) scheme and the control input of the system, i.e., the step change in load, is evaluated in order to restore the frequency. For this and the following chapters, it is assumed that the load shedding amount provided by the developed methodologies is exactly met, by employing the advanced load management infrastructure of the smart grid.

3.2 Frequency Analysis

The frequency performance of either a large power system, or an islanded portion thereof, may be represented by a simple low order SFR model that includes the essential system dynamics [12]. The transfer function of the employed model is given by (3.1) and the corresponding block diagram is given in Figure 3-1.

$$\Delta\omega = \left(\frac{R\omega_n^2}{DR + K_m} \right) \left(\frac{\left(1 + T_R s\right) P_d}{s^2 + 2\zeta\omega_n s + \omega_n^2} \right) \tag{3.1}$$

where $P_d = P_{Step}u(t)$ is the sudden load change (P_d>0 stands for a sudden increase in generation and P_d<0 for a sudden decrease in generation), P_{step} is the per unit disturbance magnitude (the base is the apparent power of the system), $u(t)$ is the unit step function, P_m is the per unit turbine mechanical power, P_e is the per unit generator electrical load power, P_a=P_m-P_e, $\Delta\omega$ is the per unit incremental speed, F_H is the fraction of the thermal energy high pressure turbine, converted into mechanical work, T_R is the reheat time constant (s), H is the inertia constant (s), D is the damping factor, R is the governor regulation constant and K_m is the mechanical power gain factor. Also, for our convenience ω_n and ζ are defined in terms of the aforementioned quantities as:

$$\omega_n^2 = \frac{DR + K_m}{2HRT_R} \tag{3.2}$$

$$\zeta = \left(\frac{2HR + \left(DR + K_m F_H\right)T_R}{2\left(DR + K_m\right)} \right)\omega_n \tag{3.3}$$

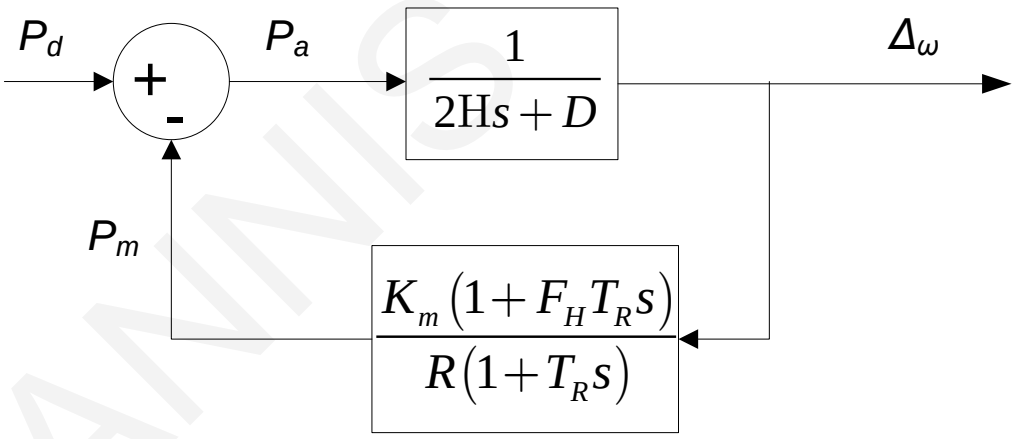

Figure 3-1: SFR model with per unit load change as an input and per unit frequency deviation as an output.

This Chapter builds on this model, by identifying its parameters online and utilizing these identified parameters in order to control it. The control objective is the accommodation of any disturbance -in the sense of sudden load change- and the minimization of the frequency deviation. The model is enhanced with an additional block containing the control system, taking a zero signal reference input. This enhanced model is shown in Figure 3-2.

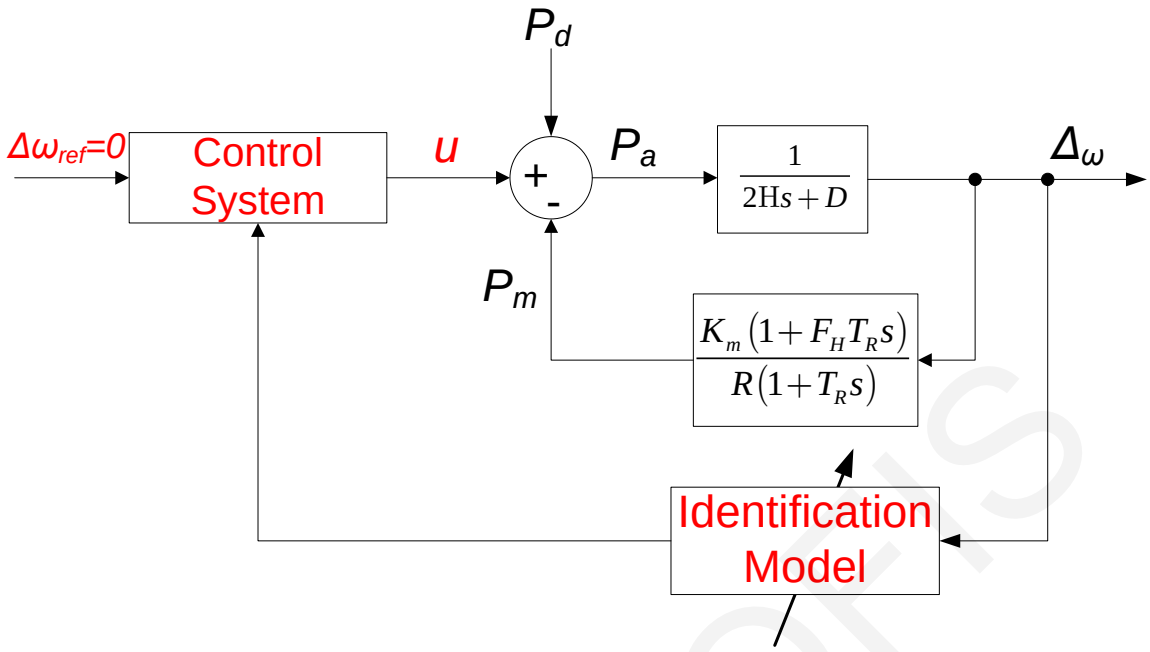

Figure 3-2. SFR controlled model

3.3 Methodology

In order to extract the state space form of (3.1) we rewrite it as:

$$\frac{\Delta\omega(s)}{P_d(s)}=\left(\frac{R\omega_n^2}{DR+K_m}\right)\left(\frac{1+T_R s}{s^2+2\zeta\omega_n s+\omega_n^2}\right)\frac{Z(s)}{Z(s)} \tag{3.4}$$

by multiplying and dividing with $Z(s)$, thus not changing the transfer function. By performing the equalization of the numerator and denominator:

$$\Delta\omega(s)=\left(\frac{R\omega_n^2}{DR+K_m}\right)(1+T_R s)Z(s) \tag{3.5}$$

and

$$P_d(s)=\left(s^2+2\zeta\omega_n s+\omega_n^2\right)Z(s) \tag{3.6}$$

Taking the inverse Laplace transform of (3.5) and (3.6) yields:

$$\Delta\omega(t) = \left(\frac{R\omega_n^2}{DR + K_m}\right)\left(T_R \frac{dz}{dt} + z\right) \tag{3.7}$$

$$P_d(t) = \frac{d^2 z}{dt^2} + 2\zeta\omega_n \frac{dz}{dt} + \omega_n^2 z \tag{3.8}$$

Since a second order system is employed, we define the two following state variables:

$$x_1 = z$$
$$x_2 = \dot{x}_1$$

and

$$\dot{x}_2 = -2\zeta x_2 - \omega_n^2 x_1 + u$$

Thus, the state space representation of (3.1) is given by:

$$\begin{bmatrix} \dot{x}_1 \\ \dot{x}_2 \end{bmatrix} = \begin{bmatrix} 0 & 1 \\ -\omega_n^2 & -2\zeta\omega_n \end{bmatrix} \begin{bmatrix} x_1 \\ x_2 \end{bmatrix} + \begin{bmatrix} 0 \\ 1 \end{bmatrix} u(t) \tag{3.9}$$

The system output is given by:

$$\Delta\omega(t) = \frac{R\omega_n^2}{DR + K_m} x_1 + \frac{R\omega_n^2 T_R}{DR + K_m} x_2 \tag{3.10}$$

The first derivative of (3.10) is given by:

$$\Delta\dot{\omega} = -ax_1 - bx_2 + cu \tag{3.11}$$

where $a = \frac{R\omega_n^4 T_R}{DR + K_m}$, $b = \frac{R\omega_n^2}{DR + K_m}\left(2\zeta\omega_n T_R - 1\right)$ and $c = \frac{R\omega_n^2 T_R}{DR + K_m}$.

The control objective of this work is to achieve $\Delta\omega \to 0$ as $t \to \infty$. In order to achieve this objective we demand:

$$\Delta\dot{\omega} = -k\Delta\omega \tag{3.12}$$

where $k \in R^+$.

Thus the controller output signal u is given by:

$$u = \frac{ax_1 + bx_2 - k\Delta\omega}{c} \tag{3.13}$$

The ultimate task of the online learning scheme employed in this Chapter is to identify the parameter estimates $\hat{a}$, $\hat{b}$ and $\hat{c}$ of the parameters *a*, *b* and *c*, provide the state estimates $\hat{x}_1$ and $\hat{x}_2$ of the real states x_1 and x_2 as well as to estimate the magnitude of the load disturbance. However, the parameters and the magnitude of the disturbance are unknown while the states are not directly measured. Therefore, a system identification is performed in order to estimate these parameters online. In addition, a disturbance estimator is applied and a full state observer is designed.

With regards to the parameter identification, we assume that only $\Delta\omega$ is available. This is a realistic assumption, since the derivative of $\Delta\omega$ might not be available in all cases and the use of differentiation to obtain $\Delta\dot{\omega}$ is not desirable [43]. In order to avoid the differentiator for $\Delta\omega$ we filter each side of the last row of (3.12) and thus we derive the parametric model:

$$\chi(t) = \frac{\lambda}{s+\lambda}\left[\Delta\dot{\omega}(t)\right] = \frac{\lambda}{s+\lambda}\left[-ax_1 - bx_2 + cu\right] \tag{3.14}$$

where $\frac{\lambda}{s+\lambda}$ is a first-order stable filter (λ>0). In this formulation we use the notation $\chi(t)=H(s)\,[x]$ where $y(t)$ is the output of the system represented by the transfer function $H(s)$ with $x(t)$ as an input.

The Error Filtering Online Learning (EFOL) scheme [44] is derived by replacing the real parameters with their estimates:

$$\hat{\chi}(t) = \frac{\lambda}{s+\lambda}\left[-\hat{a}x_1 - \hat{b}x_2 + \hat{c}u\right] \tag{3.15}$$

In order to estimate the parameters of the system online, we should derive update laws for these parameters. These laws are based on the output estimation error $e(t)$ given below:

$$e(t) = \hat{\chi}(t) - \chi(t) \tag{3.16}$$

In order to ensure stability and convergence of the estimated parameters, the differential equations of the adaptive laws are chosen by employing the Lyapunov Synthesis Method [44].

The parameter errors are defined by:

$$\tilde{\Theta} = \hat{\Theta} - \Theta = \begin{bmatrix} \hat{a} - a \\ \hat{b} - b \\ \hat{c} - c \end{bmatrix} \tag{3.17}$$

and the selected Lyapunov function is:

$$V\left(e, \tilde{\Theta}\right) = \frac{\mu}{2\lambda} e^2 + \tilde{\Theta}^T \Gamma^{-1} \tilde{\Theta} \tag{3.18}$$

where $\mu, \lambda \in R^+$ and Γ is a 3x3 matrix of the adaptive gains of the update laws. In order to ensure stability, we demand that $\dot{V}$ is at least negative semi definite:

$$V = \frac{\mu}{2\lambda} e^2 + \tilde{\Theta}^T \Gamma^{-1} \tilde{\Theta} \Rightarrow \dot{V} = \frac{\mu}{\lambda} e\dot{e} + \underbrace{\dot{\tilde{\Theta}}^T \Gamma^{-1} \tilde{\Theta}}_{=\tilde{\Theta}^T \Gamma^{-1} \dot{\tilde{\Theta}}} + \tilde{\Theta}^T \Gamma^{-1} \dot{\tilde{\Theta}} \tag{3.19}$$

If we demand $\dot{V}$ to be equal to $-\mu e^2$, we derive the following adaptive law:

$$\dot{\hat{\Theta}} = -\frac{\mu}{2} e \, \Gamma \begin{bmatrix} x_1 \\ x_2 \\ u \end{bmatrix}^{\mu=2} = -e \begin{bmatrix} \gamma & 0 & 0 \\ 0 & \gamma & 0 \\ 0 & 0 & \gamma \end{bmatrix} \begin{bmatrix} x_1 \\ x_2 \\ u \end{bmatrix} \tag{3.20}$$

In this way, the unknown parameters of the controller are obtained.

As far as the magnitude of the disturbance is concerned, we employ the procedure presented in [17]:

$$P_d = \frac{H}{\omega_n} \frac{d\omega}{dt}\bigg|_{t=t_0} \tag{3.21}$$

where ω_n is the rated value of ω. Equation (3.21) is determined at $t=t_0$, where t_0 is exactly the time that the disturbance occurs.

Finally, in order to design the full state observer we verify that the system is observable at the first stage and then apply (3.21) according to [43] in the system under consideration:

$$\begin{bmatrix}\dot{\hat{x}}_1\\ \dot{\hat{x}}_2\end{bmatrix}=\begin{bmatrix}0 & 1\\ -\hat{\omega}_n^2 & -2\hat{\zeta}\hat{\omega}_n\end{bmatrix}\begin{bmatrix}x_1\\ x_2\end{bmatrix}+\begin{bmatrix}0\\ 1\end{bmatrix}u(t)+\begin{bmatrix}L_1\\ L_2\end{bmatrix}\left(\Delta\omega-\hat{c}x_1-\hat{c}\hat{T}_R\right) \tag{3.22}$$

where the "hat" symbol indicates the estimated value of the parameter.

The observer estimation error for each state is given by:

$$\begin{bmatrix}e_1(t)\\ e_2(t)\end{bmatrix}=\begin{bmatrix}x_1(t)-\hat{x}_1(t)\\ x_2(t)-\hat{x}_2(t)\end{bmatrix} \tag{3.23}$$

Substituting (3.9) and (3.21) into (3.22) we obtain:

$$\begin{bmatrix}\dot{e}_1(t)\\ \dot{e}_2(t)\end{bmatrix}=\left(\begin{bmatrix}0 & 1\\ -\hat{\omega}_n^2 & -2\hat{\zeta}\hat{\omega}_n\end{bmatrix}-\underbrace{\begin{bmatrix}L_1\\ L_2\end{bmatrix}}_{\substack{Observer\\ Matrix}}\begin{bmatrix}\frac{c}{T_R} & c\end{bmatrix}\right)\begin{bmatrix}e_1(t)\\ e_2(t)\end{bmatrix} \tag{3.24}$$

The ultimate task of the observer procedure design is to determine the elements L_1 and L_2 of the observer gain matrix.

In order to achieve this and guarantee that both $e_1(t)$ and $e_2(t)$ tend to zero as $t\to\infty$, it is required that:

$$\det\left(\lambda\underbrace{\begin{bmatrix}1 & 0\\ 0 & 1\end{bmatrix}}_{\substack{Identity\\ Matrix}}-\begin{bmatrix}0 & 1\\ -\hat{\omega}_n^2 & -2\hat{\zeta}\hat{\omega}_n\end{bmatrix}+\begin{bmatrix}L_1\\ L_2\end{bmatrix}\begin{bmatrix}\frac{c}{T_R} & c\end{bmatrix}\right)=0 \tag{3.25}$$

The observer's desired characteristic equation is determined based on the expected settling time, a critical metric for the maintenance of frequency stability for the system under consideration. By selecting an expected settling time of less than 0.4 seconds, the characteristic equation of the observer reads:

$$\Delta_d(\lambda)=\lambda^2+16\lambda+100 \tag{3.26}$$

The characteristic equation has been selected in order for the product of damping ratio and natural frequency to be equal to 10, given a tolerance fraction of 0.02 [45].

Equating the coefficients in (3.24) and (3.25) yields:

$$\begin{bmatrix}L_1\\ L_2\end{bmatrix}=\begin{bmatrix}0.3912\\ 611.9683\end{bmatrix}$$

3.4 Case Study

A direct comparison of the adaptive controller derived in the previous section has been made to the conventional practice of load shedding frequency settings for a Six Step plan as described in [12] when two consecutive sudden load disturbances of 0.2 and 0.5 per unit load occur. Here we reproduce the example provided in [12], where typical parameters are employed for the computation of the SFR model. In this case study, the system is initially at steady state when the two consecutive disturbances occur. The maximum frequency deviation and the frequency restoration time are metrics to be compared. Another important aspect is the overshoot of the control action, before the frequency returns back to its nominal value.

The frequency responses of the proposed and conventional Load Shedding Schemes (LSS) are shown in Figure 3-3. The proposed scheme outperforms the conventional one in terms of frequency declinations and restoration time. The system's frequency of the proposed scheme recovers faster than the conventional one in both disturbance events. The frequency deviation is less than 0.6 and 1.5 Hz for each disturbance respectively. On the other hand, although the frequency declination of the conventional scheme is comparable to the proposed one, the restoration time is longer and requires about 15 seconds to reach the steady state. Even at the steady state the system operates under a low-frequency mode.

The controller effort of the proposed scheme is presented in Figure 3-4. The controller action cancels each disturbance and indicates the required amount of load that should be shed in order to ensure the operational state of the power system. Thus, for a load disturbance of 0.2 per unit, a load shedding of about 0.11 per unit would be enough for the frequency of the system to recover. However, as the magnitude of the disturbance increases, the amount of load that should be shed increases disproportionately due to the fact that the maximum mechanical power P_m of the power system under consideration reaches its maximum value, i.e., the spinning reserve is eliminated. Thus, for the major load disturbance of the system of 0.7 per unit, the proposed scheme requires more than 0.5 per unit load shedding in order to maintain the frequency stability. The remaining 0.2 per unit load is undertaken by the prime mover.

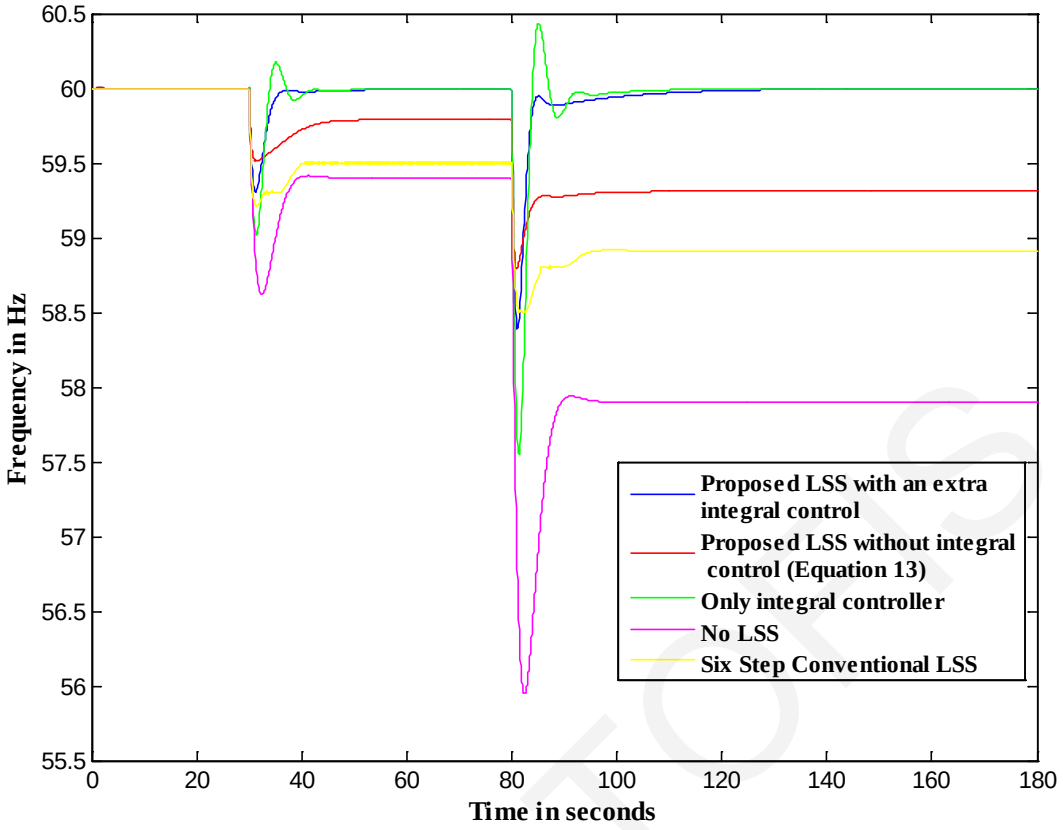

Figure 3-3. Frequency response of the proposed and conventional load shedding schemes to a load disturbance of 0.2 and 0.5 per unit.

The output estimation error shown in Figure 3-5 indicates how fast the online learning is achieved, every time that the power system changes because of the induced disturbance. It is observed that although the magnitude of the second disturbance becomes substantially larger, the output estimation error is not increased respectively during the second disturbance. This is due to the fact that initially the estimated parameters of the system are randomized. After the first disturbance the system parameters are learned and the parameter values approach the real ones with small discrepancies. As soon as the second disturbance occurs, the system changes slightly and the initial values of the parameters –before the second disturbance occurs- are closer to the real ones.

Last but not least, it is important to examine the convergence of the power system's parameters. The estimated values of the parameters are shown in Figure 3-6.

As indicated before, the estimated parameter values are initially randomized. After 30 seconds of online learning, the parameters converge until the first disturbance occurs. When the estimation error approaches the zero value, the online learning stops and the parameter values converge. When the second disturbance occurs, the online learning starts again and the parameters converge to their new values.

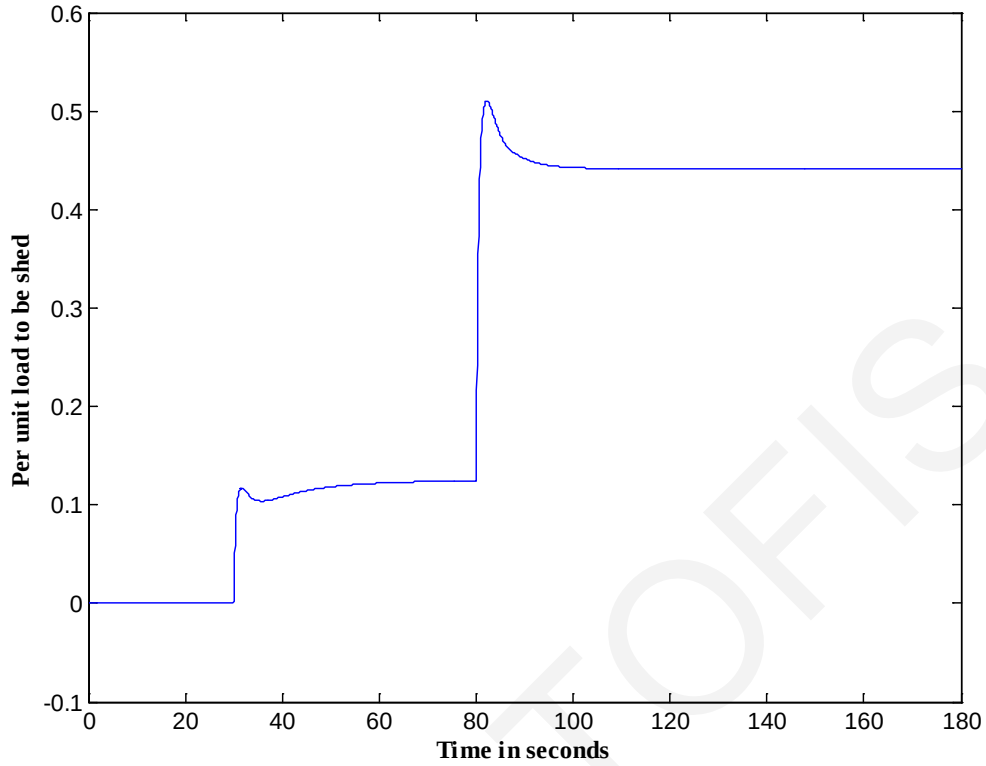

Figure 3-4: Control effort (in terms of load to be shed) of the proposed scheme.

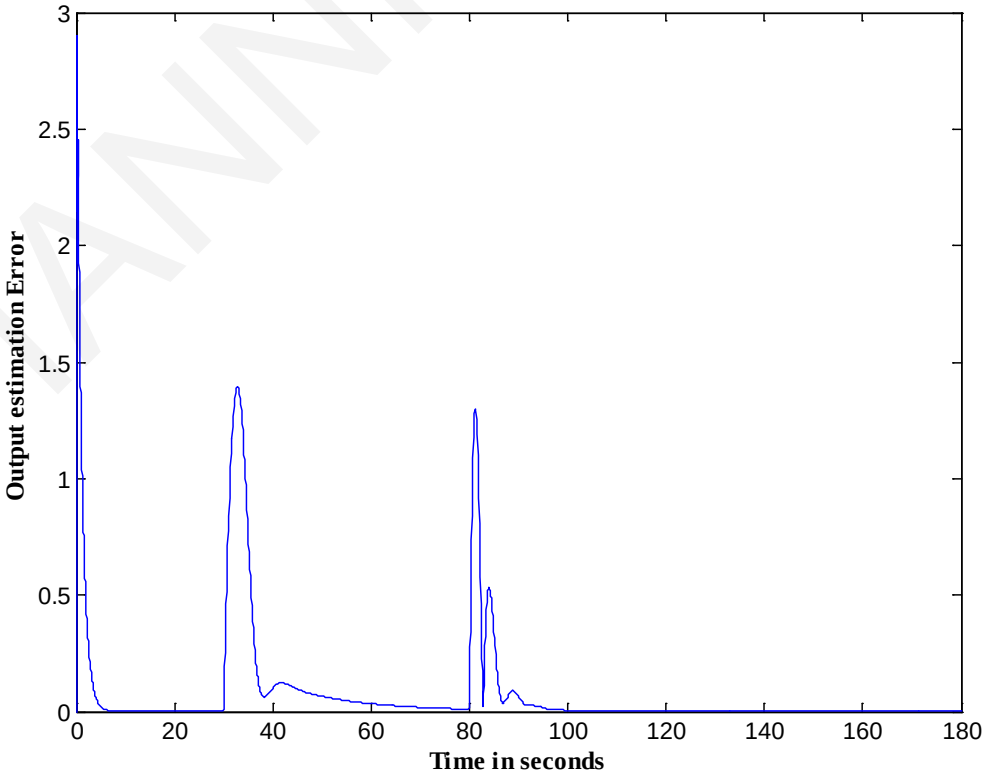

Figure 3-5: Output Estimation Error of the system given by (3.16).

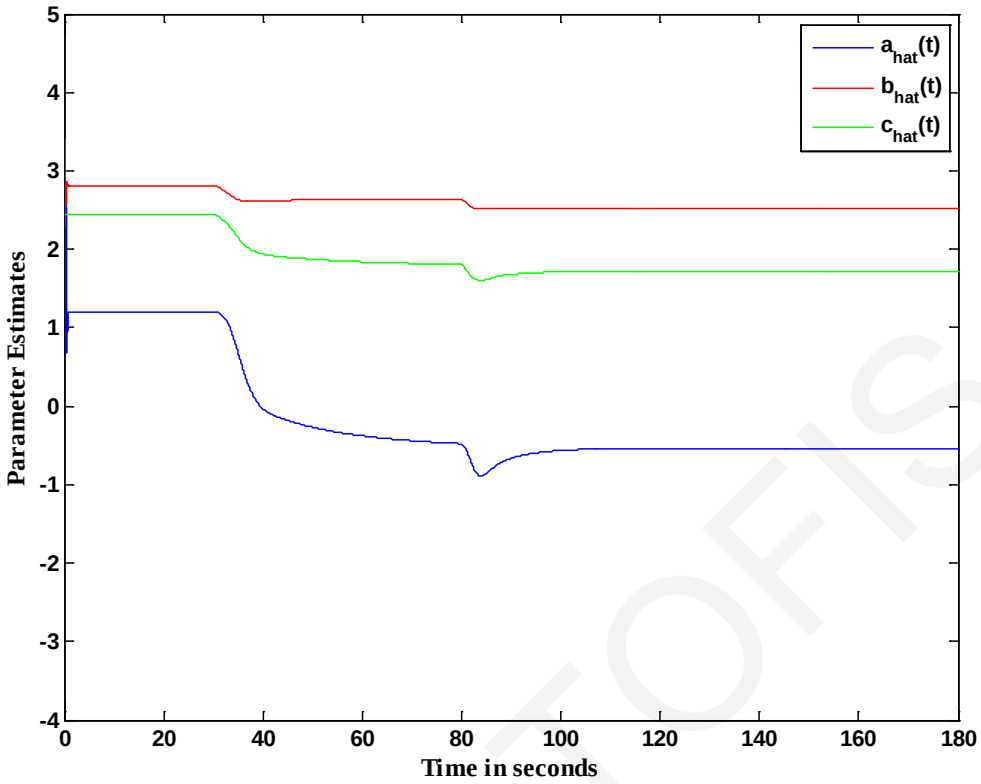

Figure 3-6: Parameter estimates given by (3.20).

3.5 Conclusions

The need for a more efficient load shedding mechanism that maintains the frequency within the desired levels and avoids catastrophic under-frequency operation is essential. Especially after the emergence of the Smart Grid, the proposed mechanism can provide exceptional performance exploiting the capability of selective distributed load shedding on the customer level. More specifically, this section provides the amount of load that should be shed in a continuous manner in order to avoid system destabilization in terms of frequency. The load shedding signal can be frequently sampled and appropriate control actions should be taken in order to track this signal consistently.

CHAPTER 4
A PLUG AND PLAY SELECTIVE LOAD SHEDDING SCHEME BASED ON THE EQUIVALENT SWING EQUATION

4.1 Introduction

As mentioned in the previous chapters, frequency is an accurate and ubiquitous indicator of the system-wide electricity supply and demand. Recently, because of the deregulation of the energy market, the increase of the demand and the large penetration of intermittent renewable resources into the power systems, the ever-decreasing spinning reserves have limited the stability margins [46], [47]. Load shedding, although the last resort to maintain or restore the generation-demand balance, is fundamental to prevent the frequency collapse when primary spinning reserve is not adequate enough to reverse the frequency decay rate. The vast majority of electric utilities employ conventional load shedding schemes because of their inherent simplicity and practicality [48]. However, the major disadvantage of this scheme is the fact that it usually fails to shed the appropriate amount of load and it performs either over- or under-shedding [17], [49], [50]. Especially the overshedding could result to unexpected power oscillations which make the sequential generation control more complicated [51], as well as to unnecessary interruptions of customers. Last but not least, there is much ambiguity in the estimation of the power imbalance due to the fact that the voltage depended loads become smaller due to the voltage decrease as a result of the load disturbance [52].

Because of the aforementioned constraints that the conventional load scheme introduces, the adaptive underfrequency load shedding has been introduced, based on the estimation of load disturbance/power imbalance. The estimation of this quantity is performed through the solution of a simplified form of the motion equation of the system. This estimation requires the average frequency time derivative [17].

Some other adaptive approaches take for granted that the equivalent system inertia is an available input [12], [53]. The estimation of the system equivalent inertia is difficult in practice due to the dynamic nature and multiple operating points of power systems. References [54]–[56] refer to intelligent schemes, the operation of which is directly dependent on the availability of real-time monitoring data of the power system. These constitute highly expensive and non-scalable solutions due to the fact that they require

complex devices for accruing these data. Finally, artificial neural networks have been proposed in [29] in order to estimate the amount of load that should be shed in an adaptive manner. However, inputs such as the total power generation, the total demand and the frequency decay rate are required for the operation of this method. Although the frequency decay rate can be obtained in high sampling rates by Phasor Measurement Units (PMUs), the other two quantities are not easily estimated due to the voltage and frequency dependent loads, as well as the intermittent nature of renewable energy sources.

In this Chapter, a new adaptive load shedding scheme is proposed, with three distinguishing features: (a) it is not system specific, (b) it does not require any prior training from historical data, and (c) it is plug and play due to the fact that the only input that it requires is the frequency at a single point of the whole grid. This is due to the role of frequency as an accurate and ubiquitous indicator of the power balance throughout the power network (as long as inter-generator oscillations are not present). The proposed scheme is robust to several contingent events, such as load disturbances, unexpected outages of generation units and short circuit faults. The dominant advantage of the proposed scheme is that it minimizes the amount of load that should be shed. The paper also introduces the concept of distributed and selective load shedding; single versus multi-area load shedding is investigated.

The 9 and 39 bus dynamic test systems are employed in order to verify the effectiveness and demonstrate the superiority of the proposed scheme versus the conventional load shedding scheme. In order to do so, several simulation events and different operating conditions have been illustrated, directly compared and evaluated.

Section 4.2 develops the theory behind the proposed method. Section 4.3 compares the proposed method with the conventional load shedding scheme using a number of scenarios and Section 4.4 concludes the chapter.

4.2 Proposed Scheme

In this Section, adaptive approximation based control is employed in order to estimate the unknown nonlinear function of electric frequency, which is known as the swing or motion equation [57]:

$$2Hf(t)\frac{df(t)}{dt} = p_{mp.u.}(t) - p_{ep.u.}(t) - Df(t) \tag{4.1}$$

where:

- H is the total normalized inertia constant in Joules/VA or per unit-seconds
- $f(t)$ is the instantaneous per unit electrical frequency
- $p_{mp.u.}$ is the per unit mechanical power out of the turbines
- $p_{ep.u.}$ is the per unit electrical power output of the generator
- D is the damping factor

These nonlinearities are due to difficulties arising in mathematically modeling a complex, rapidly changing and evolving system, such as the power system. If these unknown nonlinearities are not taken into account, severe transient performance degradation can occur and the power system can finally become unstable. Further, the unknown nonlinear functions prevent the tracking error to reach the zero value. With the proposed scheme, these unknown nonlinear functions are estimated and consequently canceled by their estimates through the control action, achieving accurate tracking of the electrical frequency with a softer load change, since the control signal is smoother.

Equation (4.1) can be rewritten in the following form:

$$\begin{aligned}\frac{df(t)}{dt} &= \frac{1}{2H}\left(\frac{p_{mp.u.}(t)}{f(t)} - \frac{p'_{ep.u.}(t)+\Delta p'_{ep.u.}(t)}{f(t)} - \frac{D}{f_{syn}}\right) \\ &= \underbrace{\frac{f_{syn}^2}{2H}\left(\frac{p_{mp.u.}(t)-p'_{ep.u.}(t)}{f(t)} - \frac{D}{f_{syn}}\right)}_{g_1^*(f)} + \underbrace{\frac{1}{2Hf(t)}}_{g_2^*(f)}\underbrace{\Delta p'_{ep.u.}(t)}_{u(t)}\end{aligned} \tag{4.2}$$

where the per unit electrical power output of the generators $p'_{ep.u.}(t)$ is equal to the non-controllable portion of the demand plus the losses related to that amount. Along the same lines, $\Delta p'_{ep.u.}(t)$ is the controllable portion of the demand. Thus, $p_{ep.u.}(t) = p'_{ep.u.}(t) + \Delta p'_{ep.u.}(t)$. Through the proposed load shedding scheme the quantity $\Delta p'_{ep.u.}(t)$ constitutes the controllable quantity and thus, the value of this quantity is determined in order to maintain the stability of the system. In other words, the proposed scheme decides the value of $\Delta p'_{ep.u.}(t)$ in order to achieve the frequency stability of the grid.

If we take into account the load disturbances, (4.2) can be written as follows:

$$\dot{f}(t) = g_1^*(f) + g_2^*(f)u(t) + d(t) \tag{4.3}$$

where $g_1^*(f)$ and $g_2^*(f)$ are unknown nonlinear functions of $f(t)$ to be approximated and u is the control law indicating how the quantity $\Delta p'_{ep.u.}(t)$ should be modified (decreased/increased in the case of load shedding/restoration) in order to achieve the control

objective: the system output $f(t)$ to be equal to the nominal value, i.e., equal to unity. Finally, $d(t)$ represents the load disturbances which can be fluctuations of the demand $p_{ep.u.}(t)$ or fluctuations of the generation $p_{mp.u.}(t)$.

The two unknown functions can be approximated with the linearly parameterized approximators, where index 1 refers to g_1 and index 2 refers to g_2 respectively,

$$g^*_{1(2)}(f) = \hat{g}_{1(2)}\left(f, \theta^*_{g_{1(2)}}\right) + \delta_{g_{1(2)}}(f) \tag{4.4}$$

where $\hat{g}_{1(2)}\left(f, \theta^*_{g_{1(2)}}\right)$ is the approximated version of the original function $g^*_{1(2)}(f)$ which is approximated by the radial basis functions approximators $\Phi_{g_{1(2)}}(f)$ and their weights $\theta^*_{g_{1(2)}} = \arg \min_{\hat{\theta}_{g_{1(2)}} \in R^N} \left\{ \sup_{f \in D} \left| g^*_{1(2)}(f) - \hat{g}_{1(2)}\left(f, \hat{\theta}_{g_{1(2)}}\right) \right| \right\}$. The quantity $\delta_{g_{1(2)}}(f)$ is the minimum functional approximation error, A is the frequency region of interest [0.95-1.02], i.e., in natural units [57-61.2 Hz] and N is the number of approximators that the functions are approximated with, such as,

$$\hat{g}_{1(2)}\left(f, \theta^*_{g_{1(2)}}\right) = \Phi_{g_{1(2)}}(f)^T \theta^*_{g_{1(2)}} = \sum_{i=1}^{N} \theta^*_{g_{1(2)i}} \varphi_{g_{1(2)}}(\| f - c_i \|) \tag{4.5}$$

The centers c_i of the approximators vector $\Phi_{g_{1(2)}}(f)$ are chosen uniformly distributed in the region of interest A.

In order for the frequency of the system to approach its nominal value exponentially fast by cancelling the nonlinearities, (4.3) is rewritten as:

$$\begin{gathered} \dot{\tilde{f}} = -a_m \tilde{f} - \Phi_{g_1}(f)^T \tilde{\theta}_{g_1} - \Phi_{g_2}(f)^T \tilde{\theta}_{g_2} u + \\ \underbrace{\Phi_{g_1}(f)^T \hat{\theta}_{g_1} + a_m \tilde{f} - v_g}_{-u_a} + \\ \Phi_{g_2}(f)^T \hat{\theta}_{g_2} u + \underbrace{\delta_{g_1}(f) + \delta_{g_2}(f) u + d(t)}_{\delta(f,u,t)} = \\ -a_m \tilde{f} - \Phi_{g_1}(f)^T \tilde{\theta}_{g_1} - \Phi_{g_2}(f)^T \tilde{\theta}_{g_2} u - u_a + \\ \Phi_{g_2}(f)^T \hat{\theta}_{g_2} u + \delta \end{gathered} \tag{4.6}$$

where $a_m > 0$ is a design constant calculated by a trial and error process and v_g is used to deal with the functional approximation errors and load disturbances δ. Thus, the control law is given by:

$$u = \frac{u_a}{\Phi_{g_2}(f)^T \hat{\theta}_{g_2}} \tag{4.7}$$

where $u_a = \Phi_{g_1}(f)^T \hat{\theta}_{g_1} + a_m \tilde{f} + \nu_g$

The adaptive laws for the unknown parameters and the bounds of $\delta(t)$ are derived based on the Lyapunov synthesis method [44] that provides inherent stability and convergence properties, such as uniform boundedness and convergence of parameter estimation errors $\tilde{\theta}_{g_{1(2)}}$.

To apply the Lyapunov synthesis method, we select the Lyapunov function

$$V = \frac{1}{2}\begin{pmatrix} \tilde{f}^2 + \tilde{\theta}_{g_1}^T \Gamma_{g_1}^{-1} \tilde{\theta}_{g_1} + \tilde{\theta}_{g_2}^T \Gamma_{g_2}^{-1} \tilde{\theta}_{g_2} + \\ \frac{1}{\gamma_L}(\hat{a}_L - a_L)^2 + \frac{1}{\gamma_U}(\hat{a}_U - a_U)^2 \end{pmatrix} \tag{4.8}$$

where $\Gamma_{g_{1(2)}}$ and $\gamma_{L(U)}$ are positive constants to be selected. By taking the time derivative of V and using the fact that θ^* is constant (i.e., $\dot{\tilde{\theta}} = \dot{\hat{\theta}}$) we obtain

$$\begin{aligned} \dot{V} = -a_m \tilde{f}^2 + \tilde{\theta}_{g_1}^T \Gamma_{g_1}^{-1} \left(\dot{\tilde{\theta}}_{g_1} - \Gamma_{g_1} \Phi_{g_1}(f) \tilde{f} \right) \\ + \tilde{\theta}_{g_2}^T \Gamma_{g_2}^{-1} \left(\dot{\tilde{\theta}}_{g_2} - \Gamma_{g_2} \Phi_{g_2}(f) \tilde{f} u \right) + \tilde{f}\left(-\nu_g + \delta\right) \\ + \frac{1}{\gamma_L}(\hat{a}_L - a_L)\dot{\hat{a}}_L + \frac{1}{\gamma_U}(\hat{a}_U - a_U)\dot{\hat{a}}_U \end{aligned} \tag{4.9}$$

In order to obtain the aforementioned stability and convergence properties, it is required for $\dot{V}$ to be at least negative semidefinite. The first term of (4.8) is negative, while the remaining terms can be positive or negative since the sign of the unknown parameters $\hat{\theta}_{g_{1(2)}}$, ν_{g_1} and $\hat{\alpha}_{L(U)}$ is unknown.

Therefore, it is necessary to force the remaining terms to zero. This can be achieved by selecting

$$\dot{\hat{\theta}}_{g_1} = \Gamma_{g_1} \Phi_{g_1}(f)(f - 1) \tag{4.10}$$

$$\dot{\hat{\theta}}_{g_2} = \Gamma_{g_2} \Phi_{g_2}(f)(f - 1)u \tag{4.11}$$

$$\nu_g = \begin{cases} \hat{a}_u \delta_u(f) & \text{if } f > 1 \\ \hat{a}_L \delta_L(f) & \text{if } f < 1 \end{cases} \tag{4.12}$$

The adaptive laws regarding the lower and upper bounds of δ(t), i.e., $a_L\delta_L(f) \le \delta(f,u,t) \le a_U\delta_U(f)$, are given by

$$\dot{\hat{a}}_u = \begin{cases} \gamma_u (f-1)\delta_u(f) & \text{if } f > 1 \\ 0 & \text{if } f < 1 \end{cases} \tag{13}$$

$$\dot{\hat{a}}_L = \begin{cases} 0 & \text{if } f > 1 \\ \gamma_L (f-1)\delta_L(f) & \text{if } f < 1 \end{cases} \tag{14}$$

where $\hat{a}_u$ and $\hat{a}_L$ are unknown parameters multiplying the bounding (lower and upper) disturbance functions $\delta_L(f)$ and $\delta_u(f)$.

4.3 Implementation of the methodology

For validation purposes of the proposed load shedding scheme, two transient stability test systems have been employed:

- The 9-bus 3-machine system [58] given in Figure 4-1, which includes three generators with power set points of 163 MW, 85 MW, and 67 MW and three large equivalent loads of a total demand of 315 MW, connected in a meshed transmission network through transmission lines.
- The IEEE 39-bus test system for dynamic studies [58] given in Figure 4-2. It is well known as the 10-machine New-England Power System. Unit 1 with a power set point of 1000 MW, represents the aggregation of a large number of generators. The system has 19 loads with a total demand of 6097 MW. The power set points of the remaining nine generators are given in Table 3.

The general approach followed includes the introduction of a load disturbance of step change to one of the buses of the test system employed. The application of the disturbance causes frequency fluctuations. Thus, load shedding schemes (both the conventional and the proposed one) perform load shedding to a part of the manageable/sheddable loads in order

to maintain the frequency stability of the system under consideration. The remaining loads are kept constant during the transient analysis simulation, representing in that way the load of the system that cannot be controlled. Without loss of generality, all the loads are considered constant power loads and the conventional controllers of the generators, such as governors and voltage regulators are on during all simulations.

For each of the test systems two cases are studied and directly compared:

1. Conventional load shedding
2. Proposed load management scheme

Several simulation events have been implemented for this work. In this Chapter, the following simulation events are shown and discussed:

a) Two consecutive load disturbances on bus 8 of the 9 bus test system.

b) Two consecutive load disturbances on bus 23 of the 39 bus test system.

c) Unexpected outage of Generator 9 in the 39 bus test system.

d) Short circuit fault on bus 25 of the 39 bus test system

Table 4-1: Power Set Points of the Machines of the IEEE 39-Bus Dynamic Test System

Unit	**Power Set Point (MW)**	**Bus Number**
Gen1	1000	39
Gen2	slack bus	31
Gen3	650	32
Gen4	632	33
Gen5	508	34
Gen6	650	35
Gen7	560	36
Gen8	540	37
Gen9	830	38
Gen10	250	30

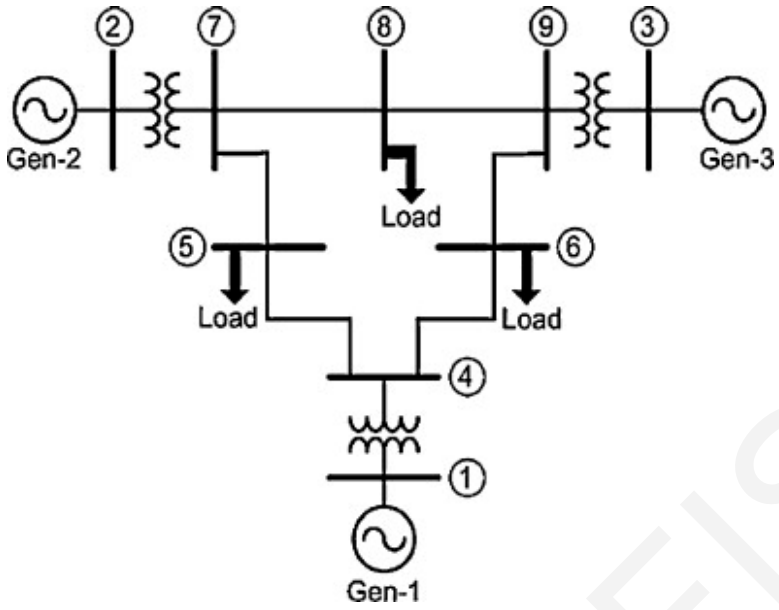

Figure 4-1: The 9-bus 3-machine test system for dynamic studies [59]

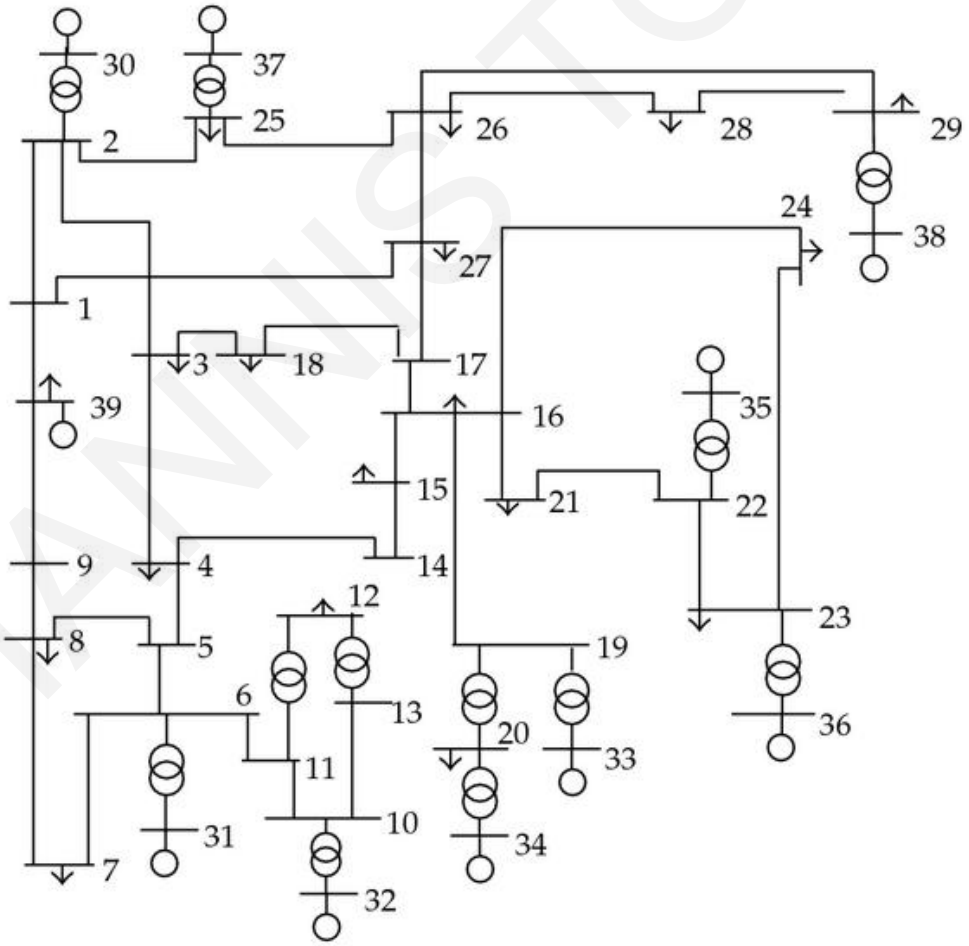

Figure 4-2: The 39-bus 10-machine test system for dynamic studies

The two test systems are simulated using DigSilent PowerFactory. The frequency of the system is monitored by a PLL (Phase Locked Loop) attached to the buses that the disturbance is applied to. The proposed scheme is implemented as described in Figure 4-3.

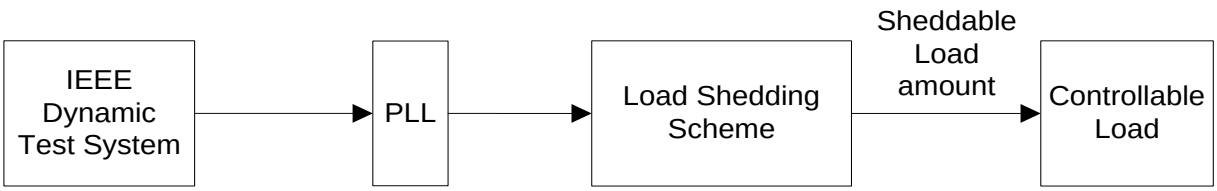

Figure 4-3: Implementation of the proposed scheme in DigSilent Powerfactory

a) Two consecutive load disturbances on bus 8 of the 9 bus test system

At first, the 9 bus test system is considered. Two consecutive disturbances of magnitude 30 MW and 50 MW are applied to bus 8, while the controllable load is the load on bus 5. The third load (load connected to bus 6) is kept constant. Frequency is measured on bus 8 where the disturbance is applied to due to the fact that, in such a small system, the disturbance constitutes a ubiquitous indicator of the balance between generation and demand The simulation results regarding the frequency response characteristic and the loading of the system for the 9 bus system are shown in Figure 4-4 and Figure 4-6 respectively. Figure 4-5 presents a closer look at the portion of the frequency characteristic when the first disturbance occurs. The conventional load shedding scheme activates its first step just after the occurrence of the first disturbance since the frequency falls below the level of 59.5 Hz. The second disturbance does not trigger the conventional load shedding mechanism. The proposed load shedding scheme achieves the control objective with a load shedding that is 14 MW less than the conventional scheme (or 4.45% of the total load of the system), without exceeding downwards the critical level of 59 Hz. An important point to note is that the conventional load shedding scheme curtails the load in steps, thus the load is interrupted in large amounts at the same point in time. In the proposed scheme the load shedding is smoother.

b) Two consecutive load disturbances on bus 23 of the 39 bus test system

Regarding the 39 bus test system, two consecutive load disturbances occur on bus 23, each one representing an increase of 371.25 MW magnitude. Figure 4-7 and Figure 4-9 depict the

frequency characteristics and the load magnitude for the controllable loads in each of the aforementioned cases.

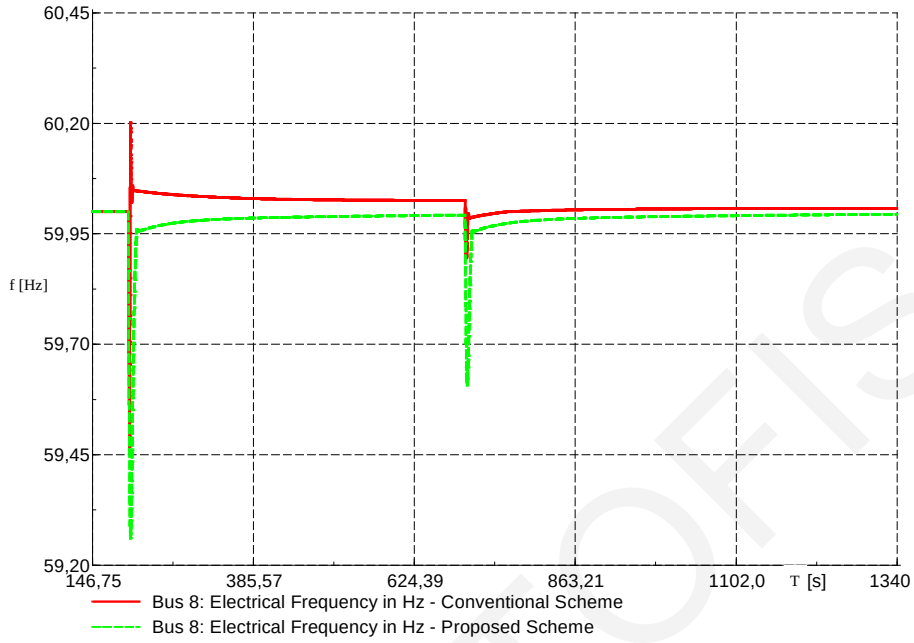

Figure 4-4: Frequency variations of the 9-bus system in the case of: (1) Conventional load shedding (Table II) and (2) Proposed load shedding

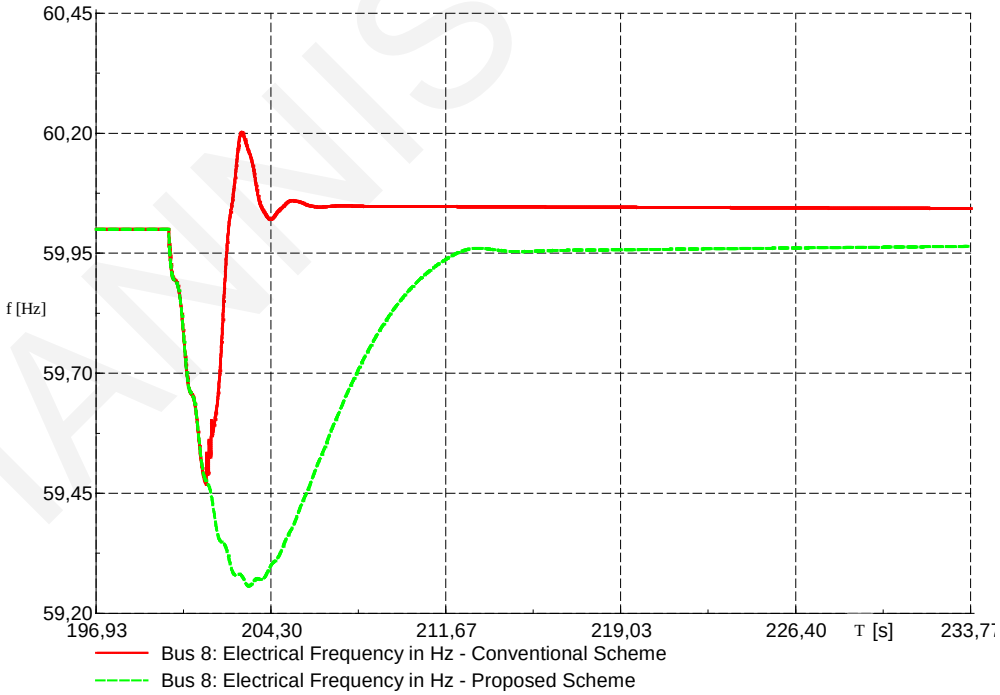

Figure 4-5: Zoomed frequency variations of Figure 4 during the first load disturbance

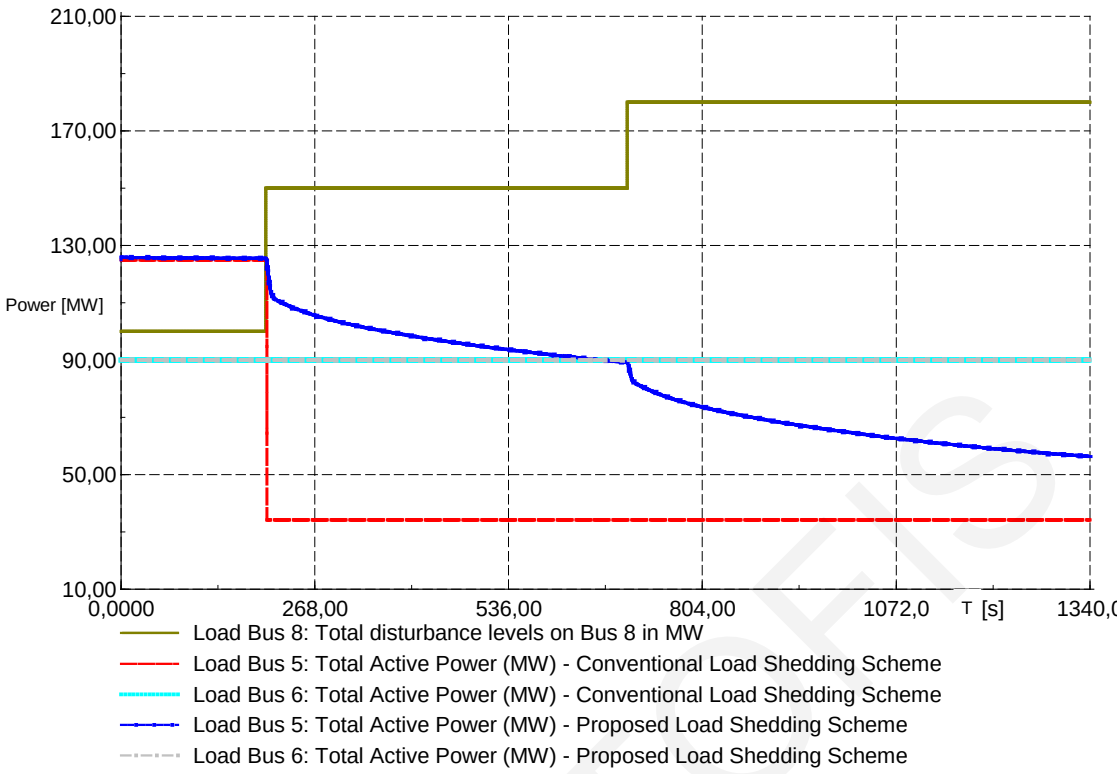

Figure 4-6: Load variations of the 9-bus system in the case of: (1) Conventional load shedding (Table II) and (2) Proposed load shedding

Two sub-cases are considered in this simulation scenario: in the first sub-case, the load shedding is performed on a single load; in the second sub-case, load shedding is distributed to three loads. It turns out that the frequency response characteristic almost coincides while the total load that has been shed is almost identical for the two sub-cases under consideration. This indicates that the frequency in an isolated system of 39 buses is agnostic to the spatial distribution of the load. Figure 4-8 presents a closer look at the portion of the frequency characteristic when the first disturbance occurs.

It can be observed from Figure 4-9 that the conventional load shedding scheme performs a total of 1494 MW of shedding while the proposed scheme 231 MW in the single load shedding scenario and 228 MW in the multiple load shedding scenario, all after the occurrence of the two disturbances. The difference of 3 MW between the two sub-cases is due to the fact that in the case of three sheddable loads the losses of the system become smaller. It is clearly shown that conventional load shedding performs an overshedding of 1260-1263 MW more than the proposed scheme, although it includes a 0.1 s of total delay (the sum of time delay of relays and circuit breakers time) that is enabled to prevent overshedding (this delay enables the conventional load shedding to obtain a reasonably accurate indication of the true frequency characteristic trend and avoid over-shedding due to the oscillatory nature of the frequency characteristic).

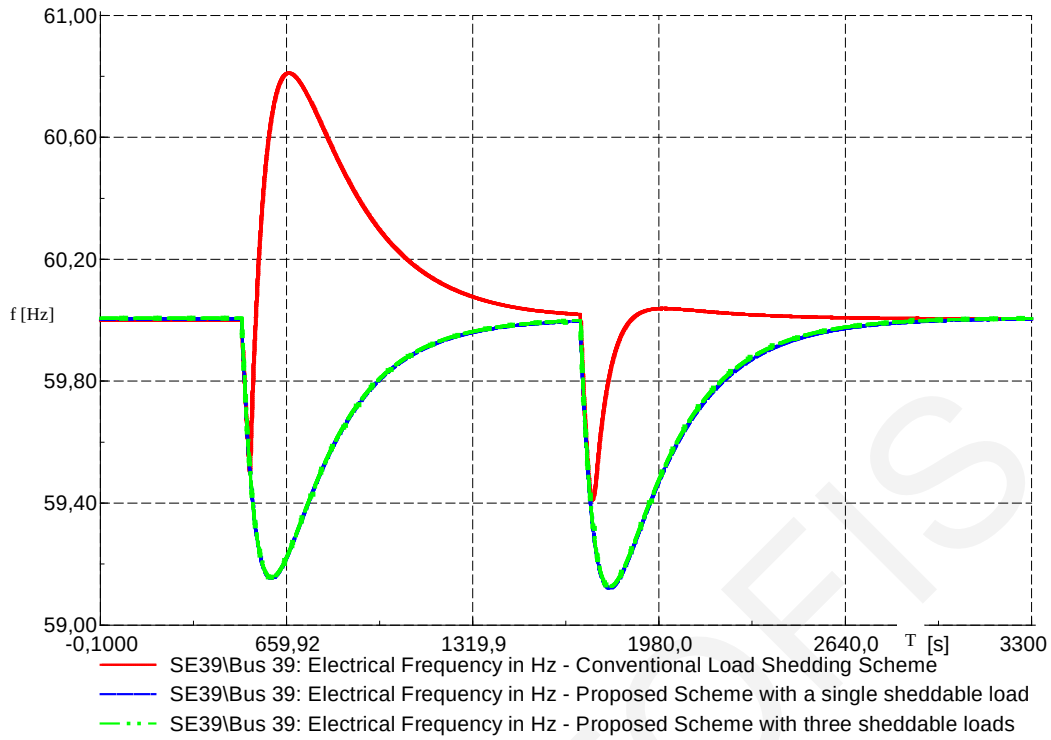

Figure 4-7: Frequency variations of the 39 bus system in the case of: (1) Conventional load shedding (Table II), (2) Proposed load shedding with shedding a single load, (3) Proposed load shedding with three sheddable loads.

Based on Table II, the first three load shedding steps are activated since the frequency response characteristic is maintained above the level of 58.5 Hz.

Furthermore, it is deduced that both schemes maintain the frequency above the critical level of 58.5 Hz, while the proposed scheme achieves the restoration to the steady state conditions about two hundred seconds faster than the conventional scheme. Moreover, the proposed scheme is robust to communication delays up to the level of 1 second because of its adaptive nature. Finally, the proposed scheme provides the capability to tune the learning rate gains of the parameters to be adapted, choosing the optimal tradeoff between the amount of load to be shed and the minimum frequency level. In this case, the learning rates have been chosen to be equal to 0.0085 in order to prevent overshooting, since the system operation for frequencies above the level of 59.4 Hz is a usual and acceptable operating condition (see Table I).

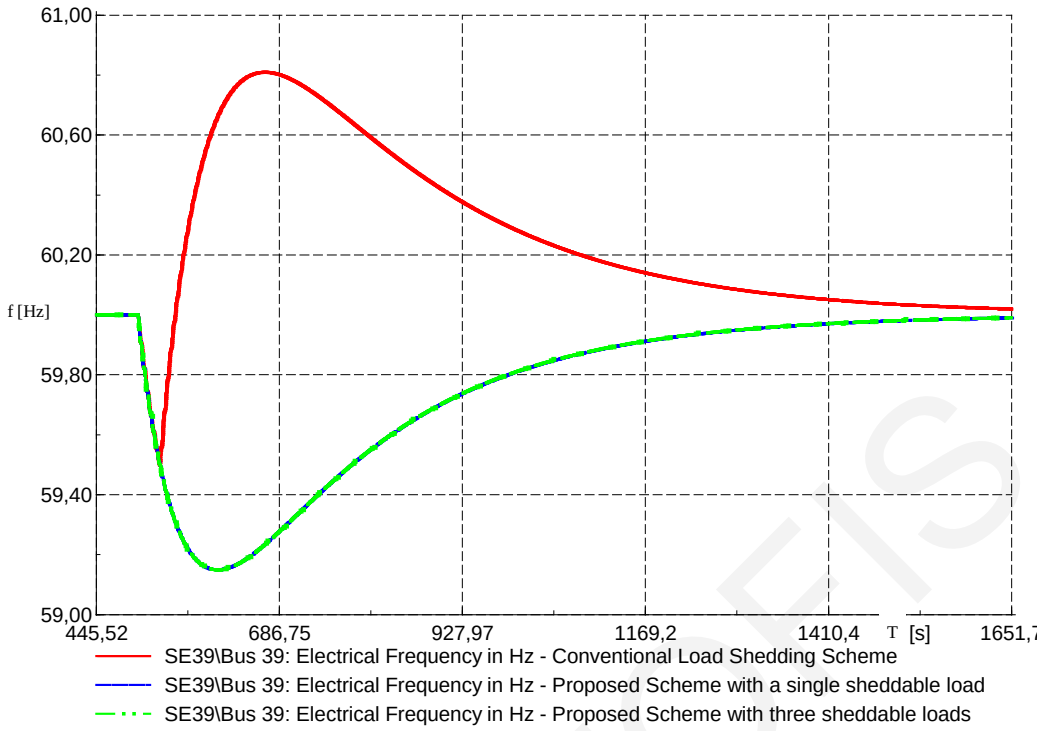

Figure 4-8: Zoomed frequency variations of Figure 5 during the first load disturbance

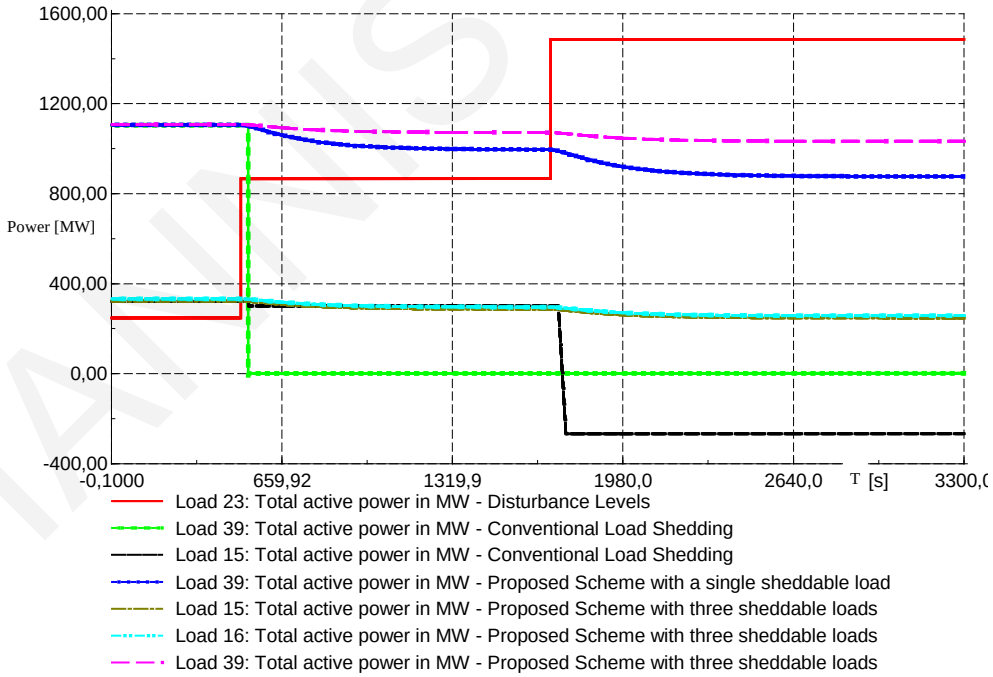

Figure 4-9: Load variations in the case of: (1) Conventional load shedding (Table II), (2) Proposed load shedding with shedding a single load, (3) Proposed load shedding with three sheddable loads.

c) Unexpected outage of Generator 9

As another simulation event, an unexpected outage of Generator unit 9 occurs at 500 seconds. The obtained results are presented in Figure 4-10 and Figure 4-11.

It can be deduced from the simulation results that the conventional load shedding scheme performs quite significant amount of over-shedding of about 987 MW. Both schemes maintain the frequency above the critical frequency level of 58.5 Hz. The conventional scheme maintains the frequency significantly above this level due to over-shedding while the proposed scheme ultimately reaches the level of 58.79 Hz.

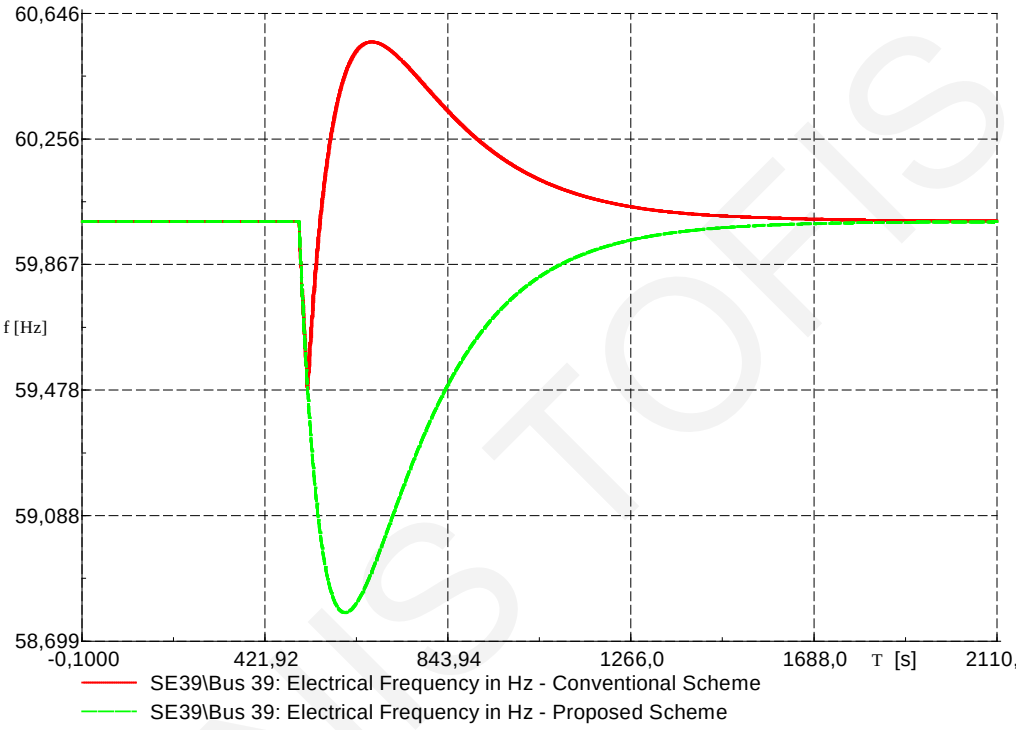

Figure 4-10: Frequency variations in the case of: (1) Conventional load shedding (Table II), (2) Proposed load shedding with shedding a single load for the event of Generator 9 unexpected outage.

d) Short circuit fault on bus 25 of the 39 bus system

In this simulation event a short circuit fault occurring on bus 25 of the 39 bus system at 50 seconds. The fault is cleared 100 ms later by disconnecting all the elements that are connected to this bus, i.e., the transformer, the load and two transmission lines, thus isolating the fault. The simulation results for this load event are presented in Figure 4-11 and Figure 4-12.

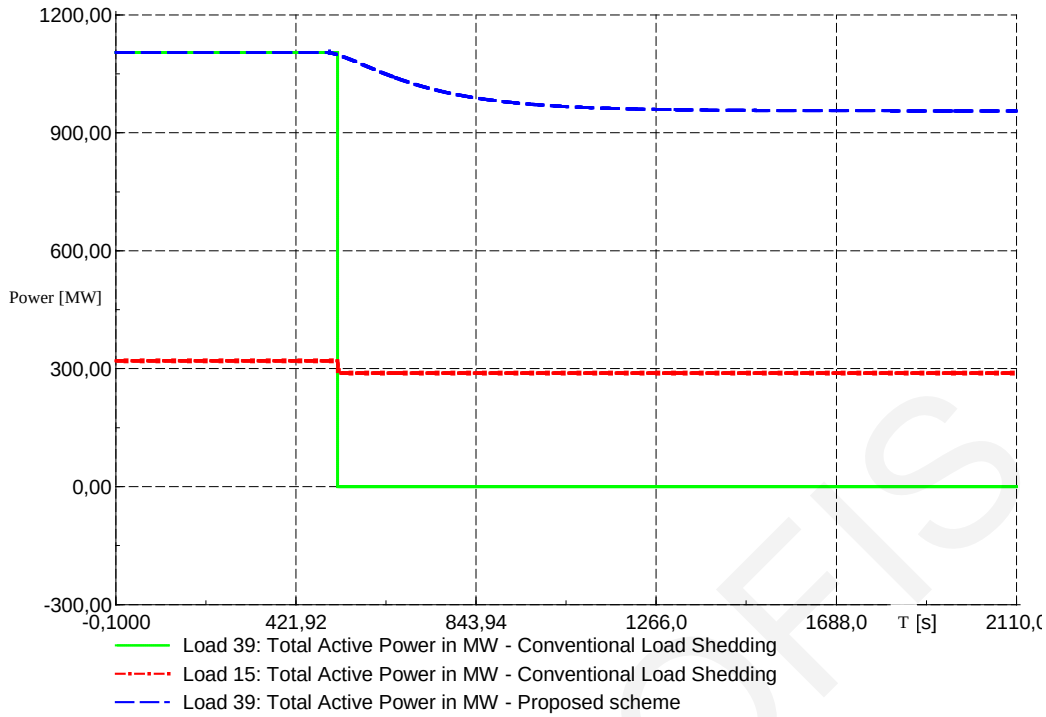

Figure 4-11: Load variations in the case of: (1) Conventional load shedding (Table II), (2) Proposed load shedding with shedding a single load for the event of Generator 9 unexpected outage.

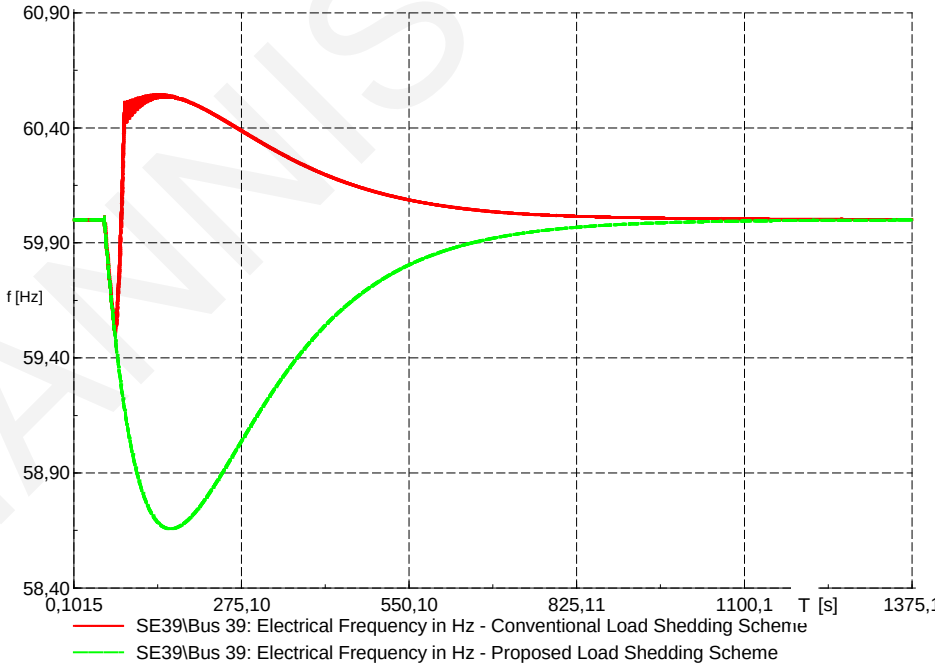

Figure 4-12: Frequency variations in the case of: (1) Conventional load shedding (Table II), (2) Proposed load shedding with shedding a single load for the short circuit event on bus 25.

4.4 Conclusions

In this chapter an adaptive load shedding mechanism was proposed that is robust to load disturbances and maintains the frequency stability of the system. The load shedding scheme is based on a single measurement of the frequency across the power system. Load disturbances as well as functional approximation errors are adaptively bounded while the unknown nonlinearities of the system's swing equation are linearly approximated online, ensuring uniform boundedness and convergence of parameter estimation errors. The performance of the proposed load shedding scheme has been compared to conventional practices and evaluated by simulation results in different dynamic test systems and scenarios. It can be deduced from the simulation results that the proposed scheme achieves the rated frequency levels faster than the conventional scheme, although it sheds significantly less amount of load than the conventional load shedding scheme requires. Furthermore, it is robust to consecutive load disturbances and it is not dependent on the magnitude of the disturbance. In general, the proposed scheme ensures the frequency stability of the system and determines online the appropriate amount of load that should be shed based only on the measurement of frequency across the whole system. This makes it plug and play and system independent, being able to tackle unforeseen disturbance events that have not been experienced in the past.

CHAPTER 5
MINIMUM LOAD SHEDDING BY ANALYTICALLY SOLVING THE SWING EQUATION

5.1 Introduction

As stated in Chapter 2, load shedding is a highly unwanted situation for the electricity consumers, causing significant financial impact. However, it is usually an unavoidable action, taken to prevent the total collapse of the power system. It is essential to minimize the curtailed load, minimizing at the same time the consequences to the customers and the economy. The design of a load shedding scheme is a very challenging, tedious and long term procedure which is usually system specific, requires a large amount of historical data and deep study and understanding of the disturbance events [52], [53]. Conventional and contemporary load shedding techniques fail to prevent over-shedding due to the sequence of control and protection actions that need to be taken step-by-step and the inherent time delays introduced [6]. Conventional load shedding schemes are step-wise processes based on prescheduled load shedding tables that are determined based on a rule of thumb and past experience [60]. These tables indicate the amount of load that should be shed at every step depending on the frequency variation. This chapter provides the minimal amount of load shedding by analytically solving the swing equation.

5.2 Methodology

Based on the swing equation and given the ramp up limit and the rated capacity of each committed generating unit, we find in this chapter the minimum load shedding that ensures that the frequency is always larger from or equal than the operator-chosen minimum frequency level, $f_{\min}^{req}$, that maintains the frequency stability of the system. The proposed scheme is based on the dependence of the electric frequency on the active power as modeled by the swing equation of the power system

$$2Hf(t)\frac{df(t)}{dt} = p_{mp.u.}(t) - p_{ep.u.}(t) - Df(t) \tag{5.1}$$

where:

- H is the total normalized inertia constant for the entire system in per unit-seconds (assumed to be known)
- $f(t)$ is the per unit instantaneous electrical frequency of the center of inertia
- $p_{mp.u.}(t)$ is the per unit mechanical power of the turbines
- $p_{ep.u.}(t)$ is the per unit electrical power output of the generators
- D represents the damping power

As soon as a power deficiency between the mechanical power out of the turbines and the electric power out of the generators of magnitude p_d occurs at time $t=t_0$, the electric frequency starts to decline. In response to such a disturbance (e.g., an unexpected outage of a generator) the governor of each unit increases the produced mechanical power to compensate for the disturbance with a ramp limit rate ρ_i for turbine i. The total ramping rate is a monotonically decreasing piecewise-constant function of time, because as time increases different turbines reach their maximum power output $p_i^{\max}$. Let $t_1 \le \ldots \le t_i \le \ldots \le t_N$, with $t_i = (p_i^{\max} - p_i(t_0))/\rho_i$ denoting the time that generator i out of N generators, reaches its maximum power output and $p_i(t_0)$ the initial mechanical power of turbine i. Let also section i denote the time span between t_i and t_{i-1}. The total ramp rate in section i is $R_i = \sum_{j=i}^{N} \rho_j$ and the disturbance magnitude is denoted by p_d. The total mechanical power for $t \in [t_{i-1}, t_i]$ can be written as:

$$\begin{aligned} p_{mp.u.}(t) &= p_{mp.u.}(t_0) - p_d + \sum_{j=1}^{i-1} R_k \left(t_j - t_{j-1}\right) + R_i \left(t - t_{i-1}\right) \\ &= p_{mp.u.}(t_{i-1}) + R_i \left(t - t_{i-1}\right) \end{aligned} \tag{5.2}$$

Let $f(t^{\min}) = \min_{t \ge t_0} f(t)$, denote the minimum frequency experienced by the system. The optimal amount of load that should be shed, p_{LS}^{OPT}, yields the maximum total demand:

$$p_{ep.u}(t) = p_{ep.u}(t_0) - p_{LS}^{OPT}, \; t > t_0 \tag{5.3}$$

that maintains stability, i.e. $f(t^{\min}) \ge f_{\min}^{req}$. Although this problem is difficult to solve in the general case due to the piecewise linear nature of $p_{mp.u.}(t)$, considering a section-by-section approach with constant load shedding, p_{LS}^{cand}, yields an analytical expression for the frequency of section i, $f_i(t)$. Let $f_i(t_i^{\min}) = \min_{t \ge t_{i-1}} f_i(t)$. The minimum frequency of the system

$f(t^{\min})$ is equal to $f_i\left(t_i^{\min}\right)$ only if $t_i^{\min} \in \left[t_{i-1}, t_i\right]$. This is because $p_{mp.u.}(t)$ is a monotonically increasing function of time so that after reaching a frequency minimum, the frequency response will be monotonically increasing. In mathematical terms, the minimum frequency in section *i* is reached at time $t_i^{\min}$ given by:

$$\left.\frac{df(t)}{dt}\right|_{t=t_i^{\min}} = p_{mp.u.}\left(t_{i-1}\right) + R_i\left(t_i^{\min} - t_{i-1}\right) - p_{ep.u.}(t_0) + p_{LS}^{cand} = 0$$
$$\Rightarrow t_i^{\min} = t_{i-1} + \frac{p_{ep.u.}(t_0) - p_{LS}^{cand} - p_{mp.u.}\left(t_{i-1}\right)}{R_i} \tag{5.4}$$

Analytically solving (5.1) for section *i* yields:

$$f_i(t)\frac{df_i(t)}{dt} = \frac{1}{2H}\left(p_{mp.u.}\left(t_{i-1}\right) + R_i\left(t - t_{i-1}\right) - p_{ep.u.}\left(t_0\right) + p_{LS}^{cand}\right) \Rightarrow$$
$$\frac{f_i^2(t)}{2} = \frac{1}{2H}\left(p_{mp.u.}\left(t_{i-1}\right)t + \frac{R_i\left(t - t_{i-1}\right)^2}{2} - \left(p_{ep.u.}\left(t_0\right) - p_{LS}^{cand}\right)t\right) + C_i \tag{5.5}$$

Assuming that at time $t=t_0$ the frequency is at its rated value, i.e., $f\left(t = t_0\right) = 1$p.u., the integration constant C_i is given by:

$$C_i = \frac{f_{i-1}^2\left(t_{i-1}\right)}{2} - \frac{1}{2H}\left(p_{mp.u.}\left(t_{i-1}\right)t_{i-1} - (p_{ep.u.}(t_0) - p_{LS}^{cand})t_{i-1}\right) \tag{5.6}$$

The quantity p_{LS}^{cand} takes values in the interval [0, p_d]. The optimal p_{LS}^{cand}, denoted as p_{LS}^{OPT}, is found using the *bisection method* by repeatedly bisecting the p_{LS}^{cand} interval and selecting the subinterval which ensures that $\min_{t \geq t_0} f\left(t\right) \geq f_{\min}^{req}$, as outlined below. The computational complexity of the proposed scheme is O(*N*log(*1/ε*)), where *ε* is the optimality tolerance.

Algorithm

While $\left|P_{LS}^{\max} - P_{LS}^{\min}\right| \geq \varepsilon$

1. $p_{LS}^{cand} = \left(P_{LS}^{\min} + P_{LS}^{\max}\right)/2$
2. for *i*=1…N
   Calculate $t_i^{\min}$ from (5.4)
   if $t_i^{\min} \in [t_{i-1}, t_i]$ then break;
3. Solve (5.5) for $f_i\left(t_i^{\min}\right)$ using $t_{\min}$
4. If $f_i\left(t_i^{\min}\right) \geq f_{\min}^{req}$ then $P_{LS}^{\max} = p_{LS}^{cand}$; $p_{LS}^{OPT} = p_{LS}^{cand}$
   else $P_{LS}^{\min} = p_{LS}^{cand}$

5.3 Case Study

The IEEE three generator nine bus test system has been employed to demonstrate the method [4]. It is assumed that $f_{\min}^{req}$ is 48.5 Hz. The ramp rates of generators 1, 2 and 3 are 15, 10 and 8 MW/min respectively. The load disturbance P_d is equal to 50 MW and it is assumed that it can be exactly met.

Figure 5-1 depicts the response of the three schemes that are examined: (a) the proposed scheme (b) the conventional load shedding scheme used in practice by several transmission operators [3], and (c) an "ideal" conventional load shedding scheme with optimally designed steps to exactly achieve $f_{\min}^{req}$.

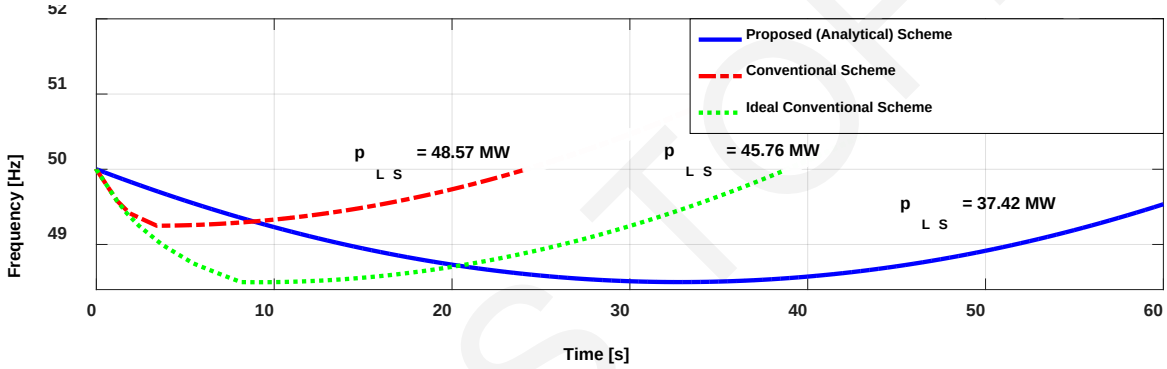

Figure 5-1. Response of proposed and conventional load shedding schemes with a 50 MW disturbance and respective required load shedding amount (p_{LS}).

The number of steps of the "ideal" scheme has been fixed in advance and the load to be shed per each step has been determined on a trial and error basis.

It is deduced that the proposed scheme outperforms the conventional one even when an ideal conventional scheme is used. The proposed scheme achieves a load shedding of 37.42 MW compared to 45.76 MW required by the "ideal" conventional scheme. The extra load shedding required for the conventional load shedding is due to the step wise nature of the scheme and the elapsed time between the decisions (consecutive steps). This time is not present in the proposed scheme since the decision is taken as soon as the disturbance occurs and requires only milliseconds to provide a solution.

It should be stressed that the extra load shedding amount of 8.34 MW (or 22.2% extra load shedding) is the minimum difference that can be achieved between the two schemes. This is because in actual practice there exists a time trip delay associated to each step of the conventional load shedding (from the instant of the load shedding decision to the opening of

the circuit breakers). Further, the steps of the conventional load shedding scheme are chosen in a very conservative manner ending up in over-shedding which is accumulated to the above determined quantity and is presented in Figure 5-1 with the red color. In this scheme the required load shedding amount is 48.57 MW, 11.15 MW or 30% more than the load shedding of the proposed scheme.

The proposed scheme outperforms the "Plug and Play" scheme proposed in Chapter 4, as far as the amount of required UFLS amount is concerned for maintaining the frequency stability. Especially, for a disturbance of magnitude 80 MW, the proposed scheme does not activate the UFLS at all, while the "Plug and Play" scheme presented in Chapter 4 requires a load shedding amount of 70 MW. This is due to the fact that the proposed scheme does not only provide the optimal UFLS amount, but it prevents the triggering of the phenomenon if this is not needed, "predicting" if the governors' actions are able to accommodate the extra loading of the system.

5.4 Conclusions

In this chapter a new analytical load shedding scheme is presented that maintains the frequency stability of the grid while achieving a minimal load shedding. The proposed scheme is computationally lightweight and does not present any processing delays due to its analytical nature that allows for a very fast solution. The proposed scheme outperforms all the previously proposed UFLS schemes in terms of the execution time as well as the amount of load to be shed in order to maintain the frequency stability of the power system. The performance of the scheme is dependent on the communication infrastructure that the commands are sent through. The larger the communication delays are, the larger is the amount of load to be shed. Chapter 6 quantifies this behavior and examines all the components of the total response time of the proposed load shedding scheme.

CHAPTER 6
THE EFFECT OF TIME DELAYS ON THE UNDER FREQUENCY LOAD SHEDDING

6.1 Introduction

Time delays inevitably play a detrimental role to the performance of UFLS schemes. In fact, the frequency reserves are classified into primary, secondary and tertiary according to their action times from the beginning of a disturbance [61]. In conventional UFLS schemes the time delay and frequency settings as well as the amount of load to be shed are constant and independent from the magnitude of the disturbance, varying from 0.1 to 1.5 seconds, depending on the capabilities of the underfrequency relays, the circuit breakers and the system operator configurations [6]. Chapter 5 introduced an innovative UFLS that performs the total load shedding amount in a single step, assuming zeros time-delays. In [62], two load shedding schemes are proposed that take into account the time-delays, while the time-delay settings are adaptively determined based on the disturbance magnitude. Time delays occurring on different power network topologies are discussed for different UFLS schemes in [5], indicating that local load shedding is usually preferable since it minimizes communication delays. The paper also deals with the intentional time delays and explains how these are applied based on the application, the step size and the magnitude of the disturbance.

The total response time of an UFLS scheme is disaggregated into the following time delay components:

1. **Processing delay** is the computational time needed to decide about the amount of UFLS to be performed; depending on the computational burden of the algorithm used this delay can considerably vary (from some tens of μs to a couple of s).
2. **Propagation delay** is the time needed for the command signal to be propagated from the control center to the underfrequency relay (up to 0.13 ms).
3. **Transmission delay** is the time for the data packet of the command signal to be sent based on the data rate of the communication channel (~10μs).
4. **Circuit breaker delay** is the time needed to physically disconnect the load (up to 300 ms)

5. **Relay time delay** is configurable time set from the operator (up to 1.5s)
6. **Inter-step delay of the conventional scheme** is the time between successive steps of the conventional UFLS scheme (of the order of seconds).

Although the processing, propagation, transmission and circuit breaker delays are unavoidable, the relay time and inter-step delays can be configured from the power system operator. Also note that the latter two are the dominant delay components. There is a gap in the literature in regard to the quantification of the effects of time delays on the required load shedding amount.

Failing to take the effect of time-delays into account, challenges the robustness of the UFLS scheme and jeopardizes the frequency stability of the power system. This Chapter expands the analysis of Chapter 5, evaluating the effects of the time delays on the UFLS schemes based on the equivalent swing equation of the power system, quantifying the "penalty" that should be paid in terms of the extra load shedding amount as a function of the time delay of the underfrequency relays. It also demonstrates the existence of a certain time threshold which constitutes a point of no return. If this time threshold is exceeded, then a complete blackout cannot be prevented by any means.

6.2 Methodology

It is assumed that the power system frequency response is adequately represented from the equivalent swing equation of the power system with negligible damping power.

$$2Hf(t)\frac{df(t)}{dt} = p_{mp.u.}(t) - p_{ep.u.}(t) \tag{6.1}$$

where:

- H is the total normalized inertia constant for the entire system in per unit-seconds (assumed to be known)
- $f(t)$ is the per unit instantaneous electrical frequency of the center of inertia
- $p_{mp.u.}(t)$ is the per unit mechanical power of the turbines
- $p_{ep.u.}(t)$ is the per unit electrical power output of the generators

It is assumed that as soon as a disturbance is introduced at time $t=t_0$, the N generating units

of the power system start to ramp up at maximum rate. Unit *j* ramps up from an initial value $p_j(t_0)$ to its maximum power output $p_j^{\max}$ with a ramping rate, ρ_j, (ramp up limit), such that saturation occurs at $t_j = (p_j^{\max} - p_j(t_0))/\rho_j + t_0$. Without loss of generality it is further assumed that $t_0 \le t_1 ... \le t_N$, such that the total ramping rate for time section *i*, $t \in [t_{i-1}, t_i), i = 1,...,N$, is constant and equal to $R_i = \sum_{j=i}^{N} \rho_j$. It is further assumed that the system experiences steady state conditions at rated frequency levels before the occurrence of the disturbance. The quantity $p_{LS}^{cand}(T_d)$ indicates the candidate load shedding amount that is performed at time $t=T_d>t_0$. For the whole spectrum of potential load disturbances, the minimum time of each section of the frequency characteristic is given by [2]

$$t_i^{\min} = t_{i-1} + \frac{p_{ep.u.}(t_0) - p_{LS}^{cand}(t_d) - p_{mp.u.}(t_{i-1})}{R_i} \tag{6.2}$$

while the solution of the swing equation at each section is

$$\begin{aligned} f_i^2(t) = {} & H^{-1}\left(p_{mp.u.}(t_{i-1})t + R_i(t - t_{i-1})^2\right) \\ & - 2tH^{-1}\left(p_{ep.u.}(t_0) - p_{LS}(T_d)\right) + C_i \end{aligned} \tag{6.3}$$

where C_i is the integration constant given by [63]

$$C_i = 0.5\left(f_{i-1}^2(t_{i-1}) - H^{-1}\left(p_{mp.u.}(t_{i-1})t_{i-1} - \left(p_{ep.u.}(t_0) - p_{LS}(T_d)\right)t_{i-1}\right)\right) \tag{6.4}$$

Finally, $p_{LS}(T_d)$ is the load shedding amount applied at time T_d with a time delay $T_d - t_0$ in (6.1) and (6.2) and is given by the following expression

$$p_{LS}(T_d) = \begin{cases} 0, & t < T_d \\ p_{LS}^{cand}, & t \ge T_d \end{cases}$$

where the candidate load shedding amount $p_{LS}^{cand}(T_d)$ is employed in a bisection method to find the minimal load shedding amount, denoted as p_{LS}^{MIN}, for each candidate disturbance p_d and time delay $T_d - t_0$. This is achieved by repeatedly bisecting the p_{LS}^{cand} interval and selecting the subinterval which ensures that $\min_{t \ge t_0} f(t) \ge f_{\min}^{req}$, where $f_{\min}^{req}$ is the minimum required frequency level as presented in [63].

At first, we define the quantity $p_{d\_NLS}^{\max}$ that indicates the maximum magnitude of p_d that can be accommodated from the system without performing any load shedding. In other words,

$p_{d\_NLS}^{\max}$ indicates the maximum disturbance magnitude that maintains the frequency stability of the power system, i.e., $p_{d\_NLS}^{\max} = \sup_{p_d}\left(\min_{t\geq t_0} f(t) \geq f_{\min}^{req}\right)$.

Algorithm I scans the full range of the potential time delays T_d and for a certain load disturbance magnitude p_d it determines the minimal load shedding amount $p_{LS}^{MIN}(T_d; p_d)$ associated with this combination that ensures the frequency stability of the power system. In this case, the time is divided into N+1 sections, since the section that the load shedding is applied is divided into two, at time T_d. At time T_d the frequency characteristic experiences another discontinuity which is treated as the time that a new section starts.

Algorithm I

For time delay T_d *: 0 : 3 sec*

Calculate $f(T_d)$ from (6.3) and $C(T_d)$ from (6.4)

While $\left|P_{LS}^{u} - P_{LS}^{l}\right| \leq \varepsilon$

$p_{LS}(T_d) = \dfrac{\left(P_{LS}^{l} + P_{LS}^{u}\right)}{2}$

for i=1…N +1

Calculate $t_i^{\min}$ *from* (6.2)

if $t_i^{\min} \in [t_{i-1}, t_i] \,||\, t_{i-1} \geq T_d$ *then*

break;

Calculate $f_i\left(t_i^{\min}\right)$ *using* $t_i^{\min}$ *from* (6.3)

If $f_i\left(t_i^{\min}\right) \geq f_{\min}^{req}$ *then*

$P_{LS}^{u} = p_{LS}(T_d); p_{LS}^{MIN} = p_{LS}(T_d)$

else $P_{LS}^{l} = p_{LS}^{cand}(T_d)$

6.3 Case Study

In order to illustrate the proposed methodology, the IEEE nine bus, dynamic test system has been employed, having three machines and three loads of 90, 100 and 125 MW [60]. In Figure 6-1, the frequency characteristic of the test system is presented, for load disturbance levels P_d equal to 120, 150, 200 and 300 MW. The lowest allowed frequency level $f_{\min}^{req}$ is chosen equal to 47 Hz and the ramp rates of generators 1, 2 and 3 are 15, 10 and 8 MW/min

respectively. Figure 6-1 provides an overview of the effects of the time delays to the load shedding amount for certain critical load disturbance levels and stresses that for large load disturbances which exceed the half of the total system loading, the Transmission System Operator (TSO) has a margin of less than two seconds in order to exhaust all the load shedding actions. This raises some questions about the current practice in regards to the underfrequency timer settings of the “up to 20 cycles underfrequency (per step) timer setting” adopted in the conventional UFLS schemes [6], since it becomes apparent that in this case and in the name of avoiding overshedding, the TSO jeopardizes having a total blackout. After the expiration of this time margin, the disturbance is cancelled in full, i.e., the amount of load shedding becomes equal to the level of the load disturbance. If the frequency is still above the safety limit of 47 Hz, then the right part of (6.1) becomes equal to zero and the governors pick up in order to restore the frequency back to the nominal levels and prevent the total blackout.

Figure 6-1 also illustrates that for relatively smaller disturbances, the power system can accommodate larger time delays before experiencing a blackout. However, in this case, the "penalty" to be paid for the delays is larger as a percentage. For example, in the case of a disturbance of 120 MW, the minimum required load shedding with zero time delay is about 25 MW. By exhausting the time delays that the system can accommodate for this disturbance level, the minimum required load shedding amount rises to 125MW (five times larger). In the case of relatively larger disturbances (larger than half of the total loading of the system), the system has a limited time to react, which is reduced to less than two seconds while the "penalty" to be paid for the delays is smaller as a percentage. For example, in the case of a disturbance of 300 MW, the minimum required load shedding with zero time delays is about 200 MW. By exhausting the time delays that the system can accommodate for this disturbance level, the minimum required load shedding amount rises to 300 MW, only 50% larger than the required one for zero time delays.

A last observation in regards to Figure 6-1, is the fact that the curves can be divided into two segments; the linear one and the exponentially increasing one. The linear segment provides a penalty rate which indicates the extra amount of load shedding/sec of delay while the point of transition to the exponentially increasing one indicates the "point of no way back" has been reached. This point acts as a warning to the TSO requiring a load shedding amount equal to the disturbance level.

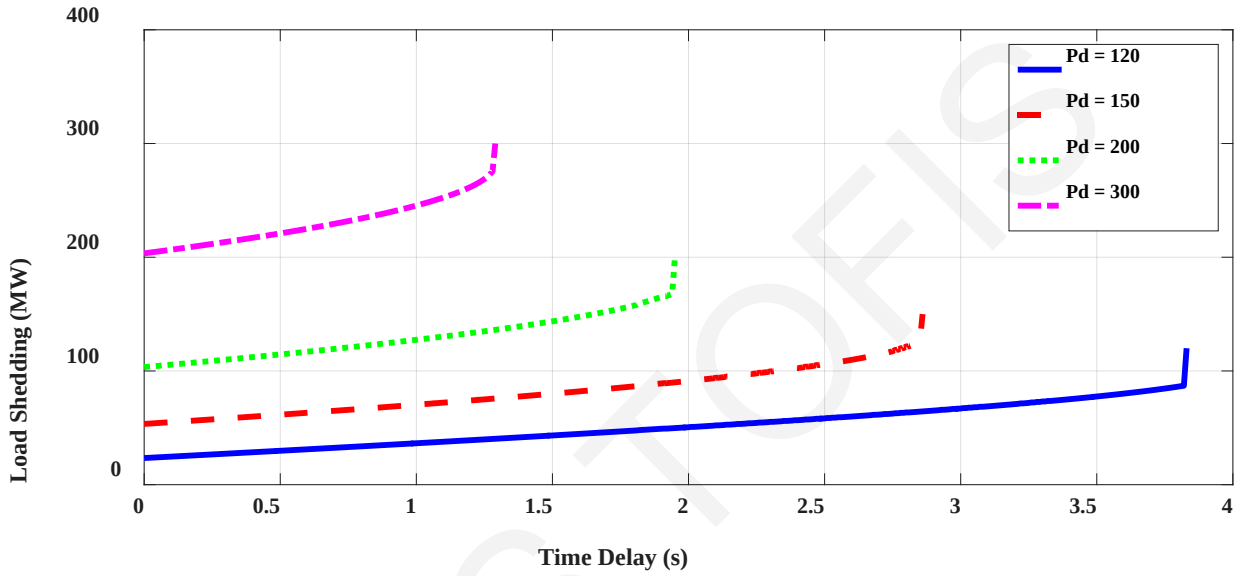

Figure 6-1: Load shedding amount as a function of time delay for certain load diturbances of 120, 150, 200 and 300 MW

Figure 6-2 superimposes planes of certain load disturbance magnitudes. Each plane, presented in different color, depicts a certain level of disturbance. It provides full information regarding the time delay associated with a certain load shedding amount and fills the gaps between the discreet disturbance levels presented in Figure 6-1. One can choose a level of disturbance from the z-axis of the figure (or for convenience from the color map), identify the plane that is associated with the certain disturbance level (color) and finally to find the time delay-amount of load shedding pairs from the projection of the plane to the x and y axes. Figure 6-2 illustrates that the minimum load disturbance that triggers the load shedding is 100 MW.

Figure 6-2 demonstrates the fact that the larger the load disturbance is, the larger is the required minimum load shedding to prevent the blackout and the smaller is the time delay that the power system can accommodate in order to maintain the system in an operational state.

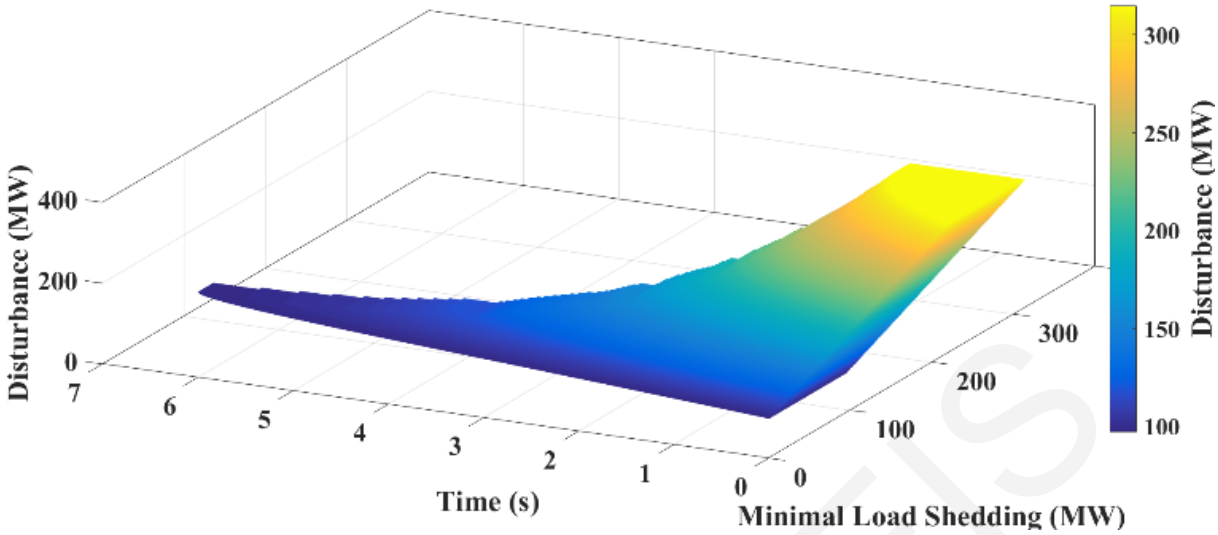

Figure 6-2: Load Shedding Amount as a continius function of time delay and the load disturbance

6.4 Conclusions

This chapter provides an insight regarding the penalty that the TSO has to pay in terms of extra load shedding amount, in the presence of time delays, arising as a result of total response time which includes the unavoidable part of the communication delays and intentional/design trip delay settings. It indicates that, beyond a certain load disturbance level, the introduction of time delay to the load shedding scheme may result in a catastrophic blackout in a “no way back” situation where no amount of load shedding is capable of preventing the blackout. Even in the case that the load disturbance is not that severe, the proposed study provides a valuable tool to the TSO to evaluate the tradeoff between introducing intentional trip delays to the load shedding schemes and undertaking the risk of overshedding in the case of direct trip. It also provides the opportunity to the TSO to asses at any time the occurring total response time of the underfrequency relays by periodically pinging them and thus to end up in a good estimation of the minimal amount of required UFLS for a given disturbance level. Last but not least, it highlights the need for the redesign of the load shedding programs, since this study quantifies the footprint of inter-step delay (as an extra cumulative part/portion of the delay) on the required amount of UFLS. Each load disturbance along with the total response time of each underfrequency relay should be examined individually to determine the amount of load shedding that needs to be performed.

CHAPTER 7
THE IMPACT OF UFLS TO THE LIFETIME OF THE GENERATING UNITS

7.1 Introduction

As discussed in the previous chapters, a large number of blackouts occurred in the past due to an improper amount of load shedding, either because of overshedding or insufficient load shedding [64]. This fact introduced questions regarding the effectiveness and reliability of conventional load shedding schemes and emphasizes the need for the introduction of new schemes that address the large size and complex nature of the smart grid. There is a lot of literature that tackles problems solely associated with UFLS. However, there is no work available in the literature that studies the impact of the underfrequency operation to the sustainability of the generating units. This work models the costs of a certain load shedding amount (which is associated with a certain frequency response) with regards to the loss of lifespan of the steam turbines of the generating units due to mechanical fatigue. This turbine fatigue cost contrasts with the unserved energy cost and in order to obtain the optimal UFLS amount, we consider the minimization of the total underfrequency operating cost as the sum of the turbine fatigue and unserved energy costs.

7.2 System Model and Problem Formulation

7.2.1 System Model

We model the frequency response of the power system by employing the equivalent swing equation without including the effect of damping:

$$2Hf(t)\frac{df(t)}{dt} = p_{mp.u.}(t) - p_{ep.u.}(t) \tag{7.1}$$

where:

- H is the total normalized inertia constant in Joules/VA or per unit-seconds
- $f(t)$ is the per unit instantaneous electrical frequency

- $p_{mp.u.}(t)$ is the total per unit mechanical power of the turbines
- $p_{ep.u.}(t)$ is the total per unit electrical power output of the generators

Equation (7.1) models the frequency response when a severe power deficiency between the mechanical power out of the turbines $p_{mp.u.}(t)$ and the electric power out of the generators $p_{ep.u.}(t)$ occurs. This imbalance is called *load disturbance* p_d, while it occurs at time $t=t_0$, which is the point that the frequency decay is initiated. In response to such a load disturbance (e.g., an unexpected outage of a generator or sudden load increment) the governor of each generating unit adjusts the opening of its valve accordingly, increasing the mechanical power out of the turbine in an effort to compensate for the load disturbance. To ensure frequency stability of the system, the minimum level of the frequency response of the system should be kept above a certain safety limit, $f_{\min}^{req}$, i.e.,

$$f(t) \geq f_{\min}^{req}, \forall t > t_0 \tag{7.2}$$

For each generating unit *i*, the rate of change of the output mechanical power is the ramp limit denoted by ρ_i [63], [65]. The total ramping rate of the system is the sum of the ramping rate of each generating unit *i* which constitutes a linear monotonically decreasing piecewise-constant function of time, due to the fact that different generating units reach their saturation power output point $p_i^{\max}$ as time evolves. In order to provide more intuition about the employed ramp up model, let $t_1 \leq \ldots \leq t_i \leq \ldots \leq t_N$, with $t_i = (p_i^{\max} - p_i(t_0))/\rho_i$ denotes the time that generator *i* reaches its saturation power output point $p_i^{\max}$ and $p_i(t_0)$ the initial mechanical power of generating unit *i* while the time span between t_{i-1} and t_i denotes the section *i*. The total ramp rate is $R_i = \sum_{j=i}^{N} \rho_j$ in section *i* while the total mechanical power out of all the turbines for $t \in [t_{i-1}, t_i]$ is given by:

$$\begin{aligned} p_{mp.u.}(t) &= p_{mp.u.}(t_0) - p_d + \sum_{j=1}^{i-1} R_j (t_j - t_{j-1}) + R_i (t - t_{i-1}) \\ &= p_{mp.u.}(t_{i-1}) + R_i (t - t_{i-1}) \end{aligned} \tag{7.3}$$

In order to obtain a better intuition of the above modelling, consider an example of a power system consisting of three generating units, denoted as G1, G2 and G3 as shown in Figure 7-1. Initially the system is at steady state conditions and thus the frequency remains at the rated level of 50 Hz while the ramp up rate of each generating unit is zero and the power

output is kept constant. At *t*=20 s, a disturbance is introduced into the system and thus the frequency starts to decay; the generating units start to increase their mechanical power with the ramp up limit until they reach their maximum power output while their power output in Figure 7-1c is increased according to the ramp up rates of Figure 7-1b. Note that the generating unit G1 was operating at the maximum power output before the occurrence of the disturbance and thus it does not ramp up and it maintains (the maximum) constant power output.

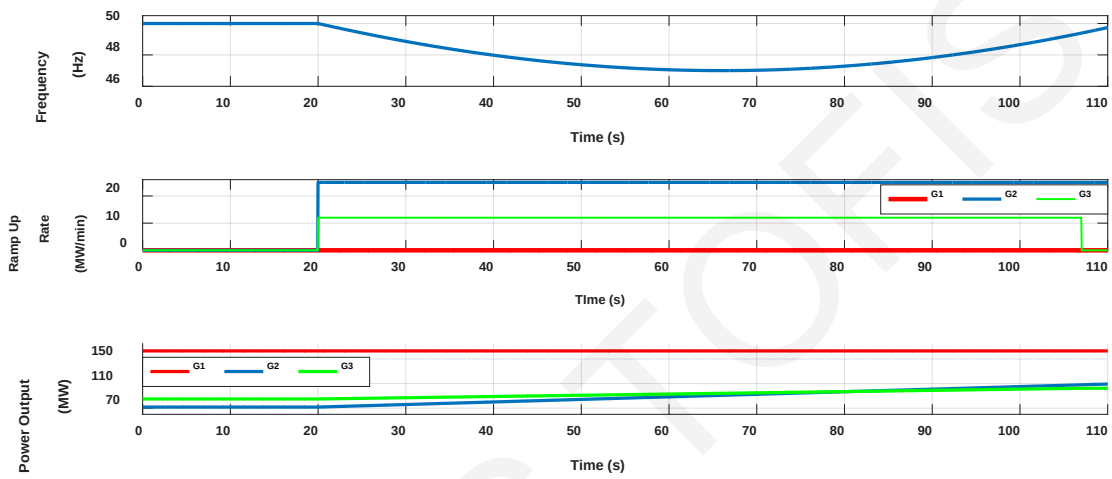

Figure 7-1: (a) Frequency characteristic, (b) Ramp up rate of each generating unit, (c) Power output of each generating unit

7.2.2 Turbine lifespan model

Severe load disturbance events cause substantial underfrequency operation that has a significant impact on the lifespan of generating units. Figure 7-2 illustrates a representative example of the underfrequency and overfrequency time limits for a steam turbine [6]. Figure 7-2 provides the estimated minimum time to cracking for some elements of the bucket structure of the turbines. The elements of the bucket structure that are more likely to crack are the tie wires and the bucket covers.

Although the crack of these elements does not constitute a catastrophic failure per se, it causes behavioral change as far as the bucket structure is concerned. This increases the possibility of shifting the natural frequencies of the bucket structure closer to the power system running frequency that causes fatigue failure to the turbine [6]. Figure 7-2 indicates that the time to damage becomes critical after a 5% departure from the nominal frequency and it is highly recommended to avoid the operation below 47 (57) Hz. It is interesting to underline that the lower frequency limit allows only one second of cumulative operation

while at a zone close to the nominal frequency the curves are flattened, indicating continuous operation without any effect on the turbines' sustainability or lifespan.

Figure 7-2 allows the mathematical definition of the Maximum Operating Time (MOT) function (in minutes) of the turbine for underfrequency operation as

$$MOT = \begin{cases} 10^{-2} & f(t) \le 47 \\ 10^{\frac{f(t)-47.1109}{0.5}} & 47 \le f(t) \le 49.5 \\ \infty & f(t) \ge 49.5 \end{cases} \quad (7.4)$$

Table 7-1 presents estimates of steam-turbine limitations as far as the under-frequency time of operation is concerned. The times shown are cumulative for the life span of a certain unit, i.e., two minutes of operation at 48.2 (58.2) Hz would leave eight minutes of operation at this frequency level, i.e., it would reduce the total lifespan of the generator by 20%.

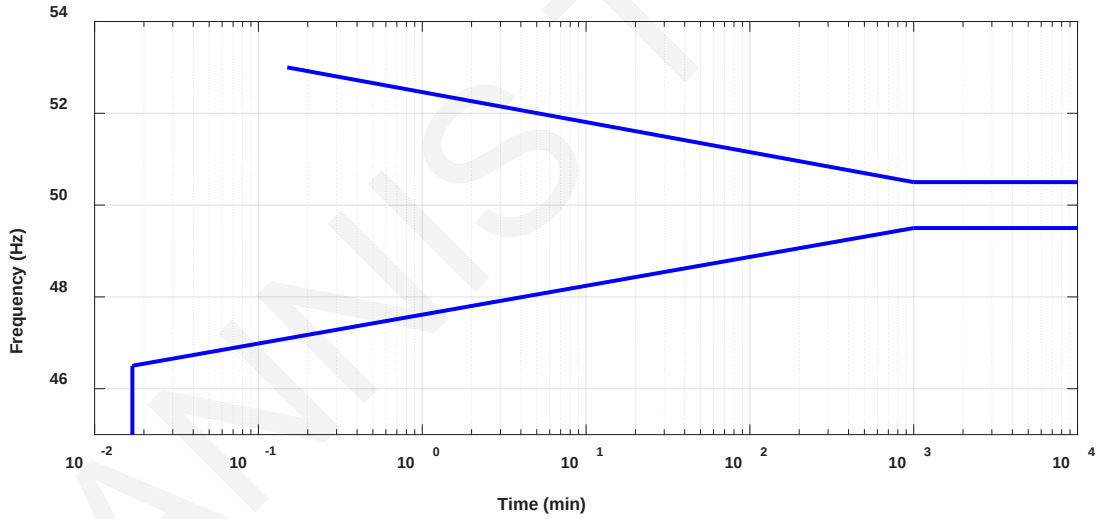

Figure 7-2: Turbine Over/Under-Frequency Limits for a 50Hz operating point [6]

Table 7-1: Cumulative time-frequency limitation for steam-turbines [6]

Frequency at Full Load - Hz	Cumulative Time to Damage
49.4 (59.4)	continuous
48.8 (58.8)	90 minutes
48.2 (58.2)	10 minutes
47.6 (57.6)	1 minute

By converting Figure 7-2 from a semi-logarithmic to a linear scale Figure 7-3 is obtained.

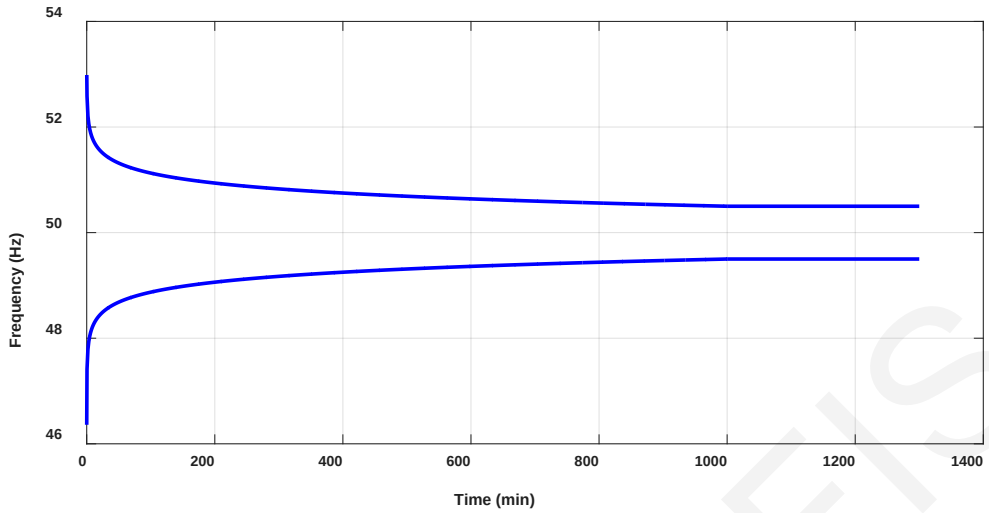

Figure 7-3: Turbine Over/Under-Frequency Limits

7.2.3 Turbine Fatigue Cost (TFC)

For a certain frequency response $f(t)$ there is a certain fatigue cost corresponding to the cumulative turbine lifespan lost due to the underfrequency operation. To obtain this cost, we project $f(t)$ to the frequency limits of the operation of a steam turbine curve (Figure 7-3). The projection function is denoted as the Maximum Operating Time function $MOT(f(t))$ which is a function of the frequency response $f(t)$. A life fraction rule is proposed here in order to determine the degree of mechanical fatigue that each steam turbine is subjected to, given a certain frequency response $f(t)$. More specifically, we split the time of the frequency characteristic into small time intervals Δt_i, in a way that the area of the frequency characteristic is approximated by the sum of vertical strips of width Δt_i, as shown in Figure 7-4. Let a certain time segment Δt_i corresponds to a certain frequency level f_i as is illustrated in the figure.

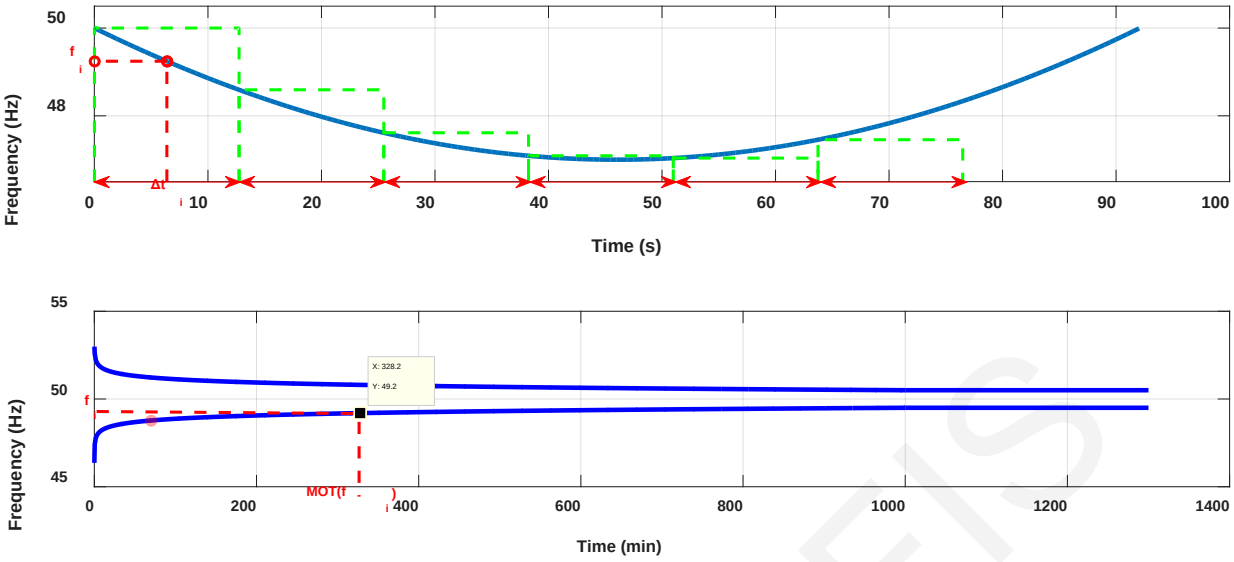

Figure 7-4: Explanation of the proposed life fraction rule

Then, by plugging the frequency level f_i to the *MOT* function (7.4), we obtain the $MOT\left(f_i\right)$, as depicted in the Figure 7-4. By summing all these time segments and by assuming that Δt_i is adequately small, the TFC of the power system with a given frequency response $f\left(t\right)$ is given by the following expression:

Normalized Turbine Fatigue Cost (NTFC) =

$$\lim_{\Delta t_i \to 0} \sum_{i=1}^{\infty} \frac{\Delta t_i}{MOT\left(f_i\left(t\right)\right)} = \int \frac{dt}{MOT\left(f_i\left(t\right)\right)} \tag{7.5}$$

In physical units, *TFC* is given by:

$$\text{TFC} = \int \frac{dt}{\text{T}\left(f\left(t\right)\right)} \times \text{C} \times \text{BC} \tag{7.6}$$

where C is the capacity of the generating units in MWs and BC is the building cost of a generating units per MW.

More intuitively, the integral is employed in order to "catch" the mixture of operation frequencies in the whole-continues underfrequency band, from the point of 49.5 Hz down to the frequency minimum and vice versa (according to the frequency restoration process).

The product of the capacity of generating units and the building cost indicates the cost of building new generating units. This cost is calculated in the literature by employing standard methods from engineering economics [66].

To minimize the turbine fatigue cost one has to perform larger load shedding amount in order to reduce the underfrequency operation time and operate at frequency values closer to the nominal one. On the other hand, performing larger load shedding amount increases the unserved energy which presents a great impact to the whole spectrum of the human activity with a significant economic cost. This cost is quantified in the next section.

7.2.4 Unserved Energy Cost due to excessive UFLS

The Unserved Energy Cost (UEC) is evaluated based on the costs incurred by customers as a consequence of unexpected outages [66]–[69]. UEC is a multivariable function of occurring frequency, duration, magnitude, timing, location, type of customer interrupted, and upfront warning defined as the length of time between notification of possible interruption and the time that the interruption actually occurs [66]. By employing a weighted average of all these factors an expected value of UEC can be determined.

For simplicity, in this chapter we employ a simpler model for estimating the UEC which is the product of the unserved load in kW and the total duration that the load is unserved in hours. Thus, for demonstration purposes of the proposed scheme, we consider in this work an UEC of 1$/kW which is in line with [70].

7.2.5 Problem Formulation

As already discussed in Sections 7.2.3 and 7.2.4 there is a tradeoff between the unserved energy cost and the turbine fatigue cost as the former decreases for increasing and the latter for decreasing the load shedding amount. Hence, to obtain the optimal UFLS amount we consider the minimization of the total underfrequency operating cost as the sum of the turbine fatigue and unserved energy costs. In mathematical terms, the considered optimization problem can be defined as

$$\begin{aligned} &\min_{p_{LS}} TFC(p_{LS}) + UEC(p_{LS}) \\ &s.t.\ (7.1), (7.2), (7.3) \end{aligned}$$

where (7.1) defines the dynamics of the considered problem, (7.2) imposes the frequency safety limit and (7.3) describes the evolution of the mechanical power of the turbines. Before discussing the solution of this optimization problem, we first optimally solve the problem by

neglecting the turbine fatigue cost, which results to the minimum possible load shedding that does not violate the frequency safety limit defined in (7.2).

7.3 Minimum Load Shedding Solution

Based on the equivalent motion equation of the power system and given the load disturbance, the ramp up limit and the rated capacity of each committed generating unit, we find the technical minimum amount of load shedding denoted as p_{LS}^{MIN} that maintains the frequency stability of the power system, i.e., that the instantaneous electrical frequency is always larger than or equal to the operator-chosen minimum frequency level, $f_{\min}^{req}$.

The minimum frequency level of the frequency response of the system is $f\left(t^{\min}\right)=\min_{t\geq t_0} f\left(t\right)$ which occurs when a minimal load shedding p_{LS}^{MIN} is performed and ensures that $f\left(t^{\min}\right)\geq f_{\min}^{req}$.

Due to the fact that R_i is a constant piecewise function of time (is $p_{mp.u.}\left(t\right)$ also is since it includes R_i), by considering a section-by-section approach with constant load shedding candidate quantity, p_{LS}^{cand}, an analytical expression for the frequency of section *i*, $f_i(t)$, is obtained. By letting $f_i\left(t_i^{\min}\right)=\min_{t\geq t_{i-1}} f_i\left(t\right)$, the minimum frequency of the system $f\left(t^{\min}\right)$ is $f_i\left(t_i^{\min}\right)$ given that $t_i^{\min}\in\left[t_{i-1},t_i\right]$ since $p_{mp.u.}\left(t\right)$ is a monotonically increasing function of time. Therefore, the frequency characteristic will be monotonically increasing after reaching a frequency minimum. In order to mathematically express the expression of the minimum frequency in section *i*, $f_i\left(t_i^{\min}\right)$ is calculated in Chapter 5 and provided here again for completeness:

$$\left.\frac{df\left(t\right)}{dt}\right|_{t=t_i^{\min}} = p_{mp.u.}\left(t_{i-1}\right)+R_i\left(t_i^{\min}-t_{i-1}\right)-p_{ep.u.}(t_0)+p_{LS}^{cand}=0$$

$$\Rightarrow t_i^{\min}=t_{i-1}+\frac{p_{ep.u.}(t_0)-p_{LS}^{cand}-p_{mp.u.}\left(t_{i-1}\right)}{R_i} \tag{7.7}$$

Solving the differential equation (7.1) for section i yields $f_i\left(t\right)$:

$$f_i(t)\frac{df_i(t)}{dt}=\frac{1}{2H}\left(p_{mp.u.}(t_{i-1})+R_i(t-t_{i-1})-p_{ep.u.}(t_0)+p_{LS}^{cand}\right)\Rightarrow$$
$$\frac{f_i^2(t)}{2}=\frac{1}{2H}\left(p_{mp.u.}(t_{i-1})t+\frac{R_i(t-t_{i-1})^2}{2}-\left(p_{ep.u.}(t_0)+p_{LS}^{cand}\right)t\right)+C_i \quad (7.8)$$

The integration constant C_i is given by (7.9), taking into account that the initial conditions prior to the introduction of the disturbance, i.e., prior to the time $t=t_0$, are known.

$$C_i=\frac{f_{i-1}^2(t_{i-1})}{2}-\frac{1}{2H}\left(p_{mp.u.}(t_{i-1})t_{i-1}-(p_{ep.u.}(t_0)-p_{LS}^{cand})t_{i-1}\right) \quad (7.9)$$

The load shedding candidate quantity p_{LS}^{cand} takes values between 0 and p_d. The technical minimum p_{LS}^{cand}, denoted as p_{LS}^{MIN}, is found by employing the bisection method in order to ensure $\min_{t\geq t_0} f(t)\geq f_{\min}^{req}$.

The minimum frequency of the frequency characteristic $f_i^{\min}(p_{LS})=\min_t f_i(t,p_{LS})$ is a monotonically increasing function of the load shedding p_{LS} i.e., the more load shedding is performed, the higher is the value of $f_i^{\min}(p_{LS})$. As a result, we can employ the bisection method to find the minimum required load shedding amount that ensures the operational state of the power system. The monotonicity can be intuitively deduced from Figure 7-5.

To mathematically prove this monotonicity result, we prove that $f_{1,i}(t,p_{LS_1})<f_{2,i}(t,p_{LS_2}),\forall t$, when $p_{LS_1}<p_{LS_2}$; this further implies that $f_{1,i}^{\min}(p_{LS_1})<f_{2,i}^{\min}(p_{LS_2})$, because at time $t_2^{\min}$ it is true that $f_{1,i}(t_2^{\min},p_{LS_1})<f_{2,i}(t_2^{\min},p_{LS_2})$. To prove that $f_{1,i}(t,p_{LS_1})<f_{2,i}(t,p_{LS_2}),\forall t$ for $p_{LS_1}<p_{LS_2}$ the induction method is employed for different segments comprised of the following three steps:

Step 1: Check the validity of the monotonicity is proved for the first segment. The frequency response of the power system for a certain amount of load shedding, say p_{LS_1}, is:

$$f_{1,i}^2(t)=\frac{1}{H}\left(p_{mp.u.}(t_{i-1})t+\frac{R_i(t-t_{i-1})^2}{2}-\left(p_{ep.u.}(t_0)-p_{LS_1}\right)t\right)+$$
$$f_{1,i-1}^2(t_{i-1})-\frac{1}{H}\left(p_{mp.u.}(t_{i-1})t_{i-1}-(p_{ep.u.}(t_0)-p_{LS_1})t_{i-1}\right)$$

The frequency response of the power system for another amount of load shedding, say p_{LS_2} is:

$$f_{2,i}^2(t) = \frac{1}{H}\left(p_{mp.u.}(t_{i-1})t + \frac{R_i(t-t_{i-1})^2}{2} - \left(p_{ep.u.}(t_0) - p_{LS_2}\right)t \right) +$$

$$f_{2,i-1}^2(t_{i-1}) - \frac{1}{H}\left(p_{mp.u.}(t_{i-1})t_{i-1} - (p_{ep.u.}(t_0) - p_{LS_2})t_{i-1} \right)$$

It is true that $f_{1,0}^2(t_0) = f_{2,0}^2(t_0)$ at time $t=t_0$. Upon removing equal terms we obtain the desired result $f_{1,1}(t) < f_{2,1}(t),\ t_0 \le t \le t_1$, since for the remaining terms it is true that $\frac{1}{H}P_{LS_1}(t-t_0) > \frac{1}{H}P_{LS_2}(t-t_0)$.

Step 2: Assume that the result is true for segment i-1, i.e., $f_{1,i-1}(t) < f_{2,i-1}(t), t_{i-2} \le t \le t_{i-1}$.

Step 3: Prove the result for segment *i*, i.e. $f_{1,i}(t) < f_{2,i}(t), t_{i-1} \le t \le t_i$. Following a similar procedure to Step 1 and removing equal terms yields $f_{1,\mathrm{i-i}}^2(t_{i-1}) + \frac{1}{H}P_{LS_1}(t-t_{i-1}) < f_{2,\mathrm{i-i}}^2(t_{i-1}) + \frac{1}{H}P_{LS_2}(t-t_{i-1})$ since:

a. $f_{1,i-1}(t_{i-1}) < f_{2,i-1}(t_{i-1})$, from the assumption made.

b. $\frac{1}{H}P_{LS_1}(t-t_{i-1}) < \frac{1}{H}P_{LS_2}(t-t_{i-1})$ because $P_{LS_1} < P_{LS_2}$

Hence it is true that $f_{1,\mathrm{i}}(t) < f_{2,\mathrm{i}}(t),\ t_{i-1} \le t \le t_i$.

This completes the proof that $f_{1,\mathrm{i}}(t) < f_{2,\mathrm{i}}(t),\ t_{i-1} \le t \le t_i, i = 1,...,N$ for $P_{LS_1} < P_{LS_2}$.

The algorithm of the methodology was developed in Chapter 5 and is provided below again for completeness. It is noted that the computational complexity of the proposed scheme is O(Nlog(1/ε)) which is proportional to the number of the generation units *N* and inverse proportional to the logarithm of *ε*, the optimality tolerance.

Although the estimation of the p_{LS}^{MIN} minimizes the amount of load to be shed in order to ensure the frequency stability of the power system, it causes the maximum mechanical fatigue to the generating units and especially to the steam turbines, due to the extended (maximum) underfrequency operation distributed in the whole allowed underfrequency band.

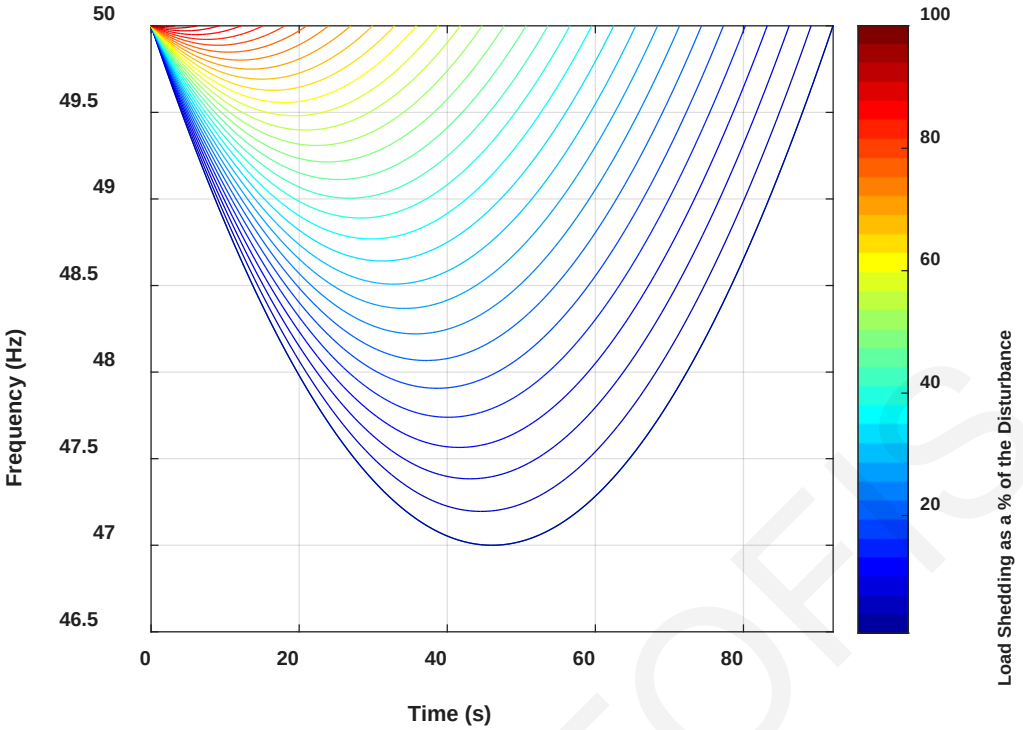

Figure 7-5: Frequency as a function of the minimal load shedding amount

Algorithm 1

While $\left|P_{LS}^{\max}-P_{LS}^{\min}\right|\le\varepsilon$

1. $p_{LS}^{cand}=\left(P_{LS}^{\min}+P_{LS}^{\max}\right)/2$
2. for i=1…N
   Calculate $t_i^{\min}$ from (7.4)
   if $t_i^{\min}\in\left[t_{i-1},t_i\right]$ then
   break;
3. Solve (7.5) for $f_i\left(t_i^{\min}\right)$ using $t_{\min}$
4. If $f_i\left(t_i^{\min}\right)\ge f_{\min}^{req}$ then $P_{LS}^{\max}=p_{LS}^{cand}$; $p_{LS}^{MIN}=p_{LS}^{cand}$
   else $P_{LS}^{\min}=p_{LS}^{cand}$

End

7.4 Optimal UFLS amount

Starting from the technical minimum amount of load shedding p_{LS}^{MIN} that was determined before, we find the amount of load shedding that is optimal from the economical point of view, in terms of the sustainability and lifetime span of the generating units (by taking into account the accumulated mechanical fatigue that the machines experience), due to the underfrequency operation, denoted as p_{LS}^{OPT}.

Although the amount p_{LS}^{MIN} constitutes the theoretical minimum amount of load shedding that can be performed, the duration and level of the underfrequency phenomenon totally exhausts the remaining life of the generating units. More specifically, the NTFC becomes greater than one, indicating permanent failures of the generating units before the frequency is restored back to the nominal level.

The real minimum amount of load shedding that fully exhausts the generating units in terms of the remaining underfrequency operation lifetime and that practically cannot be exceeded is denoted by $p_{LS}^{MIN_{re}}$. Algorithm 2 describes how $p_{LS}^{MIN_{re}}$ can be found; the initial interval of p_{LS}^{cand} that lies between zero and p_{LS}^{MIN} (as found from Algorithm 1), is bisected by selecting the subinterval that ensures that the quantity $\text{NTFC} \geq 1$.

However, $p_{LS}^{MIN_{re}}$ is still not the optimal from an economic viewpoint, as discussed in Section 7.1). This sum constitutes a unimodal function of the load shedding amount [71] due to the fact that TFC is exponentially decreased with the amount of performed load shedding while the UEC is linearly increased with the amount of load shedding ($1/kW). In order to solve this problem, the interval halving method is employed [71], which allocates an initial interval of the potential load shedding amount L_0 and equally divides it in every iteration, deleting exactly one half of the current interval of potential load shedding amount. The algorithm of the methodology is provided below. It is noted that the computational complexity of the proposed scheme is $\mathrm{O}\left(\log\left(p_{LS}^{MIN}/\varepsilon\right)\right)$. The TFC in the steps 6-8 of the algorithm is numerically calculated.

Algorithm 2

Find p_{LS}^{MIN} from Algorithm 1

$P_{LS}^{\min} = 0;\ P_{LS}^{\max} = p_{LS}^{MIN};=0;$

While $\left|P_{LS}^{\max} - P_{LS}^{\min}\right| \le \varepsilon$

$p_{LS}^{cand} = \left(P_{LS}^{\min} + P_{LS}^{\max}\right)/2$

Calculate NTFC $= \int \dfrac{dt}{\text{MOT}\ (f(t))}$

if normalized NTFC $\ge$ 1 then $p_{LS}^{cand} = P_{LS}^{\max}$

else $P_{LS}^{\min} = p_{LS}^{cand};\ p_{LS}^{MIN_{re}} = p_{LS}^{cand}$

End

Algorithm 3

1. Find p_{LS}^{MIN} from Algorithm 1
2. $a = 0;\ b = p_{LS}^{MIN};\ L_0 = [a, b];$

While $(b - a) > \varepsilon$

3. $x_0=(a+b)/2;$
4. $x_1=a+(b-a)/4;$
5. $x_2=a+3*(b-a)/4;$
6. $f_0 = UOC(x_0) + UEC(x_0)$
7. $f_1 = UOC(x_1) + UEC(x_1)$
8. $f_2 = UOC(x_2) + UEC(x_2)$
9. *if* $(f_1 < f_0)$ & $(f_0 < f_2)$ $\quad b = x_0;$

   elseif $(f1 > f_0)$ & $(f_0 > f_2)$ $\quad a = x_0;$

   else $\quad a = x_1;\ b = x_2;$

End

7.5 Case Study

The IEEE three generator nine bus test system has been employed to demonstrate the proposed methodologies [60]. The $f_{\min}^{req}$ is set to 47 Hz according to the Institute of Electrical and Electronics Engineers (IEEE) standards [5] while the ramp rates of generators 1, 2 and 3 are 15, 10 and 8 MW/min respectively. The load disturbance P_d is equal to 90 MW. The UEC is set to \$1/kW [70] while the Building Cost for steam turbines is set to \$1000/kW [72]. The minimal load shedding p_{LS}^{MIN} for this scenario is given by applying Algorithm 1 and is equal to 72.35 MW, while the realistic minimal load shedding $p_{LS}^{MIN_{re}}$ is equal to 74.76 MW.

Figure 7-6 depicts the TFC and UEC and their sum as a function of load shedding amount, starting from p_{LS}^{MIN} (72.35 MW) and scanning all the range of potential load shedding amounts up to the magnitude of the disturbance (90 MW). Figure 7-7 presents TFC and UEC as a function of the frequency.

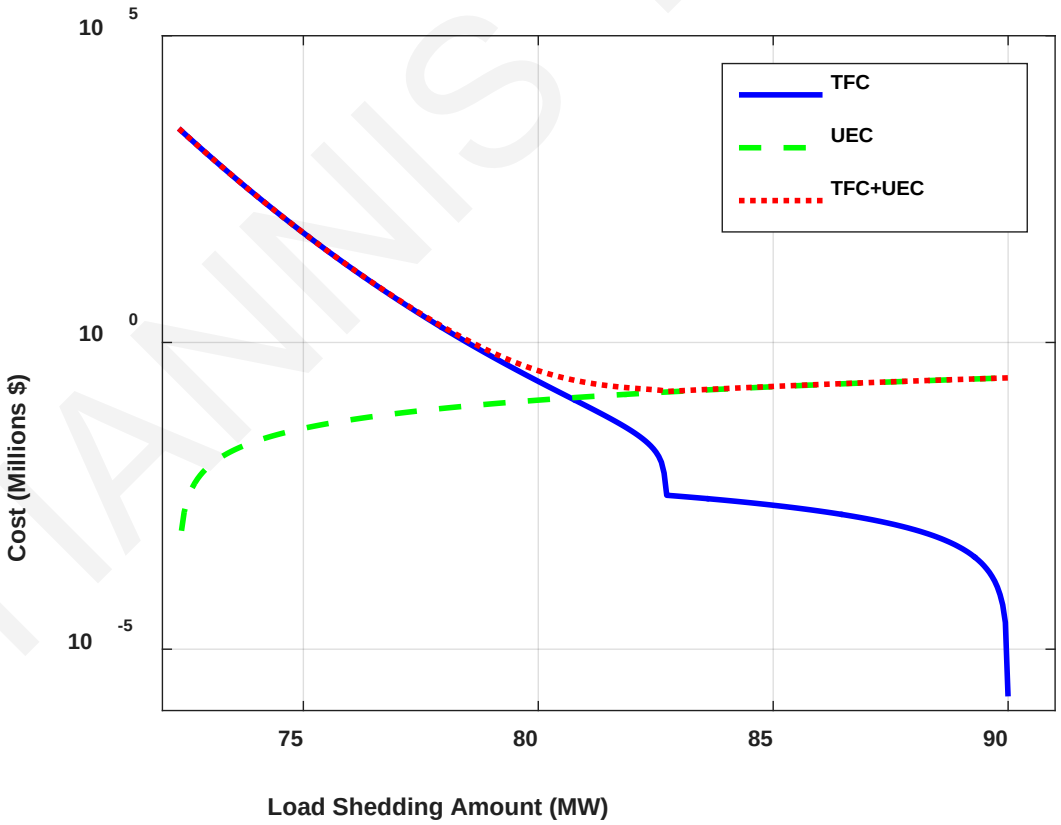

Figure 7-6: TFC, UEC and their sum as a function of load shedding amount

It is shown that the TFC increases logarithmically after exceeding downwards the 49.5 Hz

level and becomes the dominant term of the sum of TFC and UEC. The increase of TFC in the underfrequency band below the level of 49.5 Hz is “not compensated” with the corresponding reduction of the UEC, rendering the cost of operating in that band very expensive and prohibitive from a financial point of view.

Algorithm 2 yields the economically optimal load shedding amount, which is equal to 82.7

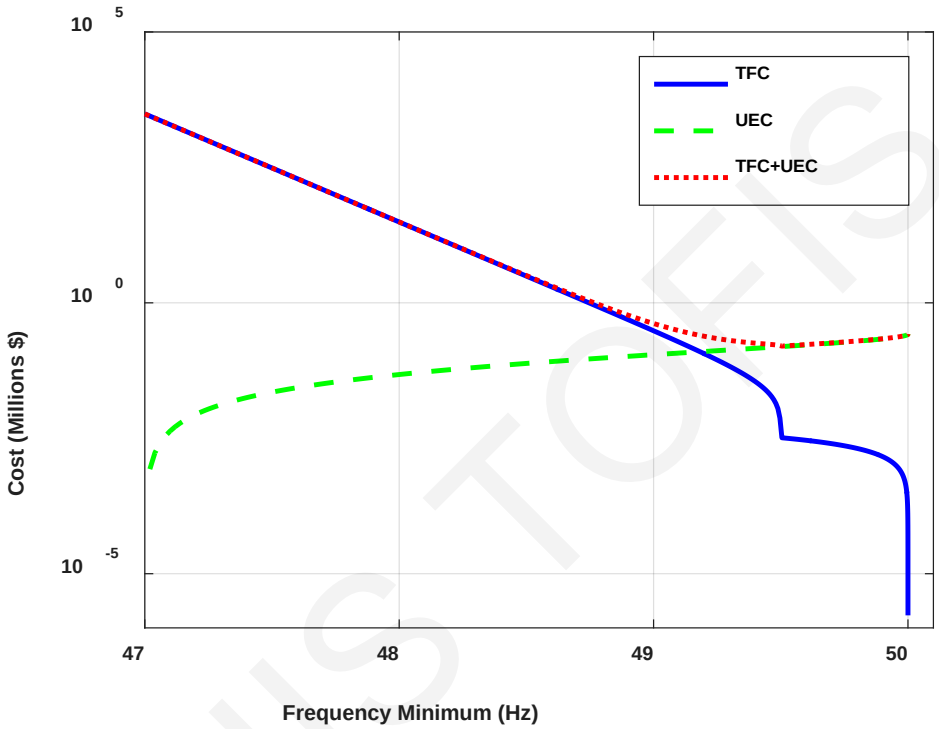

Figure 7-7: TFC, UEC and their sum as a function of the frequency minimum

MW, instead of 72.35 MW which is the minimal amount that guarantees the operating state of the power system.

Figure 7-8 presents the frequency response for the two cases of the minimal and the optimal load shedding amounts. In the first case, the frequency occupies the whole underfrequency spectrum, while in the second, the frequency lies above 49.5 Hz where the operating cost of the generating units in terms of mechanical fatigue is negligible.

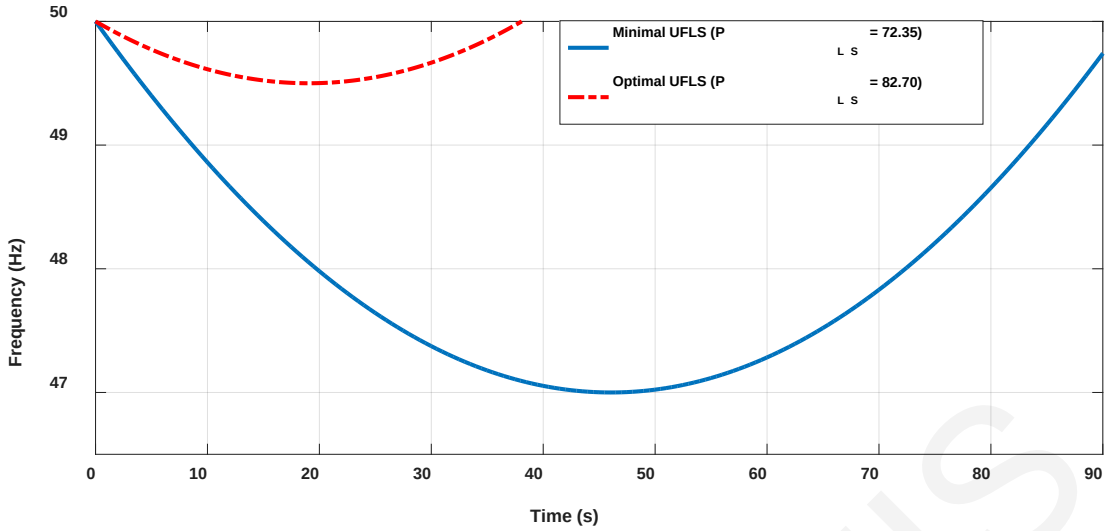

Figure 7-8: Response of the Minimal and the Optimal UFLS cases with a 90 MW disturbance and respective required load shedding amount (P_{LS}).

7.6 Conclusions

In this Chapter, a novel optimal load shedding scheme is presented that takes into account the effect of the mechanical fatigue of the generating units due to their operation in the underfrequency band. This cost, in conjunction with the unserved energy cost, is employed to estimate a new optimal load shedding amount which is significantly larger than the technical minimum amount of load shedding.

The proposed algorithms are of utmost importance for the estimation of the frequency stability margins of the power system. According to the findings of this work, the current building cost of the generating units and the existing energy mix in the energy markets renders the underfrequency operation below 49.5 Hz prohibitive from a financial point of view. However, there is an ever increasing drastic change in the energy mix due to the introduction of the converter based renewables which are not prone to underfrequency operation. This, along with the constant increasing cost of the unserved energy, especially for the critical loads, as well as the constant reduction of the building cost of new generating units, opens new research avenues with regards to the estimation of the future frequency stability margins since the underfrequency operation of the power system is expected to become more flexible.

CHAPTER 8
CONCLUSIONS AND FUTURE WORK

This Ph.D. thesis covers topics of advanced UFLS methods, where different UFLS schemes have been studied covering the whole spectrum of UFLS proposed in academia and industry so far, as discussed in Chapter 2. Conventional UFLS schemes have been thoroughly discussed, from Conventional UFLS schemes, semi-adaptive and fully adaptive schemes. The principles of operation of each scheme have been discussed and their algorithms have been described and illustrated. Also, an introduction was presented regarding the footprint on load shedding on the power system rotating equipment and especially the generating units.

A model based UFLS scheme has been proposed in Chapter 3, based on a simplistic low order frequency response model that includes the essential dynamics. The model has been excited accordingly from load disturbances and identified online, estimating the parameters of the model under different operating conditions. The scheme provides the exact amount of load shedding that should be performed following the occurrence of the disturbance.

In Chapter 4, an intelligent UFLS scheme has been proposed that approximates online the swing equation of the power system based on a single measurement of the frequency across the power system. For a more accurate approximation, the frequency of the center of inertia can be employed, as the frequency of the center of mass of all rotating masses. Load disturbances as well as functional approximation errors are adaptively bounded, while the unknown nonlinearities of the system's swing equation are linearly approximated online, ensuring uniform boundedness and convergence of parameter estimation errors. The performance of the proposed load shedding scheme has been compared to conventional practices and evaluated by simulation results in different dynamic test systems and scenarios. Load disturbance scenarios include the sudden increase of load representing the unexpected connection to the system of a large customer such as an industrial facility or the unexpected outage of a generating unit, as well as the occurrence of a short circuit on a transmission line. It can be deduced from the simulation results that the proposed scheme achieves the rated frequency levels faster than the conventional scheme, although it sheds significantly less amount of load than the conventional load shedding scheme requires. Furthermore, it is robust to consecutive load disturbances and it is not dependent on the magnitude of the disturbance, i.e., it can operate adequately and generalizes well even in the cases of unseen load disturbances. The proposed scheme in Chapter 4 ensures the frequency stability of the

system and determines online the appropriate amount of load that should be shed based only on the measurement of frequency across the whole system. This makes it plug and play and system independent, being able to tackle unforeseen disturbance events that have not been experienced in the past.

In Chapter 5 a new analytical load shedding scheme is presented that maintains the frequency stability of the grid while achieving a minimal UFLS amount. The proposed scheme is computationally lightweight and does not present any inter-step processing delays due to its analytical nature that allows for a very fast solution. The proposed scheme outperforms all the previously proposed UFLS schemes in terms of the execution time as well as the amount of load to be shed in order to maintain the frequency stability of the power system. The minimal amount of UFLS arises due to the fact that the scheme exploits the whole allowed underfrequency band, maximizing the underfrequency operational time.

Chapter 6 provides an insight regarding the penalty that the TSO has to pay in terms of extra load shedding amount, in the presence of time delays, arising as a result of total response time which includes the unavoidable part of the communication delays and intentional/design trip delay settings. It indicates that, beyond a certain load disturbance level, the introduction of time delay to the load shedding scheme may result in a catastrophic blackout in a “no way back” situation where no amount of load shedding is capable of preventing the blackout. Even in the case that the load disturbance is not that severe, the proposed study in Chapter 6, provides a valuable tool for the TSO to evaluate the tradeoff between introducing intentional trip delays to the load shedding schemes and undertaking the risk of overshedding in the case of a direct trip. It also provides the opportunity to the TSO to assess at any time the occurring total response time of the underfrequency relays by periodically pinging them and thus to end up in a good estimation of the minimal amount of required UFLS for a given disturbance level. Last but not least, it highlights the need for the redesign of the load shedding programs, since this study quantifies the footprint of inter-step delay (as an extra cumulative part/portion of the delay) on the required amount of UFLS. Each load disturbance along with the total response time of each underfrequency relay should be examined individually to determine the amount of load shedding that needs to be performed.

In Chapter 7 a novel optimal load shedding scheme is presented that takes into account the effect of the mechanical fatigue of the generating units due to their operation in the underfrequency band. This cost, in conjunction with the unserved energy cost, is employed

to estimate a new optimal load shedding amount which is significantly larger than the technical minimum amount of load shedding.

The proposed algorithms of Chapter 7 are of utmost importance for the estimation of the frequency stability margins of the power system because of the ongoing drastic change in the energy mix due to the introduction of the converter based renewables which are less prone to underfrequency operation. This, along with the constant increasing cost of the unserved energy, especially for the critical loads, as well as the constant reduction of the building cost of new generating units, opens new avenues with regards to the estimation of the future frequency stability margins.

Both adaptive and analytical schemes have been proposed and compared with the conventional scheme and the "ideal UFLS conventional scheme" as a proposed benchmark. In the absence of a benchmark in the area of UFLS, the "ideal UFLS conventional scheme" has been proposed as the scheme that can achieve the best theoretical performance as far as the amount of load to be shed, given a certain load disturbance. This Ph.D. thesis outlines the following important conclusive points:

- Fully adaptive schemes constitute a good candidate for UFLS schemes since they are able to identify and control the system online and achieve operating conditions after network changes and load disturbances of different nature. However, their computational footprint which is associated with the size and the complexity of the power system and thus the number of the approximators employed, renders the scheme prone to delays. These delays have been studied in Chapter 7 and it arises that for a certain power system and a load disturbance, UFLS can achieve the frequency stability of the grid if it is performed in a timely manner, subjected to a maximum delay threshold. Operating in this threshold, the system's operating condition is guaranteed. However, the larger the delay of the UFLS application is, the larger is the amount of load to be shed in order to maintain the frequency stability.
- Analytical schemes have been employed in Chapters 5 and 7, incurring a negligible computational burden due to the analytical nature of the solutions. These schemes require an a priori good estimate of the load disturbance and they can be performed almost instantaneously, minimizing in this way the "penalty" of extra load shedding due to delays. The key feature of these UFLS schemes is the fact that they fully exploit the underfrequency operating band achieving minimum load shedding.

- Although a substantial effort has been made from the academic community in developing UFLS schemes that minimize the amount of load shedding to be performed avoiding the overshedding, the effects of underfrequency operation to the generating units dictated by the UFLS have not been studied. There is a tradeoff between the amount of load shedding and the damage that the generating units are subjected to due to the underfrequency operation which is addressed in Chapter 7. The smaller the amount of load shedding performed, the lower is the frequency minimum of the underfrequency operation, incurring larger damage to the generating units due to subsynchronous resonance.

The proposed schemes are in line with the nowadays industrial practice for managing and performing UFLS centrally, from the control center.

As a future work, we would like to go another step further by introducing the selectivity with regards to transmission system equivalent loads which constitute candidate loads to be shed. More specifically, we would like to illustrate the dependence of the amount of required load shedding with the electric proximity of the candidate load to the disturbance. A systematic technique for optimally selecting candidate load buses for UFLS is going to be proposed. The selection is expected to take place based on the electrical proximity of the load disturbance to the candidate bus that the load shedding will be performed. The electrical proximity will be obtained by employing a routing algorithm to the network graph representation of the power system under consideration.

The proposed methodology is based on a co-simulation process launched separately for each equivalent load *k* as soon as the disturbance occurs, in parallel with the evolving dynamic simulation of the dynamic test system.

Load shedding will be performed for each one of the *N* equivalent loads of the transmission system under consideration and the optimal amount of load shedding for each load *k*, denoted as $p_{LS_k}^{OPT}$, will be calculated using the bisection method, by repeatedly bisecting the candidate amount of load shedding $p_{LS_k}^{cand}$ interval and selecting the subinterval which ensures that the frequency of the center of inertia of the test system $f(t)$ is maintained above the required threshold $f_{\min}^{req}$. The quantity $p_{LS_k}^{cand}$ takes values in the interval $[0, p_{L_k}^{init}]$, where $p_{L_k}^{init}$ is the initial active power of the k^{th} equivalent load.

The final required optimal amount of load shedding p_{LS}^{OPT} which is the actual load shedding that will be performed on the load *k* after the execution of the pre-simulation process, is equal to the minimum $p_{LS_k}^{OPT}, \forall k \in [1, N]$. The computational complexity of the scheme to be proposed is O(*N*log(1/ε)), where ε is the optimality tolerance. The algorithm is outlined below.

Algorithm

For k=1:*N*

While $\left|P_{LS_k}^{\max} - P_{LS_k}^{\min}\right| \geq \varepsilon$

1. $p_{LS_k}^{cand} = \left(P_{LS_k}^{\min} + P_{LS_k}^{\max}\right)/2$
2. If $f(t) \geq f_{\min}^{req}$
   then $P_{LS_k}^{\max} = p_{LS_k}^{cand}; p_{LS_k}^{OPT} = p_{LS_k}^{cand}$

   else $P_{LS_k}^{\min} = p_{LS_k}^{cand}$

End

End

3. $p_{LS}^{OPT} = \min_k \left(p_{LSk}^{OPT}\right)$

The co-simulation process exploits the multi-core processor of the computer and performs the calculation of $p_{LS_k}^{OPT}$ for each *k* in parallel, minimizing in this way the computational time and the associated increased extra amount of load shedding required as the computational delay becomes larger according to the findings of Chapter 6.

In the case of power systems with a large number of load buses, the above methodology requires strong computational power and a large number of processors in parallel in order to compute the outer loop of the algorithm. Because of this, a systematic methodology for selecting the optimal equivalent load where the load shedding will take place, is proposed as a future work. In order to achieve that, a simplified model for the swing dynamics of the system will be considered [73], where the nonlinear Kuramoto oscillator type model for the swing dynamics is linearized [74]. This is a reduced state-space representation of generator dynamics which represents the topological structure of the power network. Two state variables are employed:

- The electric angle

- The electric frequency

This simple second order state space model allows us to come up with an undirected weighted network graph of the power system, whose vertices represent the buses, while the susceptances of the lines connecting the buses will be the edge weights. Afterwards, a routing algorithm will be applied, such as Dijkstra or Distance Vector algorithms, indicating the electrical distance of the disturbance to each one of the load buses.

REFERENCES

[1] "USA power blackout report," 2011. [Online]. Available: http://powerquality.eaton.com/blackouttracker. [Accessed: 11-Jul-2017].

[2] J. A. Laghari, H. Mokhlis, A. H. A. Bakar, and H. Mohamad, "Application of computational intelligence techniques for load shedding in power systems: A review," *Energy Convers. Manag.*, vol. 75, no. August 2003, pp. 130–140, Nov. 2013.

[3] J. Tang, J. Liu, F. Ponci, and A. Monti, "Adaptive load shedding based on combined frequency and voltage stability assessment using synchrophasor measurements," *IEEE Trans. Power Syst.*, vol. 28, no. 2, pp. 2035–2047, May 2013.

[4] H. Bevrani, "Robust Power System Frequency Control," *Renew. Power Gener. IET*, vol. 4, no. 1, p. 225, 2009.

[5] P. Systems, R. Committee, I. Power, and E. Society, "IEEE Std C37.117 - IEEE Guide for the Application of Protective Relays Used for Abnormal Frequency Load Shedding and Restoration," *IEEE Std C37.117-2007*, no. August. pp. c1-43, 2007.

[6] W. C. New, J. Berdy, P. Brown, and L. E. Goff, "Load Shedding, Load Restoration and Generator Protection Using Solid State and Electromechanical Underfrequency Relays," *Gen. Electr. Company, Philadelphia*, 1983.

[7] B. Delfino, S. Massucco, A. Morini, P. Scalera, and F. Silvestro, "Implementation and comparison of different under frequency load-shedding schemes," in *2001 Power Engineering Society Summer Meeting. Conference Proceedings (Cat. No.01CH37262)*, 2001, vol. 1, pp. 307–312 vol.1.

[8] H. Bevrani, G. Ledwich, Z. Y. Dong, and J. J. Ford, "Regional frequency response analysis under normal and emergency conditions," *Electr. Power Syst. Res.*, vol. 79, no. 5, pp. 837–845, May 2009.

[9] M. Sanaye-Pasand and M. Davarpanah, "A new adaptive multidimensioanal load shedding scheme using genetic algorithm," in *Canadian Conference on Electrical and Computer Engineering, 2005.*, 2005, no. May, pp. 1974–1977.

[10] H. Bevrani and T. Hiyama, "Robust load–frequency regulation: A real-time laboratory experiment," *Optim. Control Appl. Methods*, vol. 28, no. 6, pp. 419–433, Nov. 2007.

[11] "UCTE operation handbook. 2009." [Online]. Available: http://www.ucte.org.

[12] P. M. Anderson and M. Mirheydar, "An adaptive method for setting underfrequency load shedding relays," *IEEE Trans. Power Syst.*, vol. 7, no. 2, pp. 647–655, May 1992.

[13] G. Valentis and Q. Berthelot, *Intelligent Automatic Generation Control*. New York,

2011.

[14] “Final Project Report, Impact of increased DFIG wind penetration on power systems and markets.”

[15] E. Development and P. G. Committee, “IEEE Recommended Practice for Functional and Performance Characteristics of Control Systems for Steam Turbine-Generator Units,” 1991.

[16] R. Hooshmand and M. Moazzami, “Optimal design of adaptive under frequency load shedding using artificial neural networks in isolated power system,” *Int. J. Electr. Power Energy Syst.*, vol. 42, no. 1, pp. 220–228, Nov. 2012.

[17] V. V. Terzija, “Adaptive Underfrequency Load Shedding Based on the Magnitude of the Disturbance Estimation,” *IEEE Trans. Power Syst.*, vol. 21, no. 3, pp. 1260–1266, Aug. 2006.

[18] C. T. Hsu, H. J. Chuang, and C. S. Chen, “Adaptive load shedding for an industrial petroleum cogeneration system,” *Expert Syst. Appl.*, vol. 38, no. 11, pp. 13967–13974, 2011.

[19] F. Croce *et al.*, “Operation and management of the electric system for industrial plants: an expert system prototype for load-shedding operator assistance,” *IEEE Trans. Ind. Appl.*, vol. 37, no. 3, pp. 701–708, 2001.

[20] C. Hsu, H.-J. Chuang, and C. Chen, “Artificial Neural Network Based Adaptive Load Shedding for an Industrial Cogeneration Facility,” *Ind. Appl. Soc. Annu. Meet. 2008. IAS ’08. IEEE*, vol. 1, no. 1, pp. 1–8, 2008.

[21] J. A. P. Lopes, Wong Chan Wa, and L. M. Proenca, “Genetic algorithms in the definition of optimal load shedding strategies,” in *PowerTech Budapest 99. Abstract Records. (Cat. No.99EX376)*, 1999, no. 2, p. 154.

[22] M. Moazzami and A. Khodabakhshian, “A new optimal adaptive under frequency load shedding Using Artificial Neural Networks,” in *2010 18th Iranian Conference on Electrical Engineering*, 2010, pp. 824–829.

[23] D. Novosel and R. L. King, “Using artificial neural networks for load shedding to alleviate overloaded lines,” *IEEE Trans. Power Deliv.*, vol. 9, no. 1, pp. 425–433, 1994.

[24] D. Kottick and O. Or, “Neural-networks for predicting the operation of an under-frequency load shedding system,” *IEEE Trans. Power Syst.*, vol. 11, no. 3, pp. 1350–1358, 1996.

[25] M. Djukanovic, D. J. Sobajic, and Y.-H. Pao, “Neural net based determination of generator-shedding requirements in electric power systems,” *IEE Proc. C Gener.*

Transm. Distrib., vol. 139, no. 5, p. 427, 1992.

[26] C.-H. Lee and S.-C. Hsieh, "Lessons learned from the power outages on 29 July and 21 September 1999 in Taiwan," *IEE Proc. - Gener. Transm. Distrib.*, vol. 149, no. 5, p. 543, 2002.

[27] J.-J. Wong, C.-T. Su, C.-S. Liu, and C.-L. Chang, "Study on the 729 blackout in the Taiwan power system," *Int. J. Electr. Power Energy Syst.*, vol. 29, no. 8, pp. 589–599, Oct. 2007.

[28] Chien-Hsing Lee and Shih-Chieh Hsieh, "A technical review of the power outage on July 29, 1999 in Taiwan," in *2001 IEEE Power Engineering Society Winter Meeting. Conference Proceedings (Cat. No.01CH37194)*, 2007, vol. 3, no. C, pp. 1353–1358.

[29] C.-T. Hsu, M.-S. Kang, and C.-S. Chen, "Design of adaptive load shedding by artificial neural networks," *IEE Proc. - Gener. Transm. Distrib.*, vol. 152, no. 3, p. 415, 2005.

[30] M. H. Purnomo, C. A. Patria, and E. Purwanto, "Adaptive load shedding of the power system based on neural network," in *2002 IEEE Region 10 Conference on Computers, Communications, Control and Power Engineering. TENCOM '02. Proceedings.*, 2002, vol. 3, pp. 1778–1781.

[31] M. a. Mitchell, J. a. P. Lopes, J. N. Fidalgo, and J. D. McCalley, "Using a neural network to predict the dynamic frequency response of a power system to an under-frequency load shedding scenario," in *2000 Power Engineering Society Summer Meeting (Cat. No.00CH37134)*, 2000, vol. 1, no. c, pp. 346–351.

[32] E. J. Thalassinakis, E. N. Dialynas, and D. Agoris, "Method Combining ANNs and Monte Carlo Simulation for the Selection of the Load Shedding Protection Strategies in Autonomous Power Systems," *IEEE Trans. Power Syst.*, vol. 21, no. 4, pp. 1574–1582, Nov. 2006.

[33] S. A. M. Javadian, M.-R. Haghifam, S. M. T. Bathaee, and M. Fotuhi Firoozabad, "Adaptive centralized protection scheme for distribution systems with DG using risk analysis for protective devices placement," *Int. J. Electr. Power Energy Syst.*, vol. 44, no. 1, pp. 337–345, Jan. 2013.

[34] S. K. Tso, T. X. Zhu, Q. Y. Zeng, and K. L. Lo, "Investigation of extended fuzzy reasoning and neural classification for load-shedding prediction to prevent voltage instability," *Electr. Power Syst. Res.*, vol. 43, no. 2, pp. 81–87, Nov. 1997.

[35] E. Hobson and G. N. Allen, "Effectiveness of artificial neural networks for first swing stability determination of practical systems," *IEEE Trans. Power Syst.*, vol. 9, no. 2, pp. 1062–1068, May 1994.

[36] A. M. A. Haidar, A. Mohamed, and A. Hussain, “Vulnerability control of large scale interconnected power system using neuro-fuzzy load shedding approach,” *Expert Syst. Appl.*, vol. 37, no. 4, pp. 3171–3176, Apr. 2010.

[37] H. Mokhlis, J. A. Leghari, and A. H. A. Bakar, “A Fuzzy based Load Shedding Scheme for an Islanded Distribution Network,” in *Power and Energy Systems*, 2013, vol. 7, no. AsiaPES, pp. 137–141.

[38] B. F. Rad and M. Abedi, “An optimal load-shedding scheme during contingency situations using meta-heuristics algorithms with application of AHP method,” in *2008 11th International Conference on Optimization of Electrical and Electronic Equipment*, 2008, pp. 167–173.

[39] C.-T. Hsu, M.-S. Kang, and C.-S. Chen, “Design of adaptive load shedding by artificial neural networks,” *IEE Proc. - Gener. Transm. Distrib.*, vol. 152, no. 3, p. 415, 2005.

[40] C.-R. Chen, Wen-Ta Tsai, H.-Y. Chen, Ching-Ying Lee, Chun-Ju Chen, and Hong-Wei Lan, “Optimal load shedding planning with genetic algorithm,” in *2011 IEEE Industry Applications Society Annual Meeting*, 2011, pp. 1–6.

[41] Y.-Y. Hong, M.-C. Hsiao, Y.-R. Chang, Y.-D. Lee, and H.-C. Huang, “Multiscenario Underfrequency Load Shedding in a Microgrid Consisting of Intermittent Renewables,” *IEEE Trans. Power Deliv.*, vol. 28, no. 3, pp. 1610–1617, Jul. 2013.

[42] Y. Y. Hong and P. H. Chen, “Genetic-based underfrequency load shedding in a stand-alone power system considering fuzzy loads,” *IEEE Trans. Power Deliv.*, vol. 27, no. 1, pp. 87–95, 2012.

[43] D. G. Luenberger, “Observing the State of a Linear System,” *IEEE Trans. Mil. Electron.*, vol. 8, no. 2, pp. 74–80, 1964.

[44] J. A. Farrell and M. M. Polycarpou, *Adaptive Approximation Based Control*. Hoboken, NJ, USA: John Wiley & Sons, Inc., 2006.

[45] A. Sánchez, “Modern control systems, 9th edition, Richard C. Dorf and Robert H. Bishop, Prentice-Hall, Upper Saddle River, NJ, 2001, 831 pages, ISBN 0-13-030660-6,” *Int. J. Robust Nonlinear Control*, vol. 16, no. 7, pp. 372–373, May 2006.

[46] L.-R. Chang-Chien, L. N. An, T.-W. Lin, and W.-J. Lee, “Incorporating Demand Response With Spinning Reserve to Realize an Adaptive Frequency Restoration Plan for System Contingencies,” *IEEE Trans. Smart Grid*, vol. 3, no. 3, pp. 1145–1153, Sep. 2012.

[47] A. Saffarian and M. Sanaye-Pasand, “Enhancement of Power System Stability Using Adaptive Combinational Load Shedding Methods,” *IEEE Trans. Power Syst.*, vol. 26,

no. 3, pp. 1010–1020, Aug. 2011.

[48] H. Mokhlis, M. Karimi, A. Shahriari, A. H. Abu Bakar, and J. A. Laghari, "A new under-frequency load shedding scheme for islanded distribution network," *2013 IEEE PES Innov. Smart Grid Technol. Conf. ISGT 2013*, 2013.

[49] H. Mohamad, H. Mokhlis, A. H. A. Bakar, and H. W. Ping, "A review on islanding operation and control for distribution network connected with small hydro power plant," *Renew. Sustain. Energy Rev.*, vol. 15, no. 8, pp. 3952–3962, 2011.

[50] A. J. A. R. DeBlasio, S. Chalmers, *IEEE Recommended Practice for Utility Interface of Photovoltaic (PV) Systems*, vol. 2000, no. 30 January. 2000.

[51] J. Mickey, "Using load resources to meet ancillary service requirements in the ERCOT market: A case study," in *IEEE PES General Meeting*, 2010, pp. 1–2.

[52] U. Rudez and R. Mihalic, "Analysis of Underfrequency Load Shedding Using a Frequency Gradient," *IEEE Trans. Power Deliv.*, vol. 26, no. 2, pp. 565–575, Apr. 2011.

[53] U. Rudez and R. Mihalic, "Monitoring the First Frequency Derivative to Improve Adaptive Underfrequency Load-Shedding Schemes," *IEEE Trans. Power Syst.*, vol. 26, no. 2, pp. 839–846, May 2011.

[54] F. Shokooh *et al.*, "Intelligent load shedding," *IEEE Ind. Appl. Mag.*, vol. 17, no. 2, pp. 44–53, 2011.

[55] J. Jung, Chen-Ching Liu, S. L. Tanimoto, and V. Vittal, "Adaptation in load shedding under vulnerable operating conditions," *IEEE Trans. Power Syst.*, vol. 17, no. 4, pp. 1199–1205, Nov. 2002.

[56] D. Andersson, P. Elmersson, A. Juntti, Z. Gajic, D. Karlsson, and L. Fabiano, "Intelligent load shedding to counteract power system instability," *IEEE/PES Transm. Distrib. Conf. Expo. Lat. Am.*, pp. 570–574, 2004.

[57] J. D. Glover, M. S. Sarma, and T. Overbye, "Power System Analysis and Design, Fifth Edition." p. 848, 2011.

[58] T. Athay, R. Podmore, and S. Virmani, "A Practical Method for the Direct Analysis of Transient Stability," *IEEE Trans. Power Appar. Syst.*, vol. PAS-98, no. 2, pp. 573–584, Mar. 1979.

[59] H. Bevrani and T. Hiyama, "On Load – Frequency Regulation With Time Delays : Design and Real-Time Implementation," *Ieee Trans. Energy Convers.*, vol. 24, no. 1, pp. 292–300, 2009.

[60] A. A. F. Paul M. Anderson, *Power System Control and Stability, 2nd Edition*, 2nd ed. New York: Wiley-IEEE Press.

[61] A. Molina-Garcia, F. Bouffard, and D. S. Kirschen, “Decentralized Demand-Side Contribution to Primary Frequency Control,” *IEEE Trans. Power Syst.*, vol. 26, no. 1, pp. 411–419, Feb. 2011.

[62] M. Sanaye-Pasand and H. Seyedi, “New centralised adaptive load-shedding algorithms to mitigate power system blackouts,” *IET Gener. Transm. Distrib.*, vol. 3, no. 1, pp. 99–114, Jan. 2009.

[63] Y. Tofis, S. Timotheou, and E. Kyriakides, “Minimal Load Shedding Using the Swing Equation,” *IEEE Trans. Power Syst.*, vol. 32, no. 3, pp. 2466–2467, May 2017.

[64] P. Pourbeik, P. S. Kundur, and C. W. Taylor, “The anatomy of a power grid blackout - Root causes and dynamics of recent major blackouts,” *IEEE Power Energy Mag.*, vol. 4, no. 5, pp. 22–29, Sep. 2006.

[65] P. A. Ruiz and P. W. Sauer, “Spinning Contingency Reserve: Economic Value and Demand Functions,” *IEEE Trans. Power Syst.*, vol. 23, no. 3, pp. 1071–1078, Aug. 2008.

[66] E. G. Neudorf *et al.*, “Cost-benefit analysis of power system reliability: two utility case studies,” *IEEE Trans. Power Syst.*, vol. 10, no. 3, pp. 1667–1675, 1995.

[67] G. Wacker and R. Billinton, “Customer cost of electric service interruptions,” *Proc. IEEE*, vol. 77, no. 6, pp. 919–930, Jun. 1989.

[68] R. Billinton and J. Oteng-Adjei, “Utilization of interrupted energy assessment rates in generation and transmission system planning,” *IEEE Trans. Power Syst.*, vol. 6, no. 3, pp. 1245–1253, 1991.

[69] L. Goel and R. Billinton, “A procedure for evaluating interrupted energy assessment rates in an overall electric power system,” *IEEE Trans. Power Syst.*, vol. 6, no. 4, pp. 1396–1403, 1991.

[70] Guodong Liu, Bailu Xiao, M. Starke, O. Ceylan, and K. Tomsovic, “A robust load shedding strategy for microgrid islanding transition,” in *2016 IEEE/PES Transmission and Distribution Conference and Exposition (T&D)*, 2016, vol. 2016–July, pp. 1–5.

[71] S. S. Rao, *Engineering Optimization*. Hoboken, NJ, USA: John Wiley & Sons, Inc., 2009.

[72] “Cost and Performance Characteristics of New Generating Technologies , Annual Energy Outlook 2017 The tables presented below will be incorporated in the Electricity Market Module chapter of the,” 2017. [Online]. Available: https://www.eia.gov/outlooks/aeo/assumptions/pdf/table_8.2.pdf.

[73] J. J. Sanchez-Gasca and J. H. Chow, “Power system reduction to simplify the design

of damping controllers for interarea oscillations," *IEEE Trans. Power Syst.*, vol. 11, no. 3, pp. 1342–1349, 1996.

[74] F. Dorfler, M. Chertkov, and F. Bullo, "Synchronization in complex oscillator networks and smart grids," *Proc. Natl. Acad. Sci.*, vol. 110, no. 6, pp. 2005–2010, Feb. 2013.

LIST OF PUBLICATIONS

[1] A. Kamilaris, Y. Tofis, C. Bekara, A. Pitsillides, and E. Kyriakides, “Integrating Web-Enabled Energy-Aware Smart Homes to the Smart Grid,” *Int. J. Adv. Intell. Syst.*, vol. 5, no. 1 and 2, pp. 15–31, 2012.

[2] Y. Tofis, Y. Yiasemi, and E. Kyriakides, “A Plug-and-Play Selective Load Shedding Scheme for Power Systems,” *IEEE Syst. J.*, vol. 11, no. 4, pp. 2864–2871, Dec. 2017.

[3] Y. Tofis, S. Timotheou, and E. Kyriakides, “Minimal Load Shedding Using the Swing Equation,” *IEEE Trans. Power Syst.*, vol. 32, no. 3, pp. 2466–2467, May 2017.

[4] Y. Tofis, S. Timotheou, and E. Kyriakides, “Optimizing Under Frequency Load Shedding under Delays,” *IEEE Trans. Power Syst.*, pp. 1-3 (Submitted, May 2018).

[5] Y. Tofis, S. Timotheou, and E. Kyriakides, “The Impact of UFLS to the Lifetime of the Generating Units,” *IEEE Trans. Power Syst.*, pp 1-8 (Submitted, May 2018).

[6] Y. Tofis, L. Hadjidemetriou, and E. Kyriakides, “An intelligent load shedding mechanism for maintaining frequency stability,” in *2013 IEEE Grenoble Conference PowerTech, POWERTECH 2013*, 2013, pp. 1–5.

[7] Y. Tofis, Y. Yiasemi, and E. Kyriakides, “A plug and play, approximation-based, selective load shedding mechanism for the future electrical grid,” *Lect. Notes Comput. Sci. (including Subser. Lect. Notes Artif. Intell. Lect. Notes Bioinformatics)*, vol. 8328 LNCS, pp. 74–83, 2013.

[8] Y. Tofis, Y. Yiasemi, E. Kyriakides, and K. Kansala, “Adaptive frequency control application for a real autonomous islanded grid,” in *2014 IEEE PES General Meeting | Conference & Exposition*, 2014, pp. 1–5.

[9] Y. Tofis, S. Timotheou and E. Kyriakides, "Minimal load shedding using the swing equation," in *2017 IEEE Manchester PowerTech*, Manchester, 2017, pp. 1-3.